Water tunnel experiments on flow separation and vortex control by applying suction

Ram Sivakumaran

Recommended Citation

To the Graduate Council:

I am submitting herewith a thesis written by Ram Sivakumaran entitled "Water tunnel experiments on flow separation and vortex control by applying suction." I have examined the final electronic copy of this thesis for form and content and recommend that it be accepted in partial fulfillment of the requirements for the degree of Master of Science, with a major in Aerospace Engineering.

Jain-Ming Wu, Major Professor

We have read this thesis and recommend its acceptance:

A. D. Vakili, Edward Kraft
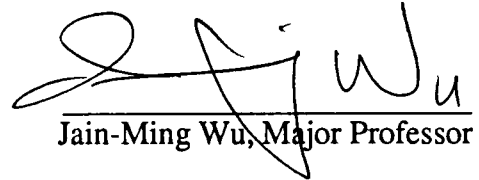
Accepted for the Council:
Carolyn R. Hodges

Vice Provost and Dean of the Graduate School

(Original signatures are on file with official student records.)

To the Graduate Council:

I am submitting herewith a thesis written by Ram Sivakumaran entitled "Water tunnel experiments on flow separation and vortex control by applying suction". I have examined the final copy of this thesis for form and content and recommend that it be accepted in partial fulfillment of the requirements for the degree of Master of Science with a major in Aerospace Engineering.

Jain-Ming Wu, Major Professor

We have read this thesis and
and recommend its acceptance:

Accepted for the Council:

Vice Provost and Dean of
the Graduate School

STATEMENT OF PERMISSION TO USE

In presenting this thesis in partial fulfillment of the requirements for a Master's degree at the University of Tennessee, Knoxville, I agree that the Library shall make it available to borrowers under the rules of the Library. Brief quotations from this thesis are allowable without special permission, provided that accurate acknowledgement of the source is made.

Permission for extensive quotation from or reproduction of this thesis maybe granted by my major professor or in his absence, by the Head of Interlibrary Services when, in the opinion of either, the proposed use of the material is for scholarly purposes. Any copying or use of the material in this thesis for financial gain shall not be allowed without my written permission.

Signature _____Ram Sivakumaran_____

Date _____November 26, 1991_____

WATER TUNNEL EXPERIMENTS ON FLOW SEPARATION AND VORTEX CONTROL BY APPLYING SUCTION

A Thesis

Presented for the

Master of Science

Degree

The University of Tennessee, Knoxville

Ram Sivakumaran

December, 1991

DEDICATION

This thesis is dedicated

to my parents

K. S. Sivakumaran and Pushpa Sivakumaran

who taught me how invaluable an education is and guided me onto the never ending

path of quest for knowledge

and

to my late uncle

Veluppillai Vigneshwarakumaran

who gave me the opportunity to pursue my higher education without whose generous

and timely help I would not be where I am today

ACKNOWLEDGEMENTS

ABSTRACT

In this experimental study, the effectiveness and methods of applying suction as a tool for flow control, specifically to prevent flow separation and to curtail vortices that promote separation, were studied utilizing a water tunnel facility. All tests were conducted at moderately low Reynolds numbers ranging from 1,550 to 21,180. Experiments were conducted with four different configurations: (1) Cylinder model of diameter 4.83 cm, (2) Cylinder - flat plate junction model with a cylinder diameter of 11.43 cm, (3) Streamlined body - flat plate junction model, where the streamlined body is a wing with NACA 0012-64 airfoil and chord length 18.1 cm, and (4) 30° swept-forward wing with NACA 0012-64 airfoil and of chord length 16.2 cm at angles of attack of 30° and 40°.

Instead of random, large-scale, brute-force applications of suction, in this study suction was applied discretely only at certain selected locations (determined based on guiding principles that were drawn from some fundamental study of the physics of the flow), and at moderately low suction rates. Tests were conducted at suction rates ranging from 0 to 21.0 cc/sec. The suction coefficients, $C_Q = Q/AV_\infty$ ranged from 0.0028 to 0.0760 at various Reynolds numbers.

With suction applied at low suction rates and only at selected locations, very effective flow control was achieved around the models tested. In a severe case of flow over the cylinder, separation was delayed up to a maximum of 19°. In the cases of the cylinder and streamlined body - flat plate junctions, the horse-shoe vortex was almost totally eliminated. In the case of the swept-forward wing, a 'horn' vortex which forms as a consequence of reversed flow was moved towards the root of the wing. Flow reversal was avoided, and nearly full-chord attached flow was established up to 45% span.

TABLE OF CONTENTS

LIST OF FIGURES

LIST OF TABLES

LIST OF SYMBOLS

A	reference area (frontal or blockage area of model)
A_H	suction hole area
A_S	suction slot area
AOA	angle of attack, also α
AR	aspect ratio $= b^2/S$
b	wing span
c	wing chord
C_D	drag coefficient $= D / 2\rho V^2_\infty$
$C_{D(total)}$	total drag coefficient (form drag + suction drag)
C_f	coefficient of friction
C_L	lift coefficient $= L / 2\rho V^2_\infty$
$C_{L(max)}$	maximum lift coefficient
C_Q	coefficient of suction $= Q/AU_\infty = -v_s A_S/U_\infty A = -v_s A_H/U_\infty A$
D	diameter, also drag force
D_H	diameter of suction hole
L	lift force
L_S	length of suction slot
Q	volume of fluid removed per unit time (suction rate)
Re_C	Reynolds number based on chord $= V_\infty c/\nu$
Re_D	Reynolds number based on diameter $= V_\infty D/\nu$
Re_L	Reynolds number based on length $= V_\infty L/\nu$
Re_S	suction slot / hole Reynolds number $= v_s W_S/n = v_s D_H/\nu$
S	wing area
U_∞	free-stream velocity
V_P	tunnel propeller speed
v_s	suction velocity $= Q/A_S = Q/A_H$
V_T	tunnel flow velocity
W_S	width of suction slot
α	angle of attack
β	side slip angle

Λ	wing angle of sweep back
μ	dynamic viscosity
ν	kinematic viscosity
θ	angle of separation
θ_U	angle of separation on the upper half of the cylinder
θ_L	angle of separation on the lower half of the cylinder
ρ	density

CHAPTER I
INTRODUCTION

In this chapter, the overall objective of the study is presented, followed by a detailed review of previous research pertaining to flow control and improved aerodynamic performance (e.g. increased lift, decreased drag, etc.) using the technique of suction. The latter part of the chapter briefly discusses the guiding principles of applying suction as a tool for flow control. The final section contrasts previously performed work with the work done in this study, pointing out the differences and variations.

§ 1.1 OBJECTIVE

The objective of this study is to demonstrate a method for controlling the flow over and around various aerodynamic configurations (refer to § 2.3 for configurations investigated) in such ways that are beneficial to the aerodynamics of the body in question. The desired result is to achieve minimum flow separation by application of continuous suction through slots and holes located at selected regions on the surfaces of the bodies. The proper location of such suction slots and holes were determined, taking into consideration the specific physics of the flow for the different cases. Also, a minimal number of slots/holes were utilized together with the minimal required suction to achieve the desired objective. All experiments reported here were conducted in a water tunnel (in a low speed, moderately low Reynolds number scenario).

In general, flow separation occurs because of one or all of the following effects: (i) Viscosity effects (ii) Adverse pressure gradient (iii) Geometry. Depending on the case at hand, for a given geometry, the technique of applying suction may help curtail the two underlying mechanisms causing flow separation, namely viscosity effects and adverse pressure gradient effects. By applying the appropriate amount of suction at the wall near the separation point, the viscous shear layer is weakened because of the transfer of fluid mass at the wall. This in turn reduces the viscosity effect and prevents boundary layer growth since a new boundary layer forms downstream from where suction was applied (see e.g., Chang, 1976). Also, application of suction reduces the adverse pressure gradient. Consequently, flow stagnation and reversal are delayed or at best avoided. This implies a delay in flow separation. Hence, by applying suction in the vicinity of the separation point, flow separation over and around bodies may be

1

delayed and or curtailed. In this study, suction was applied primarily to change the adverse pressure gradient or associated vorticity pattern, and thereby delay separation.

There are many practical advantages in reducing flow separation and thereby achieving better aero/hydrodynamic characteristics of various everyday practical vehicles: Firstly, if flow separation is delayed, an airplane can be pushed to higher angles of attack without stalling, which translates into an increase in lift. Secondly, since laminar flow is maintained and transition to turbulent flow is prevented or delayed, a reduction in drag can be accomplished. Thirdly, the separated region may be significantly reduced and therefore a smaller or a weaker wake flow is established, which is advantageous from many applications points of view. According to Saric (1985) a reduction of about 60-80% in skin friction drag is achieved when a laminar instead of a turbulent boundary layer is maintained. In commercial aircraft for instance, where the viscous drag accounts for about 50% of the overall drag, a reduction in overall drag of about 25% maybe realized if the flow is fully laminar over the wings. Finally, the overall stability of the flow and hence that of the lifting surface is improved. The technique of suction may be utilized as an effective tool for minimizing flow separation. The amount of fluid that need be removed by suction to achieve successful flow control is relatively small which can be achieved by a pump with minimal expenditure of energy. One must weigh the above advantages against the required power or energy input (for the purpose of suction) that is needed to achieve them. In other words, what is the price that need be payed.

In the current study, suction, as a means to help attain flow control, is applied through holes and slots located on the surface of the bodies. Most previous researchers' investigations utilized suction through slots, holes, and perforate surfaces, generally located over the entire or most of the chord region, and the entire span region in question. However, in this study suction is applied only in selected location/s on the body encompassing a constrained area. This area was chosen after careful consideration and experimental determination of the physics of the flow (i.e. after determining, for instance, where the core of a 'horn' vortex that is a consequence of reversed flow exits in the case of a swept-wing, or where flow separation occurs in a cylinder - flat plate junction). Because of the consideration of the basic physics related to flow separation, a significant reduction in the amount of fluid that needed to be sucked was achieved. This gave rise to a simpler design, while simultaneously achieving a saving in the power required.

2

The idea behind applying suction near the separation point, as opposed to gross suction on the entire surface or region to alter the overall boundary layer is conceived, and is theoretically shown to be a correct concept by Wu and Wu (1991) (A detailed look into the guiding principles of flow control is presented in § 1.3). The principal idea is that it is relatively easy to achieve flow control and avoid flow separation if the method of flow control was implemented at the separation point (on the verge of separation) rather than at a point downstream of the separation point, i.e. after separation has taken place (e.g. In the case of flow separation on a cylinder, suppressing or removing the separating streamline at the point of separation, rather than allowing separation to develop and then trying to reduce it further downstream). In essence then, the main objective of this study is to prevent or weaken the mechanism (e.g. adverse presure gradient) that causes flow separation at the instant and location where it occurs, rather than allowing for the mechanism to substantiate and then reduce the detrimental aftereffects, caused by the mechanism.

The results and observations from the experiments are compared with the physical concept, and analyses of the observations in each case are undertaken and presented. In addition, the results are also compared, wherever permissible and applicable, with those results obtained by other researchers, who have utilized conventional methods of pursuing flow control.

§ 1.2 PREVIOUS STUDIES AND INVESTIGATION

As early as 1904, Ludwig Prandtl (1904 and 1927), experimented with various ways of artificially controlling the boundary layer, and thereby showed how great an influence external boundary layer control has on the flow field around the body in question (Betz, 1961). An extensive literature survey on the subject of flow control by suction is included in the Appendix. Some essentials to this study are explained in this section.

In his first paper published in 1904, Prandtl discussed the utilization of the method of suction (among others) to effectively control the boundary layer. He validated his idea by performing an experiment in which he considered the flow past a cylinder, with suction applied at a location in the upper half of the cylinder ($90° < \theta < 180°$) through a small slot. On the upper half, where suction was applied part of the boundary layer was removed and it is evident that the flow stays attached to the cylinder to a greater

3

extent than the lower half, and separation is delayed considerably. Consequently, the drag is minimized (refer to Figure 1.1) (Schlichting, 1968).

However, further investigations into the use of suction as a flow control method were not carried out until the early 1920's. In 1921, G. V. Lachmann tested a wing model with slotted suction in Göttingen. He achieved a 60% increase in $C_{L(max.)}$ compared to unslotted airfoils that were available at the time (Betz, 1961). In 1921, Handley Page published a paper on Boundary Layer Control (BLC), in which he reported achieving higher lift coefficients than any known up to that time by using a slotted wing.

In the late 1920's and 1930's, two experimental airplanes were built, and tested at the Aerodynamische Versuchsanstalt at Göttingen, under the supervision of O. Schrenk, with the objective of achieving increased lift due to suction (Schlichting, 1979). Suction was applied through a slot, located just ahead of the flap. Full-chord laminar flow was realized over the flap, when the flap was deflected. Figure 1.1 shows the separated flow without suction and completely attached flow with suction.

Organized and elaborate research on Boundary Layer Control intensified during the 1940's. Experimental and theoretical works were performed at the Royal Aircraft Establishment (RAE), and the National Physics Laboratory (NPL) in the United Kingdom; continued research was conducted at Göttingen in Germany; investigations were carried out at the Institute for Aerodynamics at the Federal Institute of Technology in Zurich, Switzerland; some research also took place in the United States under the auspices of National Advisory Committee for Aeronautics (NACA).

Thus far, most of the research activities using suction as a tool for BLC, were carried out in the 1950's, 1960's, and the early part of the 1970's. Suction was mostly applied in such ways that the nature of the boundary layer was altered.

In the sixties, the possibilities of using the technique of suction of the boundary layer and hence alleviating partially or completely the amplifications of the instabilities that cause transition to turbulent flow from laminar flow, became popularly referred to as Laminar Flow Control (LFC). With the advent of rising fuel costs in the late 1960's and early 1970's, the National Aeronautical and Space Administration (NASA) initiated the Aircraft Efficiency Program (ACEE) in 1976, in which suction was used as the mechanism for LFC with drag reduction in mind. Previously performed work (1950's

4
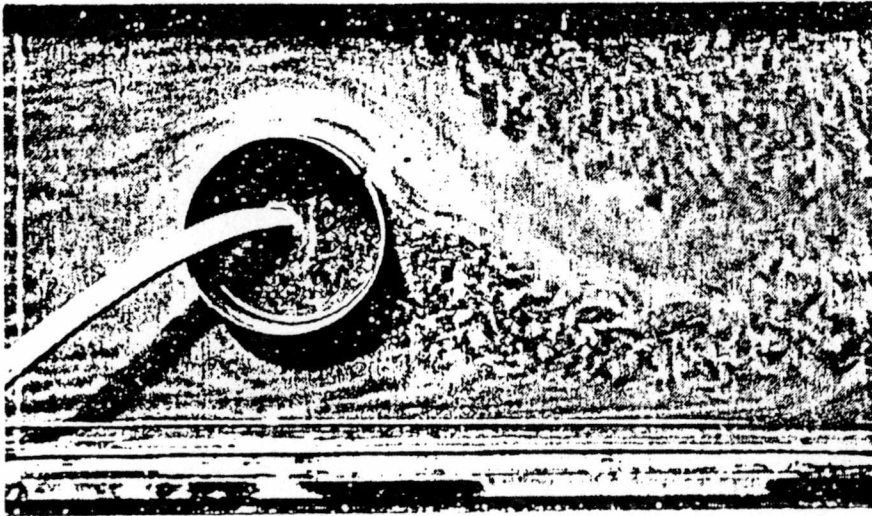
(a) Prandtl's cylinder experiment with a suction slot on the upper half
(Btez, 1961)
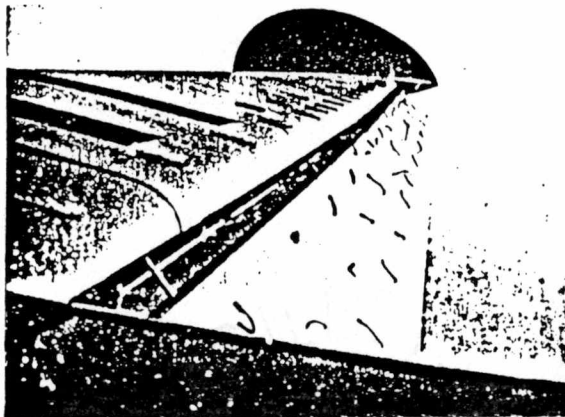
(b) Schrenk's flight experiment:
Separated flow over flap
without suction (Betz, 1961)
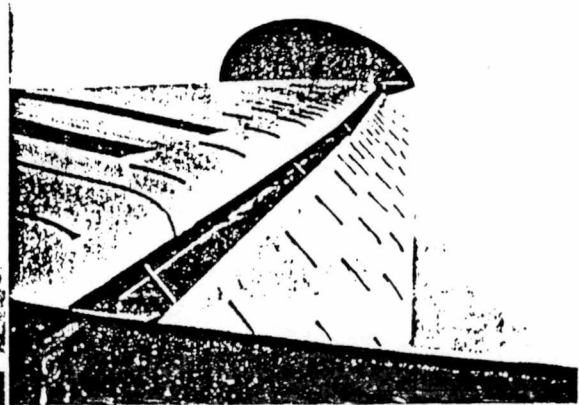
(c) Schrenk's flight experiment:
Attached flow over flap
with suction (Betz, 1961)

Figure 1.1 Prantl's cylinder experiment and Schrenk's flight experiment

and 1960's) at Northrop under W. Phenninger received much attention from NASA and became an integral part of ACEE. Northrop and Douglas aircraft companies, together with several other entities continued to carry out research on suction under ACEE well into the mid-1980's.

A chronological summary in tabular form of all major investigations where suction was used as the tool for flow control through holes, slots, perforated surfaces, and porous surfaces is presented in the Appendix. The investigations range from wind/water tunnel experiments to flight experiments, including cylinders, flat plates, tubes and wings.

The methods of applying wall suction may essentially be grouped into three categories: (1) Suction through slots (uniform suction through all slots, or distinct and different suction through each or groups of slots. For instance, the suction quantity through slots located at the leading edge of a wing may be increased, where an intense pressure peak is prevalent, and lower suction may be applied through slots located in the mid-chord area where the pressure gradient is constant and less intense and favorable). (2) Suction through holes (again, uniform suction through all holes or distinct suction through separate holes). (3) Suction through a perforated or porous surface, also referred to as area suction (for this case only continuous suction is applicable).

So far, the technique of suction for flow control has been used in a few experiments involving cylinders and flat plates. An appreciable amount of work has also been performed using various axisymmetric bodies of revolution. Research in the control of internal flow has also been performed using long tubes with small diameters. Numerous experiments have been conducted to achieve flow control over wing sections. Tests have been carried out both in wind and water tunnels, and on aircraft engaged in actual flight experiments.

CYLINDERS: Besides the experiment by Prandtl described earlier, the utilization of suction for flow control over cylinders has been minimal. In 1950, Pankhurst and Thwaites, two British researchers performed experiments with a wholly porous cylinder of diameter 3 in., with a Thwaites flap attached to the rear of the cylinder. At a flap deflection of $60°$ and a suction parameter, $(C_Q)(Re^{0.5}) = 35$ (at $Re = 0.1 \times 10^6$), circulatory flows were realized while achieving $C_{L(max.)} = 9$. The suction parameter was observed to decrease slightly with increase in deflection angle of the Thwaites flap.

FLAT PLATES: Holstein (1940), Kay (1953), and Smith (1953) have experimented with flat plates, using continuous or area suction to achieve boundary layer control. The first investigator used a perforated surface for suction, while the two latter investigators used porous surfaces. In his experiments conducted at the Cambridge University wind tunnel in 1953, Kay determined a suction-to-freestream velocity ratio, $v_s / V_\infty = 0.001$, to stabilize the flow and prevent transition from laminar to turbulent flow. Smith in 1953, achieved full chord laminarization up to Re = 8 X 10^6 during tests conducted at the Douglas El Segundo wind tunnel.

TUBES: Much, if not all of the suction research pertaining to *tubes* were conducted at Northrop under the guidance and supervision of Werner Phenninger in the time period between 1950 and 1960. Phenninger, along with Meyer, Moness, and Sipe, Jr. (1952 - 1957) performed these tests at the Northrop Norair wind tunnel.

At the early stages of research, Phenninger used 2 in. diameter tubes of length 20 ft. and 40 ft. with suction through a single circumferential slot. Suction through this single slot destabilized the flow without a favorable pressure gradient immediately downstream of the slot (see References 44, 45). He then experimented with 8 circumferential slots on the 20 ft. length tube, and achieved full-tube laminar flow up to a length Reynolds number, $Re_L = 14.7$ X 10^6 (see Reference 46). In 1953 Phenninger and Meyer (1953), performed further experiments with a tube of 1 in. diameter and 50 ft. length, again, maintaining full length laminar flow up to about $Re_L = 15$ X 10^6.

In 1957 Goldsmith and Meyer, also at Northrop, investigated the case of suction through holes on a 2 in. diameter tube, and determined that the 3-D disturbances due the holes (as opposed to slots) were destabilizing and posed an immense problem in maintaining full laminar flow at higher Reynolds numbers. In the same year, Meyer also performed hole suction experiments on an 8 in. diameter tube, where holes of 1/8 in. diameter were drilled 1/2 in. apart from each other. Again, he was not successful in achieving full laminarization, and observed destabilizing trailing vortices from the holes.

Meanwhile, in the research that culminated in 1957, Phenninger et al. (1953 - 1957) continued their research with the 2 in. tube, and increased the number of suction slots to 80. For this case full-length laminar flow was attained at $Re_L = 21.2$ X 10^6. The minimum C_Q required to maintain full-length laminar flow was 20% less than that

required in the case of 8 suction slots. In general, a 27% reduction in overall suction required over the 8 slot case was also achieved.

BODIES OF REVOLUTION: Research involving axisymmetric bodies of revolution were carried out by Groth (1953 - 1958) and, Gross (1964) at the Northrop Norair 7 X 10 ft. wind tunnel with a great degree of success. Other researchers in the area are McCormick and the Soviet investigators Kozlov and Tsyganyuk.

Groth (1958 a, b), investigated with an axisymmetric body of revolution of fineness ratio 8 and length 142 in., with continuous suction applied through a porous surface. Full-length laminar flow was achieved at an angle of attack of 3° and up to $Re_L = 14 \times 10^6$. It was determined that the total drag $C_{D(total)}$ of the body was 1.24 times the coefficient of friction, C_f of that of a flat plate.

Gross (1964) performed experiments on a body of revolution with a fineness ratio of 9 and length 12 ft., with suction through 102 circumferential holes. Full-length laminar flow was realized up to $Re_L = 20.63 \times 10^6$. At $Re_L = 20.27$, the total drag was, $C_{D(total)} = 4.18 \times 10^{-4}$, and a suction coefficient of $C_Q = 2.25 \times 10^{-4}$ was required for full laminarization. The drag was 1.4 times that of a laminar flat plate C_f. Gross then used a Sears - Haack body of revolution (see Reference 20) with suction through 120 slots, in which case full laminar flow was again achieved up to $Re_L = 18.55 \times 10^6$ at an angle of attack of 2°. The total drag for this case was 1.18 times that of a laminar flat plate C_f, at $Re_L = 19.6 \times 10^6$, with $C_Q = 1.75 \times 10^{-4}$.

McCormick conducted water tunnel and sea tests on a TRI-B buoyantly propelled axisymmetric body with circumferential slot suction. Nearly full-length laminar flow was achieved up to $Re_L = 4 \times 10^6$. Non-uniform circumferential suction prevented full-length laminar flow from being realized.

Further water tunnel experiments were conducted by Kozlov and Tsyganyuk (1976) with a cylindrical body of revolution with porous suction surface. The total drag in their experiment was reduced to 1/2 the value of the case without suction, at Re $= 3.5 \times 10^6$, with $C_Q = 6 \times 10^{-4}$.

WINGS: The following researchers used suction through slots to accomplish

LFC: Schrenk (refer also to Reference 61), Holstein (1940), Goldstein (1948), Zalovcik, Wetmore, and Van Doenoff (1944), Lighthill (1945), Moss (1947), Phenninger (1947, 1949), Phenninger et al. (1955, 1957), Pearce (1982), Poppleton (1951), Keeble (1951), Loftin, Burrows, and Horton (1952), Burrows and Schwartzberg (1952), Smith and Brazier (1953), Landeryou and Porter (1966), Stark (1964), Carlson, Phenninger, and Bacon (1964), Kosin (1964), Zozulya and Cheranovskiy (1973), and early unpublished reports from NPL in the United Kingdom (refer to Reference 68).

Continuous or area suction through porous surfaces were carried out by the following: Pankhurst and Gregory (1948), Braslow, Burrows, Tetervin, and Visconti (1951), Head and Johnson (1955), Poppleton (1951), Van Ingen (1965), Pearce (1982), and unpublished work at NPL (see also Reference 68).

Area suction through perforated surfaces were carried out by the following investigators: Carmichael and Raspet (1954), Gregory and Walker (1955), and Pearce (1982).

Wind Tunnel Tests: Between 1947 and 1949, Phenninger (1947, 1949) tested a 17% thick unswept laminar wing with several suction slots at the 7 X 10 ft. wind tunnel at the Institute for Aerodynamics at the Federal Institute of Technology in Zurich, Switzerland, and maintained full-chord laminar flow on both upper and lower surfaces of the wing up to $Re_C = 2.5$ X 10^6 with the required suction coefficient, $C_Q = 0.0014 - 0.0018$, and also achieved a 50% reduction in drag: without suction - $C_{D(Min.)} = 0.0048$ at $Re_C = 2$ X 10^6, with suction - $C_{D(Min.)} = 0.0023$ at $Re_C = 2.4$ X 10^6. Between 1957 and 1959, Phenninger, et al. (51) achieved full laminarization up to $Re_C = 1.8$ X 10^6, with $C_{D(total)} = 0.00125$ on a 12% thick, 30° sweepback wing at the 5 X 7 ft. University of Michigan wind tunnel, with suction applied through 86 slots located between 25% - 95% of chord. C_Q required to maintain full laminar flow was larger than that required for a straight wing, but smaller than theoretical values. In 1961, Phenninger together with Gault achieved full-chord laminar flow up to $Re_C = 29$ X 10^6 over a 30° swept-back wing with a NACA 66-012 airfoil, with suction applied through 93 spanwise slots, in the NASA Ames 12 ft. pressure tunnel.

At a low-speed environment, Carlson, et al. (1964) achieved 90% laminar flow on a 33° swept wing, between $Re_C = 29.4$ X 10^6 and $Re_C = 43$ X 10^6 ($C_D = 0.00088$ and

$C_D = 0.001$), with an NACA 64016 airfoil of chord length 10 ft., at the NASA Ames 12 ft. pressure tunnel. Braslow, et al. (1948, 1951), between 1948 - 1951, attained full-chord laminarization up to $Re_C = 19.8 \times 10^6$, with $C_{D(total)} = 0.0017$ at a suction velocity, $v_s = 0.5$ ft./sec (induced by a suction quantity of 1.8 lb/in^2), on a wing with NACA 64A010 airfoil of chord length 3 ft, with suction applied through a 13 in. porous surface centered at mid-span of the model. A reduction in total drag of 38% (when compared to the same airfoil without suction) was achieved. C_Q required for full-chord laminar flow was observed to decrease with increase in Reynolds number. Between 1951 - 1953 Loftin and Horton achieved full-chord laminarization up to $Re_C = 17 \times 10^6$, on a 15% thick airfoil with 17 slots on the upper surface and 13 slots on the lower surface, located between 40% c - 100% c, at the 3 × 7.5 ft. Langley TDT tunnel. Full-chord laminarization was also achieved on a wing with a NACA 66-(1.8)15 airfoil of chord length 5 ft, with suction applied through multiple suction slots, up to $Re_C = 16 - 17 \times 10^6$ ($C_{D(total)} = 0.0011$ at $Re_C = 16.3 \times 10^6$).

Gregory and Walker (1955), avoided separation up to 14° on a NACA 63 A009 airfoil with distributed suction over the nose area, with $C_Q = 23 \times 10^{-4}$ at $Re_C = 3.5 \times 10^6$.

Research conducted by Pearce (1982) at the Douglas wind tunnel with a 30° sweepback wing of chord length 7 ft. produced some revealing results regarding the overall effectiveness of using various suction techniques, namely slotted surface, porous 'Dynapore', and electron beam perforated titanium. The EB perforated titanium suction surface provided the best overall results compared to the other two candidates. At $Re = 1.35 \times 10^6$/ft. (comparable to an aircraft flying at $M = 0.75$, at 38,000 ft., at $Re = 1.6 \times 10^6$/ft.), 80% laminar flow was attained on both surfaces with suction applied up to 70% chord, and the total drags were in the order of $C_{D(total)} = 0.00175 - 0.0025$. Suction applied up to 80% chord only on the upper surface yielded better results than suction applied on both surfaces up to 70% chord.

Flight Tests: Between 1944 and 1947, Zalovcik, et al. performed flight experiments with a wing glove on a B-18 aircraft, which had a NACA 35-215 airfoil and 9 suction slots placed at a distance of 5%c from each other. 45% chord laminar flow was realized up to $Re_c = 23 \times 10^6$. The tests were later repeated with 17 slots, however, laminarization could not be improved because of 'over suction'. In his 1957

laminar flow at Re_c = 29 X 10^6 (at M = 0.7). In addition a drag reduction of about 70% - 80% over the 'no-suction' case was realized. The following year, he again achieved full chord laminar flow with porous suction on a 15% thick low drag airfoil mounted as a fin under the fuselage of an Avron Anson aircraft. Between 1955 and 1957, Phenninger, et al. performed flight experiments using the F-94 aircraft, which was fitted with a 13% airfoil similar to the NACA 65-213. Suction applied through 12 slots spaced between 41.5% and 94% chord, resulted in full-chord laminar flow up to Re_C = 25.64 X 10^6, with C_Q = 0.00034, and C_D = 0.00051, while suction through 69 slots resulted in full-chord laminarization up to Re_C = 36 X 10^6, with C_Q = 2.91 X 10^{-4}, and C_D = 4.82 X 10^{-4}. In 1964, Stark (64) in conjunction with the X-21 program, flight tested a 30° sweepback wing with spanwise suction slots, and achieved partial laminarization up to Re_C = 47 X 10^6 with speeds extending into the transonic region. Continued research on the X-21 aircraft by Kosin (1964), produced full-chord laminar flow on the outer third of the 30° swept wing utilizing 120 suction slots on the upper surface and 120 suction slots on the lower surface with slot widths varying from 0.0035 in. - 0.01 in.

§ 1.3 GUIDING PRINCIPLES OF APPLYING SUCTION

Separation occurs, in general, when portions of fluid closer to the wall gradually decelerate, come to a standstill, and eventually reverse direction due to an adverse pressure gradient. Flow separation may be delayed and at best, in some cases, totally avoided by the application of suction within the boundary layer, in the vicinity of flow separation. By removing these slower moving parts of fluid in the boundary layer and by altering the presure gradient using suction, flow reversal is avoided and the flow is kept attached, triggering no separation.

Let us define a local boundary vorticity flux $\vec{\sigma}$

$$\vec{\sigma} = \nu \frac{\partial \vec{\omega}}{\partial \vec{n}}$$

(1.1)

where, $\nu = \mu/\rho$ and $\vec{n}$ = unit normal surface vector. A complete expression for $\vec{\sigma}$ over a 3-D arbitrary body has been derived by Wu, et al. (1987) based on the full Navier-Stokes equation as

$$\rho\vec{a} = \vec{n} \times (\nabla p)_{\partial B} + (\vec{n} \times \vec{\tau}_{\partial B}) \cdot \nabla\vec{n} - \vec{n}[\vec{n} \cdot (\nabla \times \vec{\tau}_{\partial B})] \tag{1.2}$$

where, $\vec{a} = \mathcal{D}\vec{V}/\mathcal{D}t$ and the subscript ∂B indicates the value on the solid boundary. On the right-hand side of the above equation, the first term is the vorticity flux due to the tangential presure gradient, the second term is the vorticity flux due to wall curvature, and the third term accounts for the normal component of the curl of the wall shear stress, which, according to Wu, et al. (1987, 1988) introduces normal vorticity flux near any separation or attachment line, in particular around spiral points (e.g. such as lee-side separation on wings at high angle of attack as shown in Figure 1.2). Lighthill (1963) was the first to realize, and extended by Wu and Wu, 1991, that in 2-D flow the presure gradient either on the normal or on the surface will alter the vorticity pattern, and conversely, the vorticity flux change will introduce a change in presure gradient, i.e., on ∂B the following relationships hold

$$\vec{n} \times \nabla p = \frac{\partial}{\partial n}(\mu\vec{\omega}) \tag{1.3}$$

$$\frac{\partial p}{\partial n} = -\vec{n} \cdot (\nabla \times \mu\vec{\omega}) \tag{1.4}$$

In other words, these two quantities are inter-related to each other. In 3-D flow, the edges of the body, and the surface curvature will affect both the presure gradient and the vorticty gradient, especially when a 'horn' vortex or spiral singularity appears in the flow field. Applying suction near the singularity may change these two quantities significantly, especially to the τ-line pattern. Thus flow separation may be altered. This is the physical reason of conducting the present experiments. The vorticity flux due to the $\vec{\tau}$ change is expressible (see Wu, et al., 1987),

$$\vec{\sigma} = -(\vec{n} \times \nabla) \cdot (\vec{\tau n}) \tag{1.5}$$

which will introduce a change in vorticity flux in the flow field.

The effectiveness of flow control is governed by the amount of fluid removed from near the singularity points in the flow. Hence, defining a nondimensionalized parameter that is a measure of the quantity of fluid removed is helpful. Such a parameter is called the suction coefficient, C_Q and is defined as

$$C_Q = Q / AV_\infty \tag{1.6}$$

where, Q is the volume of fluid removed per unit time, A is a reference area, typically the frontal or blockage area of the model, and V_∞ is the free stream velocity. Now, if

12

$\Lambda = 55^0$
$\alpha = 33^0$

$\Lambda = 30^0$
$\alpha = 20^0$
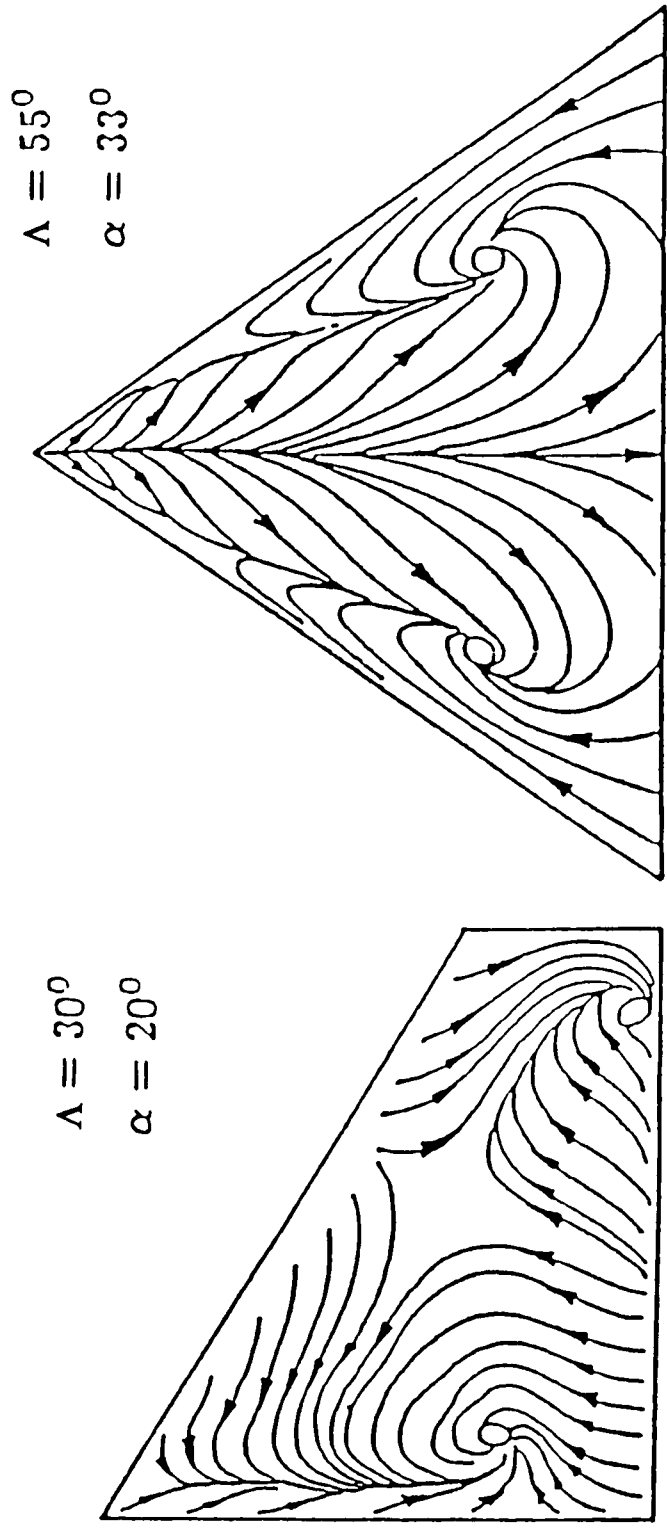
Figure 1.2 Lee-side separation on wings at high angles of attack (Liu and Su, 1985)

13

v_s is the suction velocity, then the volumetric fluid rate, Q may be expressed as

$$Q = -v_s A_S = -v_s A_H$$

where, A_S is the suction slot area, and A_H is the suction hole area. Hence, alternatively, the suction coefficient may be expressed as

$$C_Q = -v_s A_S / V_\infty A = -v_s A_H / V_\infty A \qquad (1.7)$$

Since the effectiveness of the application of suction for flow control is found to be very dependent on Reynolds numbers, and since these Reynolds numbers are appropriate nondimensional quantities that can be used to compare results of work reported herein with results of other researchers it is important to look at the definitions. The flow Reynolds numbers based on the diameter and chord are respectively defined as

$$Re_D = V_\infty D / v \;\; ; \;\; Re_c = V_\infty c / v \qquad (1.8)$$

and the suction slot and suction hole Reynolds numbers are defined as

$$Re_S = v_s W_S / v = v_s D_H / v \qquad (1.9)$$

where, W_S is the width of the suction slot, D_H is the diameter of the suction hole, and v is the kinematic viscosity (in this study, that of water)

§ 1.4 PRESENT STUDY

Previous researchers have typically used suction over large areas to achieve flow control. In this study, after careful experimental determination suction is applied only at selected locations. Figure 1.3 illustrates the difference by contrasting, for example, the wing model used in the work done by Pearce (1982) showing the large region where suction was applied, and the wing model used in the present study showing a smaller region where suction was applied. The region is restricted to a limited portion of the wing.

All models used for experimentation in this study were constructed (or modified) from existing components (or models), eliminating the need to start the fabrication process from scratch. This resulted in savings of time and money. The task of fabricating the models was also relatively eased.

Four configurations were investigated as follows: (1) Cylinder model.

14

CURRENT STUDY

3.18 cm

2.22 cm

6.03 cm

7.94 cm

REGION OF
APPIED SUCTION

SUCTION
HOLE

30°

Flow
Direction

**STUDY BY PEARCE AT
MC DONNELL DOUGLAS**

LFC SUCTION REGION

SUCTION ALONG
LEADING EDGE ONLY

LFC SUCTION REGION

FLAPERON

LFC WING GLOVE ON DC-9
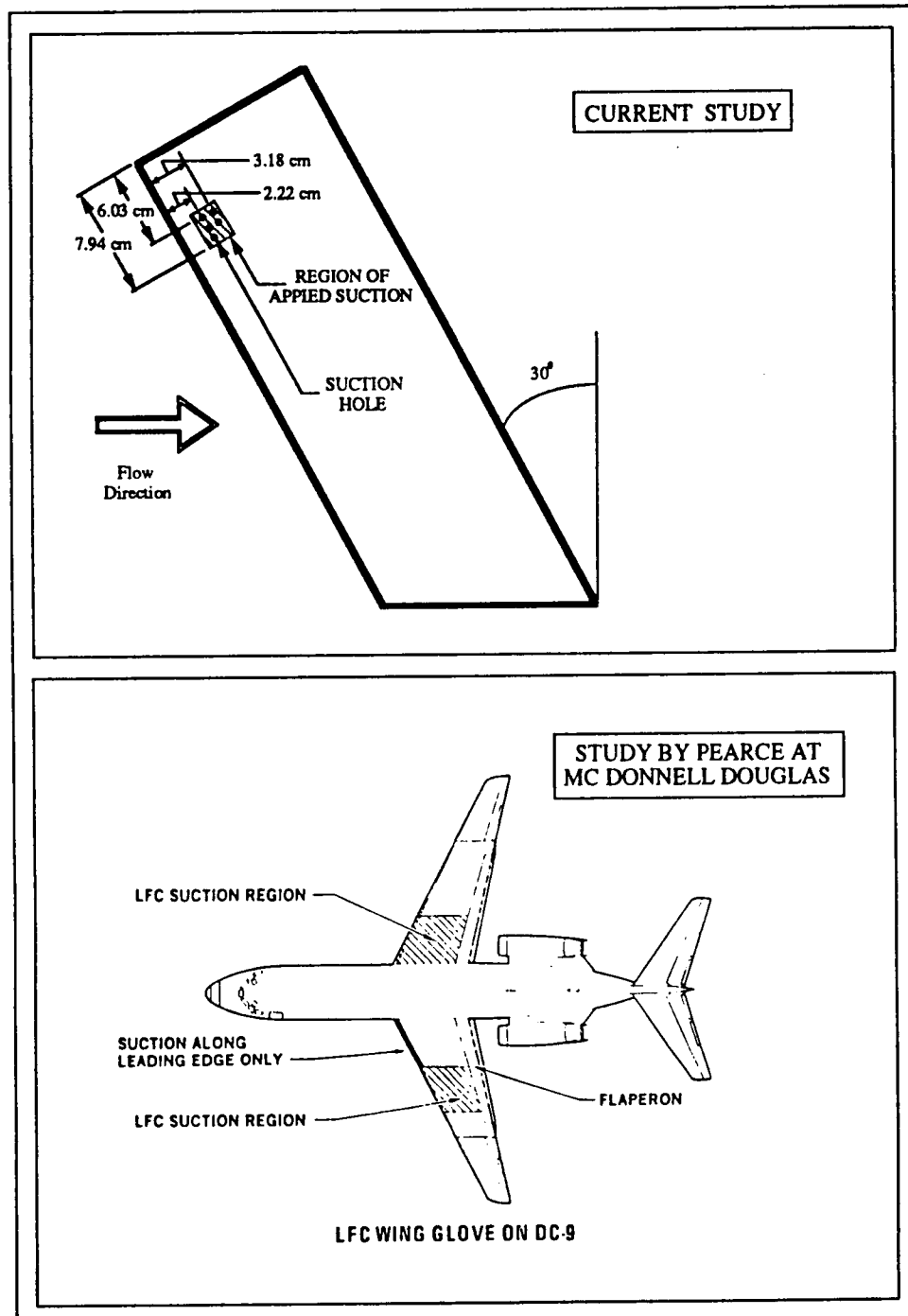
Figure 1.3 Comparison of sizes of regions where suction was applied
(current study vs. study conducted by Pearce at
McDonnell Douglas, 1982)

(2) Cylinder - flat plate junction. (3) Wing - flat plate junction. (4) Swept-forward wing at high angles of attack.

In the case of the cylinder slots were located at the vicinity on both the upper and lower halves where separation was found to occur. The next set of slots were located at points where the separation was translated to because of suction through the first set of slots, etc. Here, instead of locating slots all along the streamwise direction on the cylinder, they are located at points where separation is initiated.

In the cases of the junction models, suction was applied through holes whose locations range from immediately next to the wing and cylinder to further upstream where separation is observed to occur. In the case of the streamlined body - flat plate configuration, the wing was allowed to be pivoted about the quarter chord to attain different side slip angles, β, from the mean flow, and suction holes were placed close to the separation line that formed at various locations for $0° < \beta < 6°$.

In the case of the wing at high angle of attack, suction was applied through holes concentrated and centered in an area where the core of a 'horn' vortex forms in the absence of suction. Upon application of suction, the vortex tends to move from its original location, and hence the 'region' of holes is extended to accommodate the shifting of the vortex.

In essence then, this study has been undertaken to achieve flow control by using suction, not in an arbitrary or massive scale, but rather in a controlled specific manner in accordance with the underlying physical concepts that govern various separated flows.

CHAPTER II
WATER TUNNEL EXPERIMENTS

The first and second sections in this chapter outline the characteristics of the water tunnel facility used, and discusses the flow visualization techniques employed. Section three is devoted to the description of the design and functioning of the various configurations tested. The final section is a brief rundown of the different cases investigated.

§ 2.1 WATER TUNNEL FACILITY

A low speed closed circuit water tunnel at the University of Tennessee Space Institute (UTSI) fluid dynamics facility was used to conduct the experiments and for the purpose of flow visualization and data acquisition. Figure 2.1 shows a schematic layout of the major components of this water tunnel facility. As seen in the figure, the test section and part of the return circuit are enclosed within a building, while the motor, propeller, and the stilling chamber are located outside the building.

The tunnel is a low turbulence, closed-circuit, continuous flow facility specially designed for detailed flow visualization. The test section turbulence level is maintained at a minimal level by installation of four stainless steel screens and two honeycomb sections upstream in the stilling chamber area. Furthermore, the long return leg, with an equivalent length-to-diameter ratio of 75, helps damp out the fluctuations in the flow. The converging nozzle has an area ratio of 13.5 to 1 (from the stilling chamber to the test section). The nozzle is circular shaped at the stilling chamber and, continuously and gradually changes shape to a rectangular one at the test section.

The test section is fabricated with stainless steel and fitted with Plexiglas side wall sections all around permitting flow visualization from both vertical and horizontal sides. Another viewport, also made of Plexiglas is located downstream at the first L-bend enabling the complete flow field behind the model being tested to be visualized from a direction perpendicular to the flow direction and head-on with the on-coming flow. The test section dimensions are as follows: height = 30.48 cm (12 in.) ; width = 45.72 cm (18 in.) ; length = 152.40 cm (60 in.). The top portion of the test section was left open for this study, permitting access to various dye injection devices and probes. Since the experimental models are relatively small (the model-to-tunnel

17
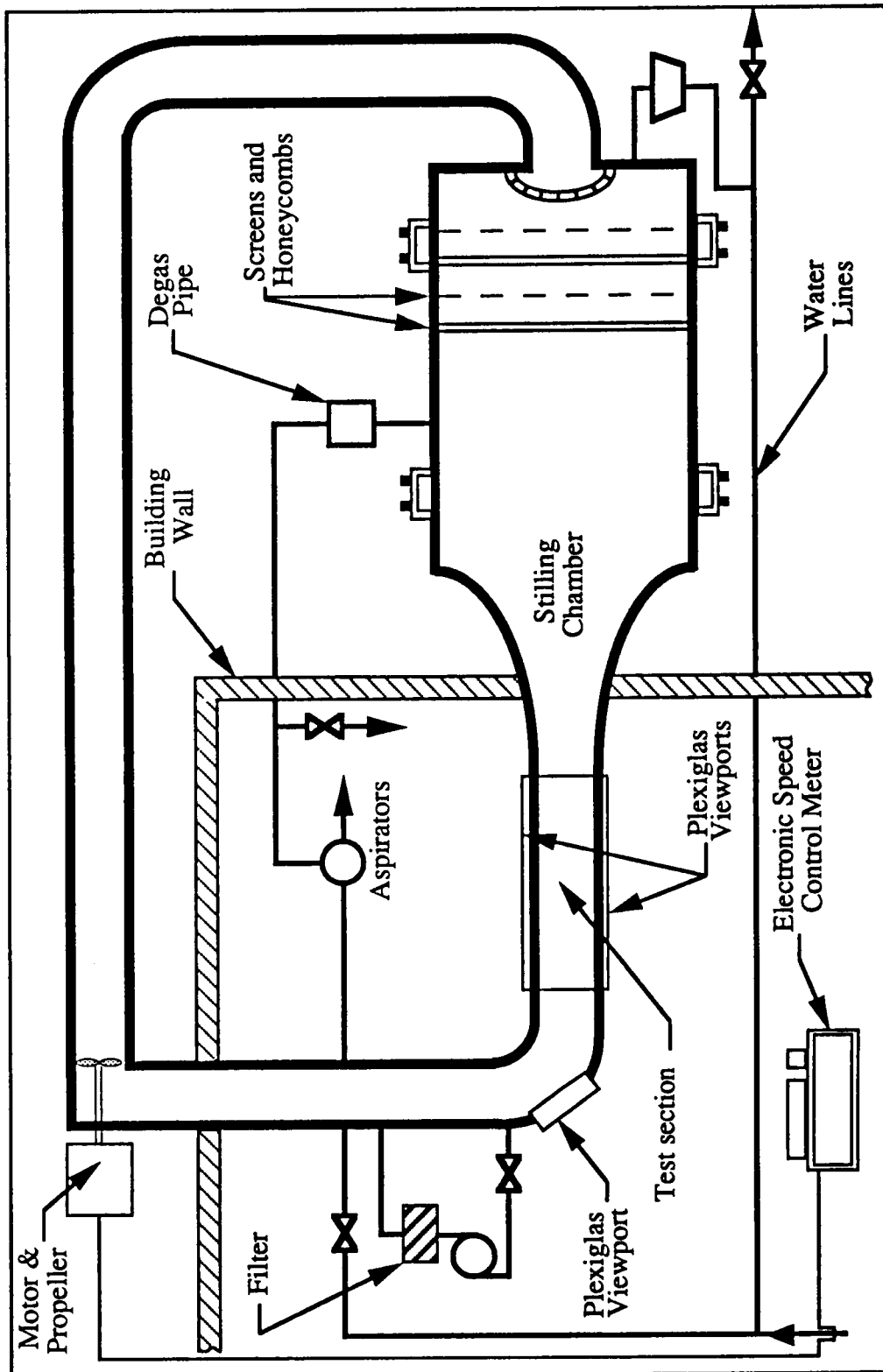
Figure 2.1   Schematic layout of water tunnel facility at UTSI

18

blockage ratio being approximately 10% for the cylinder, cylinder-flat plate configuration, and the streamlined body - flat plate junction), it was concluded that leaving the top portion of the test section open for the convenience of accessibility to models will not generate any noticeable error within the accuracy of present measurements. For the swept wing case however, when the model is set at an angle of attack tested, namely 30°, the blockage ratio is 17.5%. However, since this experiment was conducted to yield only qualitative results, the higher blockage ratio is tolerated.

The tunnel is powered by a 5 hp electric motor connected to a twin-bladed propeller of diameter of 25 cm (9.8 in.) whose location is on the second L-bend of the return circuit. This motor is capable of producing flow speeds from zero to about 50.8 cm/sec (20 in./sec). The motor is connected to an electronic speed control meter which measures and displays a digital reading of the propeller speed. A variable knob connected to the electric speed control meter allows for variation of the tunnel velocity within the capable range. The propeller speed was calibrated against the tunnel flow velocity using a cylindrical hot film probe and is given by the following empirical relationship:

$$V_T = -3.214 + 0.056 V_P \text{ (in./sec)} \tag{2.1}$$

where, V_T - tunnel flow velocity; V_P - propeller speed. Hence, the tunnel velocity can be determined given a digital readout of the propeller speed.

§ 2.2 FLOW VISUALIZATION TECHNIQUE

Flow visualization in all the experiments was carried out by continuously injecting (bleeding) colored dye through holes strategically located on the different models and configurations investigated. Whenever necessary dye was also bled through other external probes which could be placed either upstream or downstream of the model, or moved from side to side, so as to visualize the flowfield over a lateral area and a period of time.

The dye used consisted of commercial food coloring, alcohol, and milk in such proportions so as to keep the specific gravity of the dye equal to that of water. Milk was added in order to lessen the diffusion of the dye while alcohol was added to compensate for the high density of the milk. This, for instance, will prevent the dye from separating from the body, except, only at regions on the model where adverse

19

pressure gradients are experienced, at which points the flow will be forced to reverse direction and hence will be forced to detach or separate. Pressurized reservoirs supplied the dye which were carried either to the hole locations on the model or to external probes through vinyl tubings of inside diameter 1.37 mm (0.054 in.). The flow rate of the dye being bled through the holes or probes was controlled by adjusting the pressure in the reservoirs. Care was taken in adjusting the pressure to ensure that the velocity at which the dye leaves the holes or probes is negligible so that the dye itself will not influence the flow field by inducing a 'jet-effect'.

As time progressed, a detailed picture of the flowfield both around and downstream of the model could be visualized by the evolution of the dye. Both still and video photography were utilized to capture the structures of the various flowfields for further analysis.

§ 2.3 DESIGNS AND SET-UPS OF EXPERIMENTAL MODELS

The individual designs of the models including their specifications and the materials used, and the experimental set-ups of these models are discussed herein. The configurations investigated are: Cylinder, Streamlined Body - Flat Plate Junction, Cylinder - Flat Plate Junction, and Forward-Swept Wing.

§ 2.3.1 CYLINDER

The cylinder is made out of hollow aluminum piping of diameter 4.83 cm (1.9 in.) and of length 30.48 cm (12.0 in.). It is supported by two circular Plexiglas flanges glued at both ends of the cylinder. The Plexiglas flanges are of diameter 20.3 cm (8.0 in.) and of thickness 8.4 mm (0.33 in.). Since part of the cylinder on both ends is embedded within the flanges the effective length of the cylinder is 29.85 cm (11.75 in.), as shown in Figure 2.2. The circular flanges themselves have a pair of smaller rectangular flanges attached to them that keep them balanced on the tunnel floor or flat plate. This can also be seen from Figure 2.2.

Slots of width 1.27 mm (0.05 in.) are cut along the span of the cylinder for the purpose of suction. These slots are of length 29.2 cm (11.5 in.) and have a clearance of 3.175 mm (0.125 in.) on either flange as shown in Figure 2.3. The slots are located
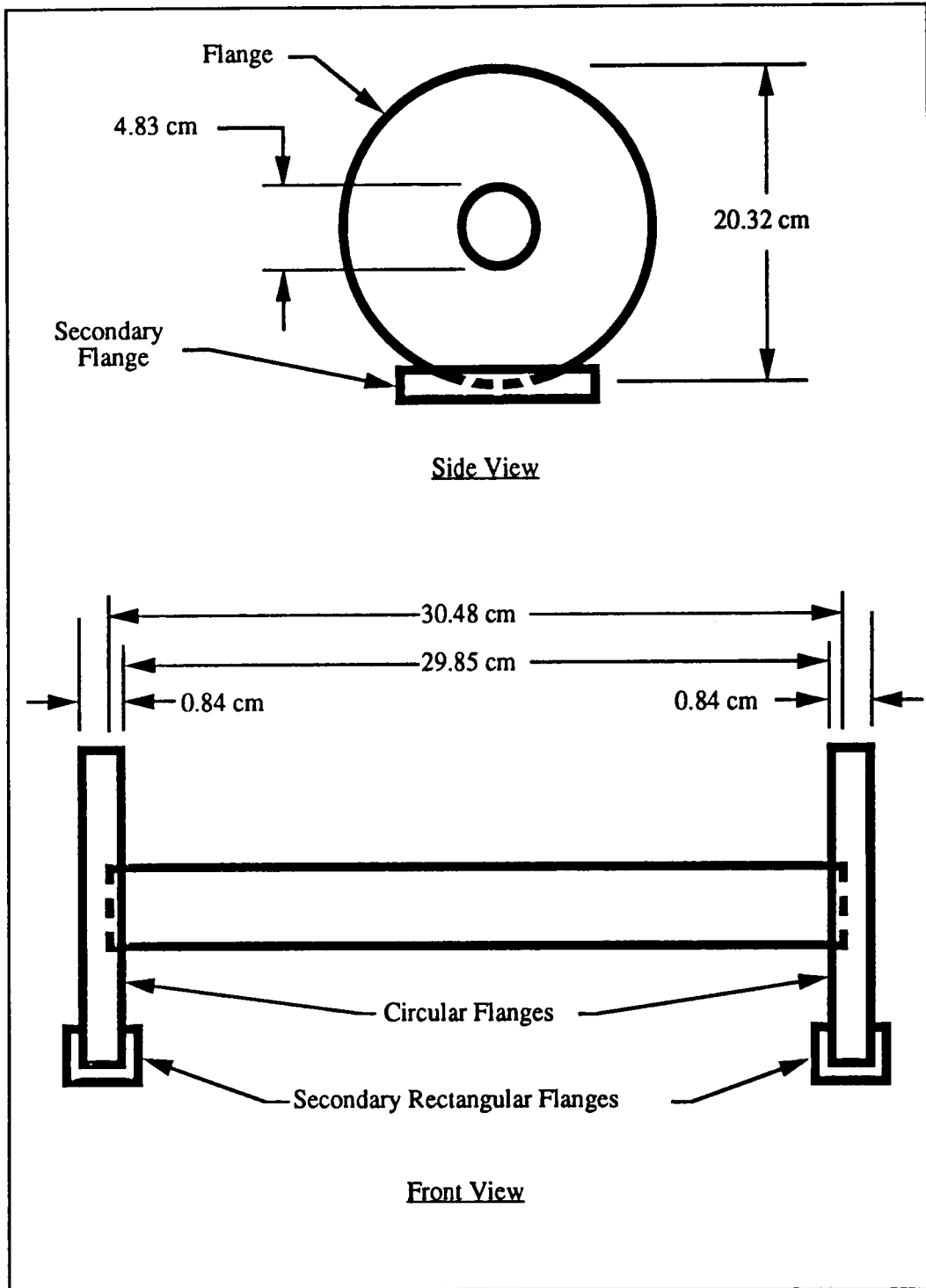
Figure 2.2 Schematic of cylinder set-up

21
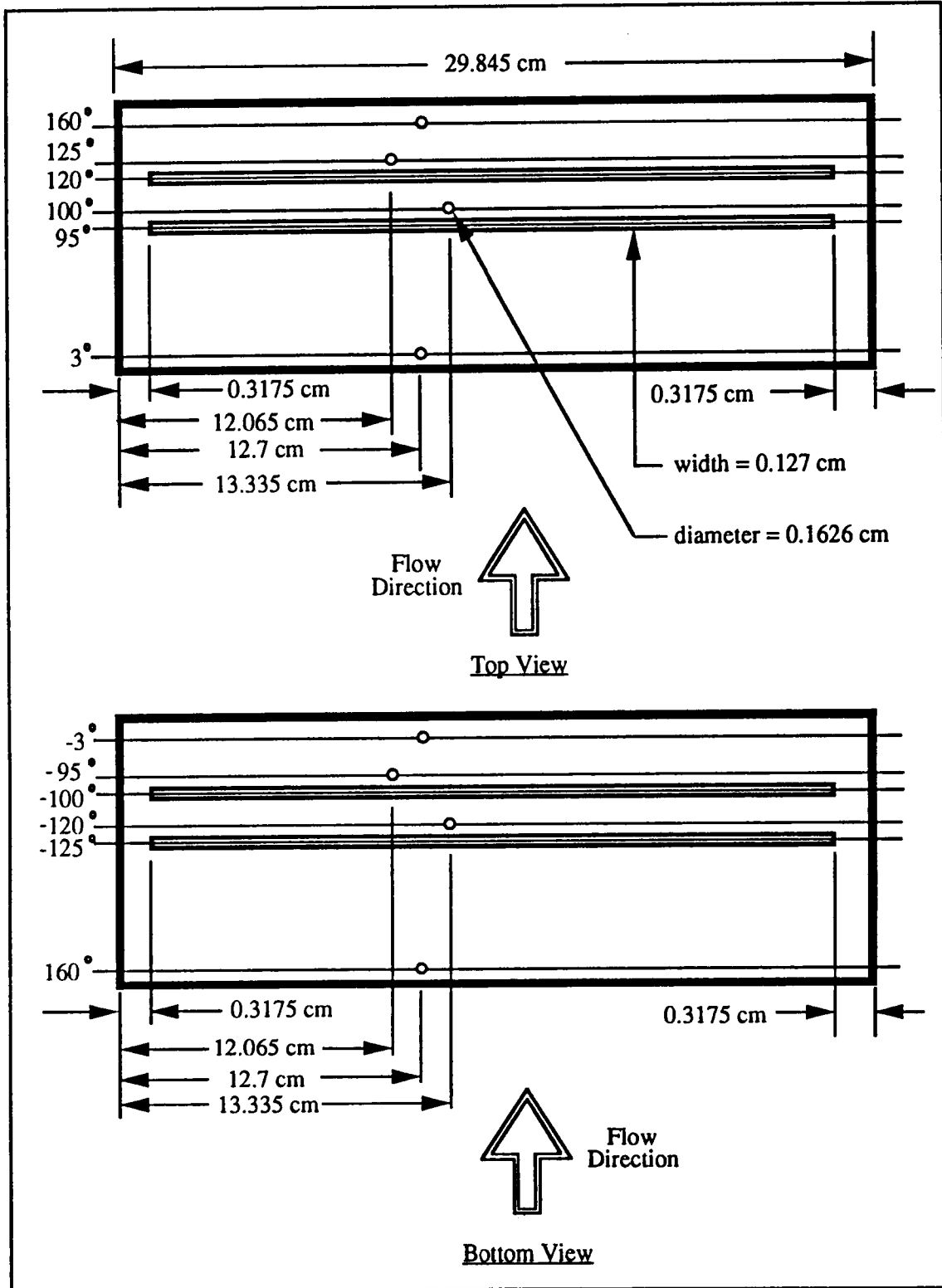
Figure 2.3   Schematic top and bottom views of cylinder
showing locations of suction slots and dye
injection holes

22

at 95°, 120°, 180°, -120°, and -95° as shown in Figure 2.4, and are referred to as slots #1 through #5 respectively as outlined in Table 2.1.

Table 2.1 Suction slit numbers and locations

Slit Number	Location (degrees)
1	95
2	120
3	180
4	-120
5	-95

At the early stages of testing, PVC piping was used to constitute the cylinder model. Slots were cut at the specified streamwise locations along the span with precision cutting machines, with the hollow piping being intact. Since the piping was still intact when the slots were fabricated, the locked-up stresses within the material of the cylinder continued to relieve themselves over time and caused a strain in the streamwise direction, which eventually led to an expansion of the material causing the slot width to decrease at different locations along the span. This not only led to the reduction in slot width but also non uniformity of the width. Possibly, the material being exposed to water, further promoted the expansion (and/or warping) of the piping material.

Due to the shortfall of the PVC piping model, the Aluminum piping was chosen as the appropriate candidate. The piping was initially cut along a diameter into two halves, and *before* fabrication of the slots, supporting structures along the locations of the slots were attached to the inside of the hollow cylindrical halves. These supporting structures are essentially circular flanges which have an outside diameter of 4.32 cm
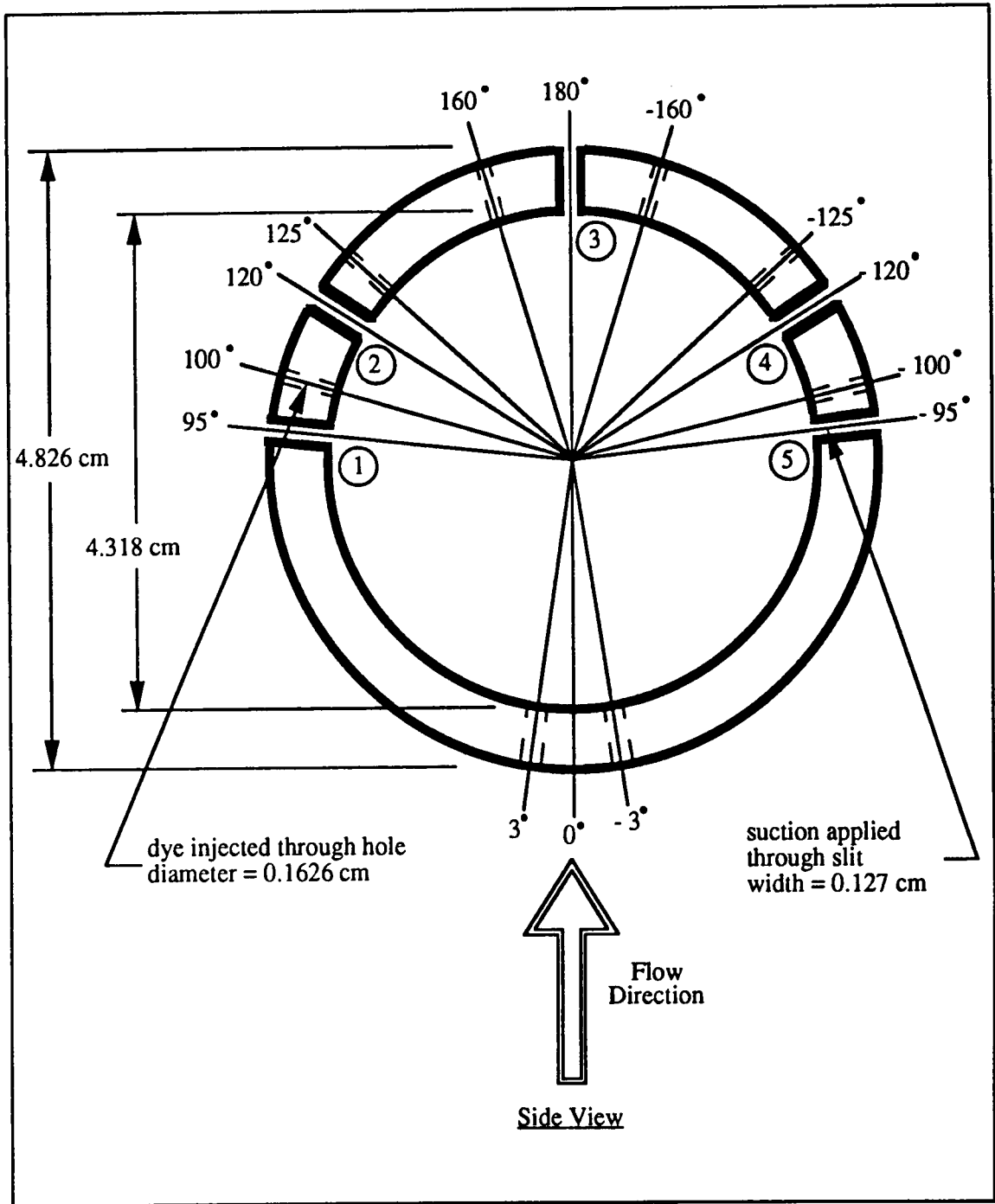
Figure 2.4 Schematic side-view of cylinder

24
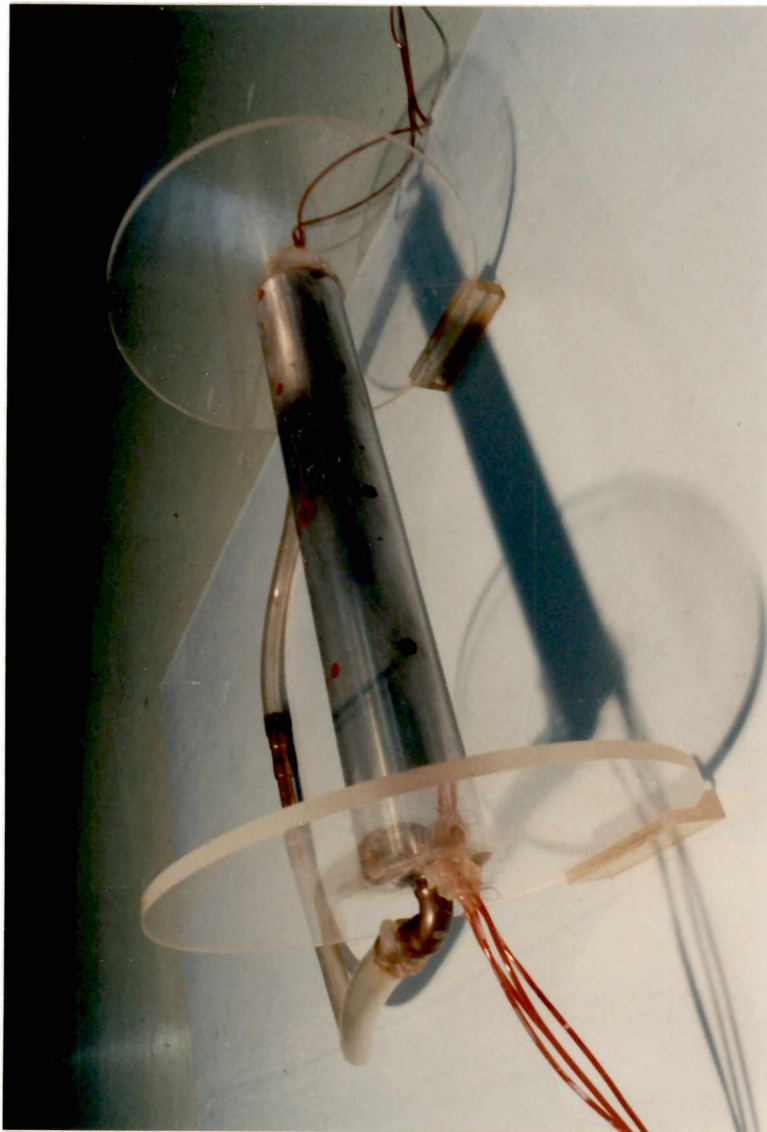
Figure 2.5 Cylinder set-up

25

(1.7 in.), an inside diameter of 3.56 cm (1.4 in.), and a thickness of 0.64 cm (0.25 in.). Circles of diameter 0.64 cm (0.25 in.) were cut on the perimeter of these flanges at locations (i.e. at various angles) where the flanges overlap the suction slots to accomadate uninterrupted passage of the incoming sucked fluid so as to keep uniformity of the sucked mass through the slots (see Figure 2.5). Three of these supporting flanges were used, centered at distances of 7.6 cm (3.0 in.), 15.2 cm (6.0 in.), and 22.9 cm (9.0 in.) respectively from either end of the cylinder (see Figure 2.6). The inclusion of the supporting flanges counteracted any stress caused by the fabrication of slots, and hence prevented any distortion in the material and maintained the slot width at the desired level throughout the course of the experiments.

Any combination of slots may be used for purpose of suction. The undesirable slots were sealed off with thin adhesive tape. When suction is applied the water is sucked through these slots and collected in the inner part of the hollow cylinder which then is transported to a flow meter by means of two 0.64 cm (0.25 in.) id vinyl tubes attached to the sides of the cylinder. Hence the rate of suction can be controlled by adjusting the flow meter to desired values. These tubes are visible in Figure 2.6, which illustrates a 3-D view of the configuration.

Dye is injected (bled) through various holes of diameter 1.625 mm (0.064 in.) located both on the upper and lower halves of the cylinder at 0°, 3°, 100°, 125°, 160°, 180°, -160°, -125°, -125°, -100°, and -3°. The holes on the upper-half surface are located between 12.07 cm (4.75 in.) and 13.34 cm (5.25 in.) from the left end of the cylinder at a lateral distance of 6.35 mm (0.25 in.) apart. The holes in the lower-half surface are also located at distances similar to the upper half, except from the right end of the cylinder. Locations of these holes in the span-wise direction and in the direction along the flow are illustrated in Figures 2.3 and 2.4 respectively. Dye is transported to these holes via tubes embedded within the hollow of the cylinder. These tubes are extended through both sides of the cylinder (see Figure 2.6) and are connected to a pressurized reservoir through which dye is bled.

§ 2.3.2 CYLINDER - FLAT PLATE CONFIGURATION

The flat plate is constructed with Plexiglas of length 60.33 cm (23.75 in.) with a rounded edge at the upstream end. The cylinder is made of PVC piping of diameter (1D) 11.43 cm (4.5 in.) and height 10.16 cm (4.0 in.), giving it a height to diameter

26
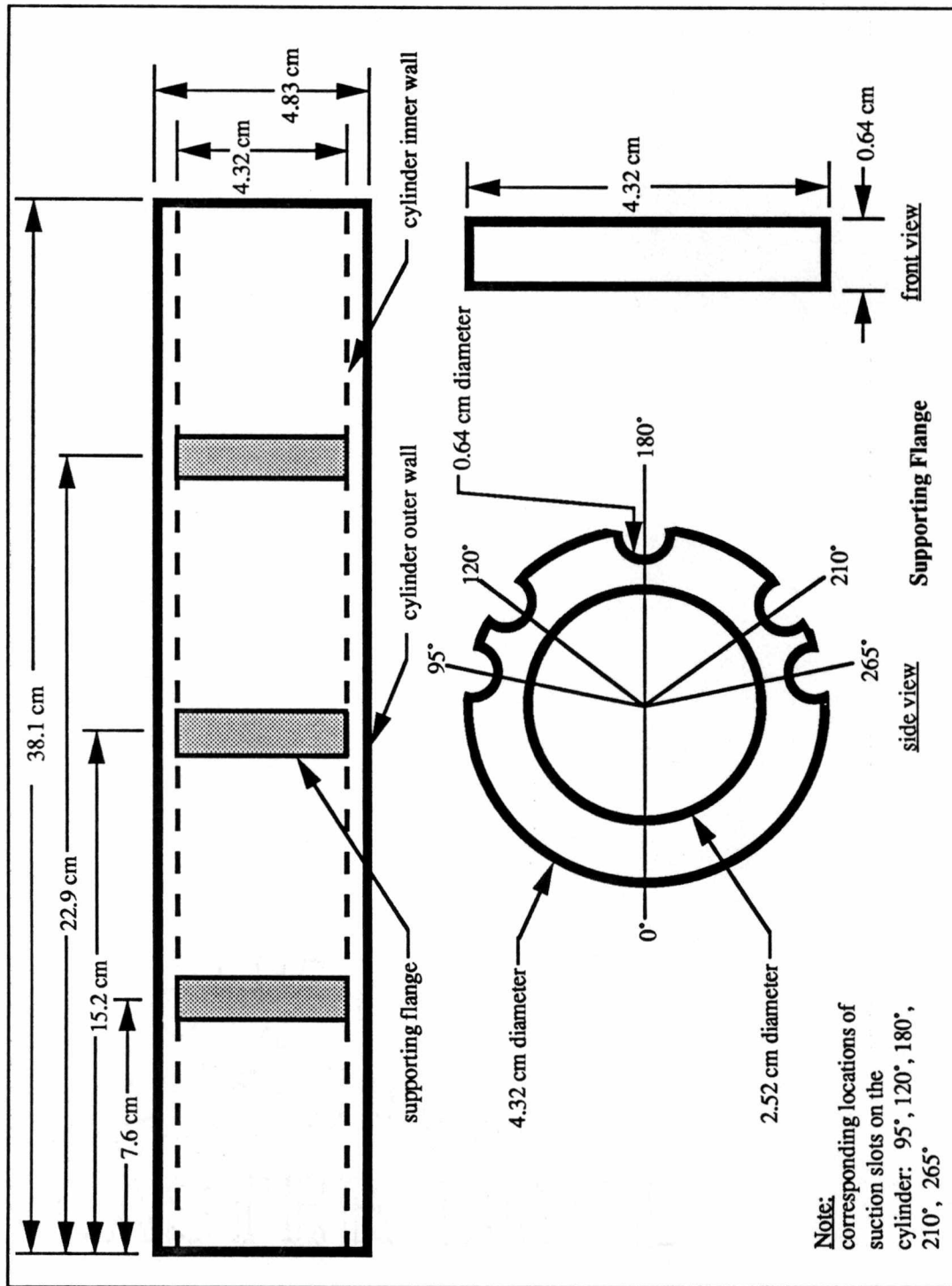
Figure 2.6 Schematic of supporting flanges and flange locations within cylinder

27

ratio, h/D = 0.89. A 11.43 cm (4.5 in.) diameter Plexiglas circular top was cut and glued on to the top of the pipe to prevent a cavity. The front of the cylinder was mounted on to the flat plate at a distance of 24.13 cm (9.5 in., 2.1 D) from the leading edge of the flat plate. The distance from the back of the cylinder to the trailing edge of the flat plate is 24.77 cm (9.75 in., 2.17 D).

Three suction holes of diameter 3.175 mm (0.125 in., 0.28 D) are drilled immediately in front of the cylinder at a radius slightly larger than that of the cylinder, at lateral distances of 1.75 cm (0.69 in., 0.153 D) apart. Three more rows of holes are drilled in a similar fashion at the same lateral distances apart at radii 7.47 cm (2.94 in., 0.653 D), 9.22 cm (3.63 in., 0.807 C), and 10.97 cm (4.32 in., 0.96 C) respectively from the center of the cylinder (refer to Figure 2.7).

A rectangular reservoir was built with Plexiglas and attached to the 'under part' of the flat plate directly below the holes and encompasses the entire region of the holes. A secondary reservoir was also built and attached to the primary for reasons discussed earlier (see Figure 2.8). A vinyl tube of inside diameter 0.64 cm (0.25 in.) carries the sucked water to a flowmeter which will control the volume of water sucked. A similar rubber tube carries the water to a drain.

§ 2.3.3 STREAMLINED BODY - FLAT PLATE CONFIGURATION

A wing with a NACA 0012-64 airfoil was chosen to be the streamlined body, together with a flat plate, to simulate a wing - body junction configuration. The wing which is made out of aluminum and has a span length (1C) of 30.48 cm (12.0 in.) and a chord length of 18.10 cm (7.125 in.) giving it a span to chord ratio of b/c = 1.68. The flat plate is fabricated with Plexiglas. The wing was mounted vertically on top of a flat plate of total length 50.47 cm (19.87 in.), as shown in Figure 2.9. The flat plate has a knife edge at its upstream end. The distance from the upstream end of the flat plate to the wing leading edge is 30.48 cm (12.0 in., 1.68 c) while the distance from the wing trailing edge to the downstream end of the flat plate is 1.91 cm (0.75 in., 0.105 c).

The wing is pivoted about its quarter-chord and is free to be side-sliped from its mean position which is aligned with the on-coming flow. The side-slip angle, ß can be varied from zero to +90° or -90°.

28

diameter = 0.3175 cm
(= 0.0278 D)

11.43 cm
(1 D)

1.75 cm
(0.1533 D)

Flow Direction

1.75 cm
(0.1533 D)

Top View

Flow Direction

5.25 cm
(0.46 D)

10.16 cm
(0.889 D)

24.13 cm
(2.111 D)

24.765 cm
(2.167 D)
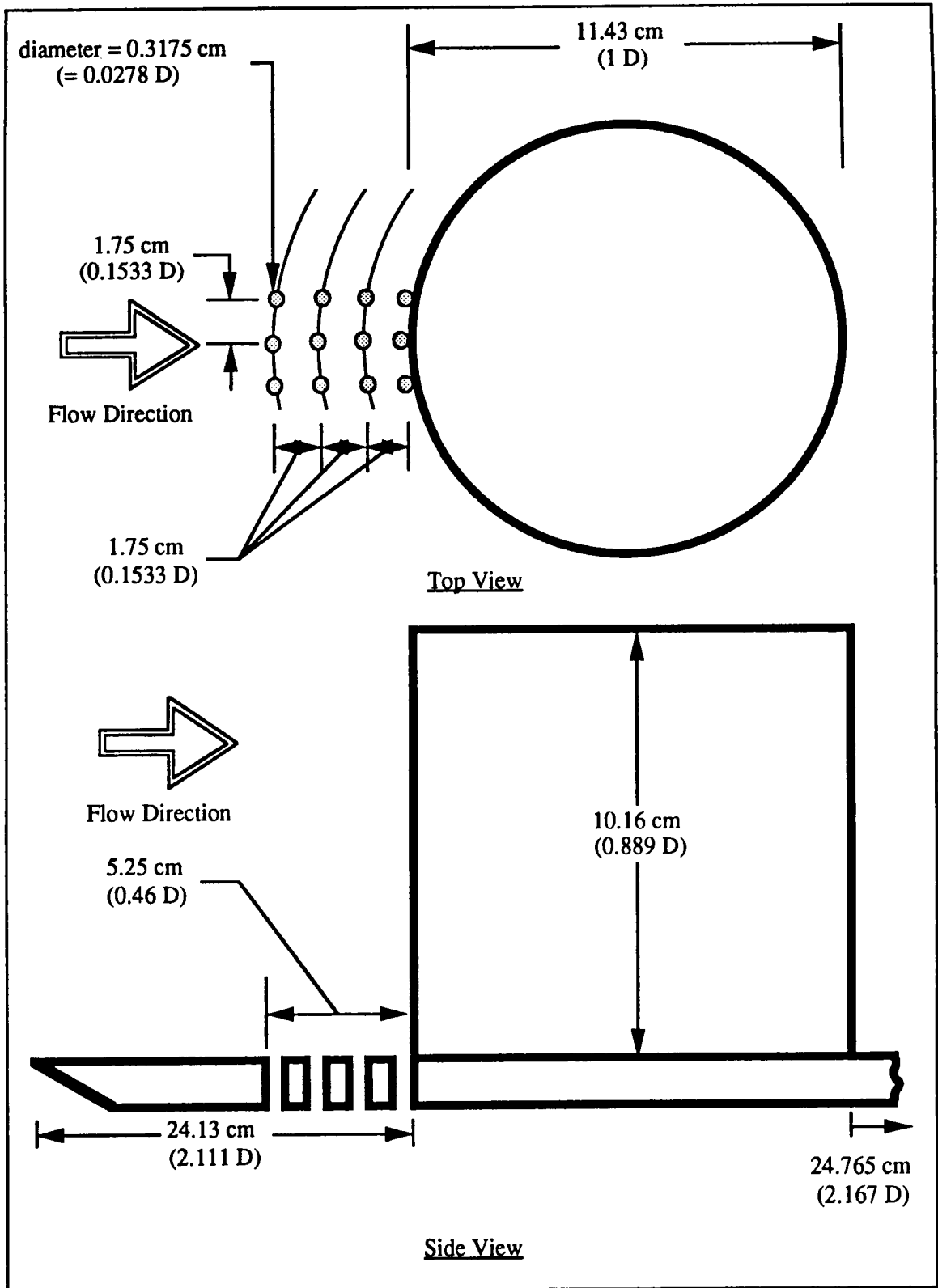
Side View

Figure 2.7 Schematic top and side views of cylinder-flat plate junction set-up

Figure 2.8 Cylinder - flat plate junction set-up
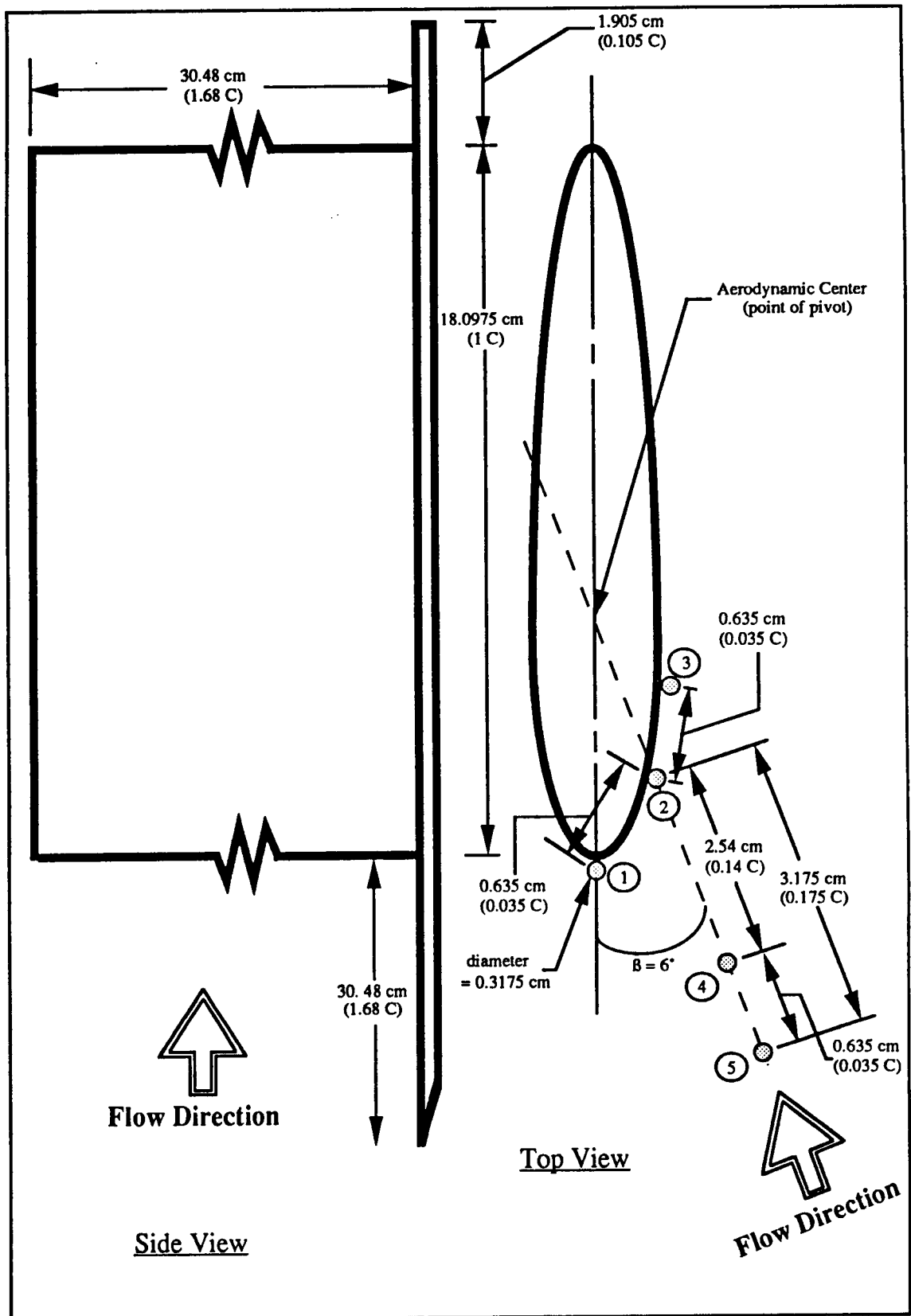
Figure 2.9 Schematic top and side view of wing - flat plate junction

31
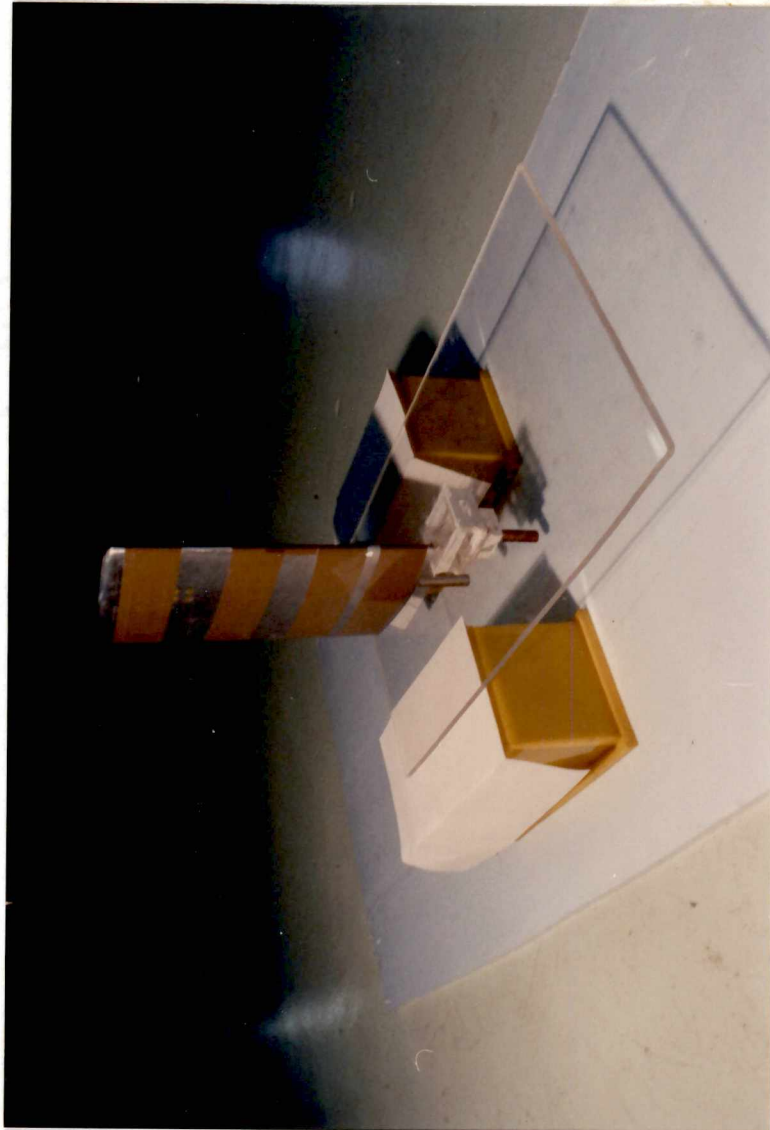
Figure 2.10 Wing - flat plate junction set-up

32

Suction is applied through any combination of holes of diameter 3.175 mm (0.125 in., 0.017 C) placed in various locations on the flat plate. The water sucked through these holes is collected in a reservoir which is attached to the 'under side' of the flat plate (see Figure 2.10). It is then drained onto another smaller reservoir from which a 0.64 cm (0.25 in.) id vinyl tubing carries the water to a flow meter which measures the flow rate. The inclusion of the reservoirs ensures that the rate of suction of the water is steady.

When the wing is aligned with the on-coming flow (i.e. at its mean position with no side-slip), suction may be applied through one, all, or any combination of holes #1, #3, #4, and #5. Similarly, when the wing is at a side-slip angle of ß = 6°, holes #1, #2, #3, #4, and #5 may be utilized. Holes #4 and #5 are aligned such that they are in the same line extension of the mean chord of the airfoil when the wing is set at a side-slip angle of 0°. These holes are placed 6.35 mm (0.25 in., 0.035 C) from each other between the region where separation is observed to occur when the wing is aligned with the on-coming flow. At ß = 0°, hole #4 is 1.91 cm (0.75 in., 0.105 C) from the wing leading edge and hole #5 is 2.54 cm (1.0 in., 0.14 C) from the leading edge. Hole #1 is set at the stagnation point at the leading edge of the wing when the wing is set at a side slip angle of $\beta = 6°$. Holes #2 and #3 are aligned along the periphery of the wing at $\beta = 6°$, hole #2 being 6.35 mm (0.25 in., 0.035 C) from hole #1 and hole #3 being 6.35 mm (0.25 in., 0.035 C) from hole #2.

§ 2.3.4   FORWARD-SWEPT WING

The wing used has a NACA 0012-64 airfoil and is fabricated with aluminum. It has a rectangular plan form and has a sweep-forward angle of 30°. The semi-span length at the leading edge is 25.4 cm (10.0 in.) and at the trailing edge is 34.75 cm (13.68 in.). The chord length (1C) is 16.19 cm (6.375 in.) and remains constant along the span. The forward-swept wing configuration was chosen since the model was already fabricated and readily available, and required minimum adjustments and additions to make it suitable for the current study.

Since the exact strategic location was not known prior to actual application of suction, suction was confined to a 'circular' area (encompassing a large horn vortex prevalent on the wing) comprised of 37 small holes of diameter 1.626 mm (0.064 in.,

diameter = 0.1626

16.1925

6.985

0.9525

0.9525

2.699

5.08

34.747

18.415

16.034

9.347

30°

Flow Direction

Note: All dimensions are in cm
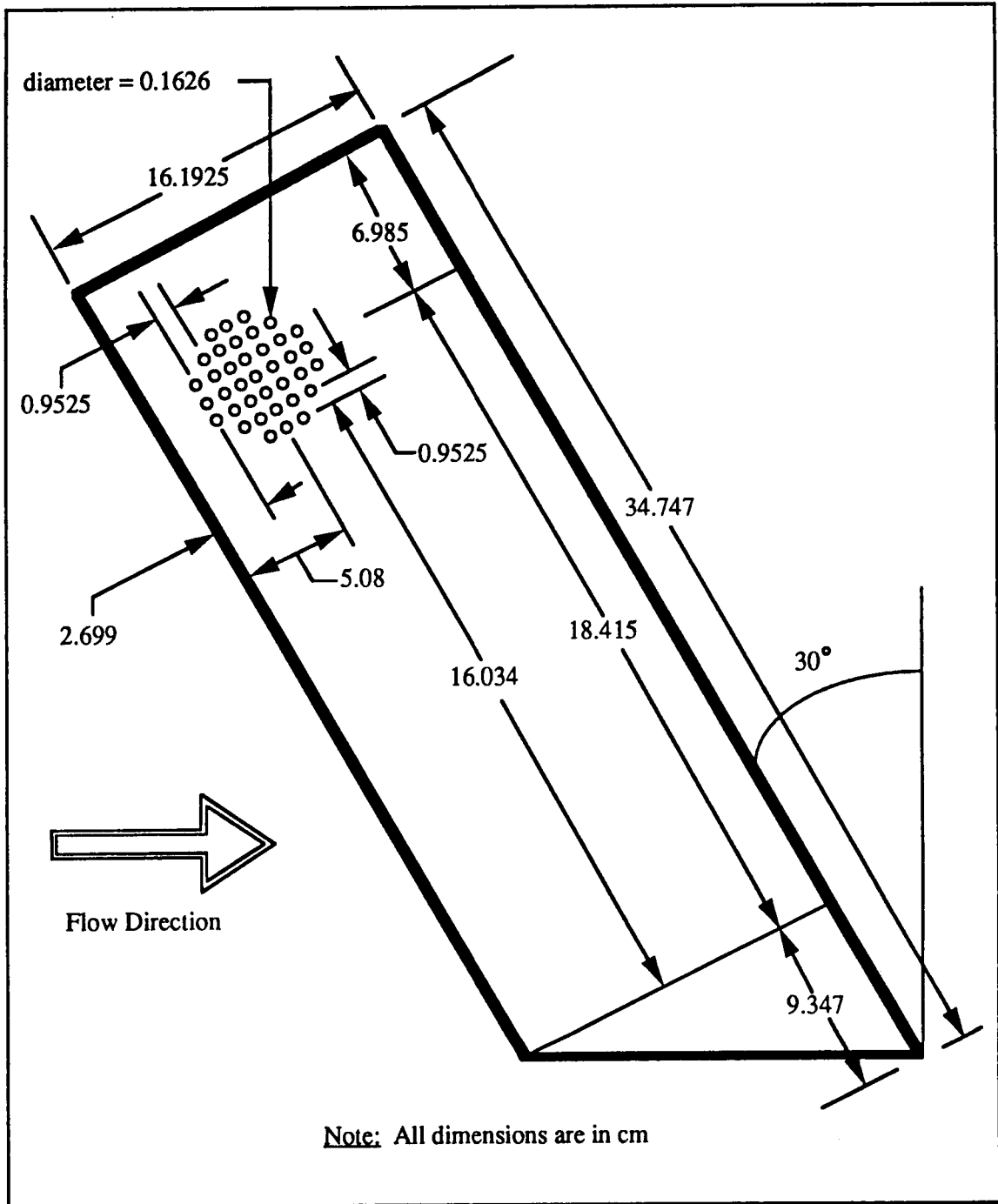
Figure 2.11 Schematic of forward-swept wing showing
hole locations through which suction was
applied

34

0.01 C), with each hole-center separated by a distance of 9.525 mm (0.375 in., 0.06 C) in all directions (see Figure 2.11). Although 37 holes were fabricated on the wing surface for the purpose of suction, in the course of the testing stage it was found that there was no need to utilize all 37 holes, and suction applied through just 5 holes was enough to accomplish the objective. The arrangement of holes are in such a way that the influence of an upstream hole on a downstream hole is avoided. Suction may be applied through any number of combinations of holes by 'opening' only the appropriate ones. The undesired holes are sealed off by means of very thin adhesive tape. The center of this 'circular' region is located 5.08 cm (2.0 in.) from the leading edge and 6.99 cm (2.75 in.) from the tip. The first 'row' of holes are at a distance of 2.699 cm (1.063 in.) from the leading edge while the last 'row' of holes are at a distance of 7.461 cm (2.938 in.) from the leading edge. The first 'column' of holes are at a distance of 4.604 cm (1.813 in.) from the tip and the last 'column' of holes are at a distance of 9.366 cm (3.688 in.) from the tip.

A diamond-shaped reservoir made of Plexiglas is attached to the bottom surface of the wing directly underneath the area where the holes are located. A secondary diamond-shaped reservoir is attached underneath the first (see Figure 2.12). Water sucked at the top surface through the holes is collected in these reservoirs and then sent to a flow meter via a 0.64 cm (0.25 in.) inside diameter vinyl tube. The amount of suction can be controlled by adjusting the flow meter to the desired volume flow rate. The water from the flow meter is then drained via another rubber tube of id 0.64 cm (0.25 in.).

§ 2.4   CASES INVESTIGATED

Various cases (i.e. running conditions with different values for the different relevant parameters like flow velocity, suction coefficient, C_Q, etc.) involving the several configurations were investigated.

In the case of the cylinder, the flow velocity, V_∞ was set at 3.22 cm/sec (1.27 in./sec, Re_D = 1,550), 6.06 cm/sec (2.39 in./sec, Re_D = 2,910), 8.90 cm/sec (3.51 in./sec, Re_D = 4,280), and 11.74 cm/sec (4.634 in./sec, Re_D = 5,650). At each of the above velocity setting, the model was tested at conditions with no suction (suction coefficient, C_Q = 0), with a suction volume rate of 0.0105 liter/sec (10.5 cm^3/sec, 10 gal/hr) [C_Q = 0.023 @ V_∞ = 3.22 cm/sec, C_Q= 0.012 @ V_∞ = 6.06 cm/sec, C_Q =

35

Figure 2.12 Forward-swept wing set - up, NACA 0012-64

36

0.008 @ V_∞ = 8.90 cm/sec, C_Q= 0.006 @ V_∞ = 11.74 cm/sec], and with a suction volume rate of 0.021 liter/sec (21.0 cm³/sec, 20 gal/hr) [C_Q = 0.046 @ V_∞ = 3.22 cm/sec, C_Q = 0.024 @ V_∞ = 6.06 cm/sec, C_Q = 0.016 @ V_∞ = 8.90 cm/sec, C_Q= 0.012 @ V_∞ = 11.74 cm/sec]. Also, for every possible combination of the two cases described above (i.e. change in velocity and change in suction rate), various combination of slots were utilized to apply suction. The combinations of slots used at any given time are as follows: #1; #1,#2; #1,#2,#3; #1,#2,#3,#4; #1,#2,#3,#4,#5; #1,#2,#4,#5; and #1,#5.

Both the cylinder - flat plate configuration and streamlined body - flat plate configuration were also run at the velocities specified above. The suction rates, as in the case of the cylinder, were 0, 10 gal/hr, and 20 gal/hr. At every combination of the various velocities and suction rates, different combination of holes were utilized to apply suction. The various combinations of holes used together with the observed results are discussed in § 3.2.1 and § 3.2.2.

The swept wing configuration was tested at angles of attack of 30° and 40°. The velocity and suction rates were varied as described for the cases discussed above. Various holes were utilized to apply suction. The specificity of these holes are outlined in § 3.3.

CHAPTER III
RESULTS AND ANALYSES

In this chapter, the results obtained from the various configurations investigated with and without suction are presented both in tabular form and by means of still photographs, and analyses pertaining to the various cases are discussed. Wherever feasible, the gathered data is reduced and presented in the form of two- and three-dimensional graphs for easier analyses and conclusions. The first section in this chapter is devoted to presentation and analysis of flow separation results from experiments conducted on the cylinder model. The second section is a qualitative look at the results from the two, body - flat plate junction configurations, namely the cylinder - flat plate model and the streamlined body - flat plate model. The final section provides the results and analysis from the swept-forward wing at higher angles of attack, again with a qualitative perspective in mind.

§ 3.1 FLOW SEPARATION AROUND CYLINDER

Experiments with the cylinder model were conducted at the following free-stream velocities, V_∞'s: 3.22 cm/s (1.27 in./s), 6.06 cm/s (2.39 in./s), 8.91 cm/s (3.51 in./s), and 11.75 cm/s (4.62 in./s). The corresponding free-stream Reynolds numbers based on the cylinder diameter, Re_D, are respectively 1550, 2910, 4280, and 5650. At these moderately low Reynolds numbers, laminar flow over the cylinder is maintained. Typically, for a cylinder, depending on various factors like surface roughness, etc., transition occurs between $Re = 1 \times 10^5 - 9 \times 10^5$.

Angles of separation, θ's, at various above mentioned free-stream velocities, for the cases of 'no suction', and suction through the following combinations of slots: #1; #1,2,3; #1,2,3,4; #1,2,3,4,5; #1,2,4,5; #1,5 are presented in Tables 3.1 and 3.2. Table 3.1 tabulates the results for the case with a total suction quantity, $Q = 10.5$ cm^3/sec (0.64 in.^{3}/sec, 10 gal/hr), while Table 3.2 outlines the results for the case with $Q = 21.0$ cm^3/sec (1.28 in.^{3}/sec, 20 gal/hr).

With the absence of suction, the natural flow separation over the 4.83 cm (1.9 in). diameter aluminum cylinder at a lower Reynolds number, $Re_D = 1550$, was observed to occur at an angle of separation, $\theta_L = 93°$ on the lower half of the cylinder, and at

Table 3.1 Separation angles on cylinder for different free-stream velocities and active suction slots at a total suction quantity, $Q = 10.5$ cm^3/sec (0.64 in^3/sec, 10 gal/hr)

Free Stream Velocity, V_∞ [cm/sec (in./sec)]	Separation Angle, Θ [degrees]		Suction Slots Open
	Uppper Half	Lower Half	
3.22 (1.27)	95°	-93°	No Suction
6.06 (2.39)	92°	-88°	
8.91 (3.51)	87°	-85°	
11.75 (4.62)	83°	-80°	
3.22 (1.27)	101°	-88°	1
6.06 (2.39)	96°	-85°	
8.91 (3.51)	93°	-82°	
11.75 (4.62)	90°	-77°	
3.22 (1.27)	114°	-88°	1,2,3
6.06 (2.39)	109°	-87°	
8.91 (3.51)	104°	-85°	
11.75 (4.62)	101°	-83°	
3.22 (1.27)	105°	-100°	1,2,3,4
6.06 (2.39)	101°	-93°	
8.91 (3.51)	95°	-85°	
11.75 (4.62)	92°	-80°	
3.22 (1.27)	107°	-107°	1,2,3,4,5
6.06 (2.39)	103°	-103°	
8.91 (3.51)	100°	-95°	
11.75 (4.62)	95°	-90°	
3.22 (1.27)	109°	-110°	1,2,4,5
6.06 (2.39)	104°	-105°	
8.91 (3.51)	98°	-95°	
11.75 (4.62)	94°	-92°	
3.22 (1.27)	105°	-120°	1,5
6.06 (2.39)	99°	-110°	
8.91 (3.51)	95°	-102°	
11.75 (4.62)	93°	-95°	

Table 3.2 Separation angles on cylinder for different free-stream velocities and active suction slots at a total suction quantity, $Q = 21$ cm^3/sec (1.28 in.^{3}/sec, 20 gal/hr)

Free Stream Velocity, V_∞ [cm/sec (in./sec)]	Separation Angle, θ [degrees]		Suction Slots Open
	Uppper Half	Lower Half	
3.22 (1.27)	95°	- 93°	No Suction
6.06 (2.39)	92°	- 88°	
8.91 (3.51)	87°	- 85°	
11.75 (4.62)	83°	- 80°	
3.22 (1.27)	105°	- 94°	1
6.06 (2.39)	100°	- 90°	
8.91 (3.51)	96°	- 83°	
11.75 (4.62)	91°	- 80°	
3.22 (1.27)	116°	- 97°	1,2,3
6.06 (2.39)	110°	- 91°	
8.91 (3.51)	105°	- 87°	
11.75 (4.62)	102°	- 85°	
3.22 (1.27)	105°	- 102°	1,2,3,4
6.06 (2.39)	101°	- 95°	
8.91 (3.51)	96°	- 90°	
11.75 (4.62)	90°	- 87°	
3.22 (1.27)	108°	- 110°	1,2,3,4,5
6.06 (2.39)	103°	- 105°	
8.91 (3.51)	100°	- 98°	
11.75 (4.62)	94°	- 93°	
3.22 (1.27)	110°	- 112°	1,2,4,5
6.06 (2.39)	104°	- 105°	
8.91 (3.51)	100°	- 96°	
11.75 (4.62)	95°	- 93°	
3.22 (1.27)	111°	- 123°	1,5
6.06 (2.39)	103°	- 116°	
8.91 (3.51)	98°	- 109°	
11.75 (4.62)	94°	- 106°	

$\theta_U = 95°$ on the upper half. At a higher Reynolds number, $Re_D = 5650$, $\theta_L = 80°$, and $\theta_U = 83°$. The difference in separation angles on the lower and upper halves may have been caused by the experimental limitation in accurately orienting the model such that flow conditions are perfectly symmetric both on the top and bottom halves of the horizontal cylindrical model (the model itself may characterize slight imperfections, in that, the alignment of the cylinder may not have been exactly parallel to the lower tunnel wall, and perpendicular to the on-coming flow). Another mechanism that may have contributed to the discrepancy is the tunnel flow speed not being uniform everywhere. External disturbances like tunnel vibrations could have also played a detrimental role. Finally, the degree of accuracy in reading the separation angle is limited to 2.5° per division. Any measure of angles less than 2.5° was eyeballed.

The location of the separation angle moved forward in the upstream sense (i.e. the value of θ reduced), with an increase in the Reynolds number (and free-stream velocity). In other words, at lower Reynolds numbers, separation was delayed to higher angles, while at higher Reynolds numbers, separation was unavoidable at lower angles. The decrease in θ with increase in Re_D (and V_∞) is observed to be a linear variation. This is consistent with results obtained in other studies.

As evident in Table 3.1 and 3.2, with the application of suction, the separation point is delayed (i.e. θ increases at varying degrees depending on the particular case (the particular combination of slots through which suction was applied)). A detailed discussion on the effect of separation for the different individual cases is presented later in this section. In general, however, the separation angles are observed to be greater for the cases with suction compared to the 'no suction' case. In other words, separation is delayed to a greater extent with suction than without suction. Once again, the variation of θ with Re_D (and V_∞) for the cases with suction is observed to be linear, with the slopes of θ vs. Re_D for the 'suction' cases approximately equaling the slope of the 'no suction' case.

Table 3.3 lists the suction slot Reynolds number, Re_S, per slot, and the suction velocity, v_s, per slot for the various cases investigated at two different total suction quantities per unit time, $Q = 10.5$ cm^3/sec (0.64 in.^{3}/sec) and $Q = 21.0$ cm^3/sec (1.28 in.^{3}/sec).

41

Table 3.3 Slot Reynolds numbers and suction velocities for various
suction quantities and combinations of suction slots
(cylinder)

Slots Open	Suction Slot Reynolds Number, Re_s / slot	Suction Velocity, v_s / slot	
		cm / sec	in. / sec
1	37.95	3.0	1.11
1, 2, 3	12.65	1.0	0.37
1, 2, 3, 4	9.49	0.75	0.28
1, 2, 3, 4, 5	7.59	0.6	0.22
1, 2, 4, 5	9.49	0.75	0.28
1, 5	18.97	1.5	0.56
Total Suction per Unit Time, Q = 10.5 cm³/ sec (0.64 in.³/ sec)			

Slots Open	Suction Slot Reynolds Number, Re_s / slot	Suction Velocity, v_s / slot	
		cm / sec	in. / sec
1	75.90	6.0	2.22
1, 2, 3	25.30	2.0	0.74
1, 2, 3, 4	18.97	1.5	0.56
1, 2, 3, 4, 5	15.18	1.2	0.44
1, 2, 4, 5	18.97	1.5	0.56
1, 5	37.95	3.0	1.12
Total Suction per Unit Time, Q = 21.0 cm³/ sec (1.28 in.³/ sec)			

For $Q = 10.5$ cm^3/sec, suction Reynolds numbers range from a high of $Re_s = 37.95$ inducing a suction velocity, $v_s = 3.0$ cm/sec (1.1 in./sec) with suction through slot #1, to a low of $Re_S = 7.59$ inducing a suction velocity, $v_s = 0.6$ cm/sec (0.22 in./sec) for the case of suction through slots #1,2,3,4,5. Similarly, at $Q = 21.0$ cm^3/sec, suction Reynolds numbers range from a high of $Re_S = 75.90$ inducing a suction velocity, $v_s = 6.0$ cm/sec (2.22 in./sec) with suction through slot #1, to a low of $Re_S = 15.18$ inducing a suction velocity, $v_s = 1.2$ cm/sec (0.44 in./sec). Since Q is kept constant, as the number of suction slots increases, both Re_S/slot and v_s/slot decrease, also evident from Table 3.3.

Suction coefficients, C_Q's, (which are based on the free-stream velocity for various Q's and V_∞'s (and Re_D's) are tabulated in Table 3.4. From the table it can be seen that for $Q = 10.5$ cm^3/sec, suction coefficients ranged from $C_Q = 0.0226$ to $C_Q = 0.006$ at $V_\infty = 3.22$ cm/sec, to $V_\infty = 11.75$ cm/sec respectively. For $Q = 21.0$ cm^3/sec, C_Q ranged from a high of 0.0452 at $V_\infty = 3.22$ cm/sec to a low of 0.0124 at $V_\infty = 11.75$ cm/sec.

Three dimensional plots describing the variations of the separation angle, θ (both on the upper and lower half of the cylinder) with both Reynolds number, Re_D and suction rate, Q, are shown in Figures 3.1 through 3.6, for all the combinations of slots through which suction was applied. From these plots, it is evident that, in general (for all cases), the separation angle increases with increasing suction rates (i.e. separation is further delayed by increasing the suction rate), and decreases with increasing Reynolds numbers (i.e. flow detaches at an earlier stage while the Reynolds number is increased).

First, let us look at cases where *unsymmetrical* suction is applied (i.e. suction is applied through slots located only on the upper half of the cylinder). Figures 3.1 and 3.2 describe the behavior of flow separation for the cases of suction through slot #1 and through slots #1, 2, 3. Since slot #1, 2, and 3 are located on the upper half of the cylinder and since suction is applied only through these slots (with the absence of suction through any of the slots in the lower half), an unsymmetrical suction pattern over the entire body of the cylinder is created. This lack of symmetry in the applied suction induces different flow patterns on the two halves of the cylinder (i.e. flow separates at different locations on the upper and lower halves). In general for these cases of non-symmetry, flow separation is observed to be delayed or attachment is

43

Table 3.4 Coefficient of suction for various velocities and Reynolds numbers
for $Q = 10.5$ cm^3/sec, and $Q = 21.0$ cm^3/sec (cylinder)

Free - Stream Velocity, V_∞		Reynold's Number, Re_D	Suction Coefficient, C_μ	
cm/sec	in./sec		$Q = 10.5$ cm^3/sec $= 1.28$ in^3/sec	$Q = 21.0$ cm^3/sec $= 0.64$ in^3/sec
3.22	1.27	1550	0.0226	0.0452
6.06	2.39	2910	0.0120	0.0240
8.91	3.51	4280	0.0082	0.0164
11.75	4.62	5650	0.0062	0.0124

44
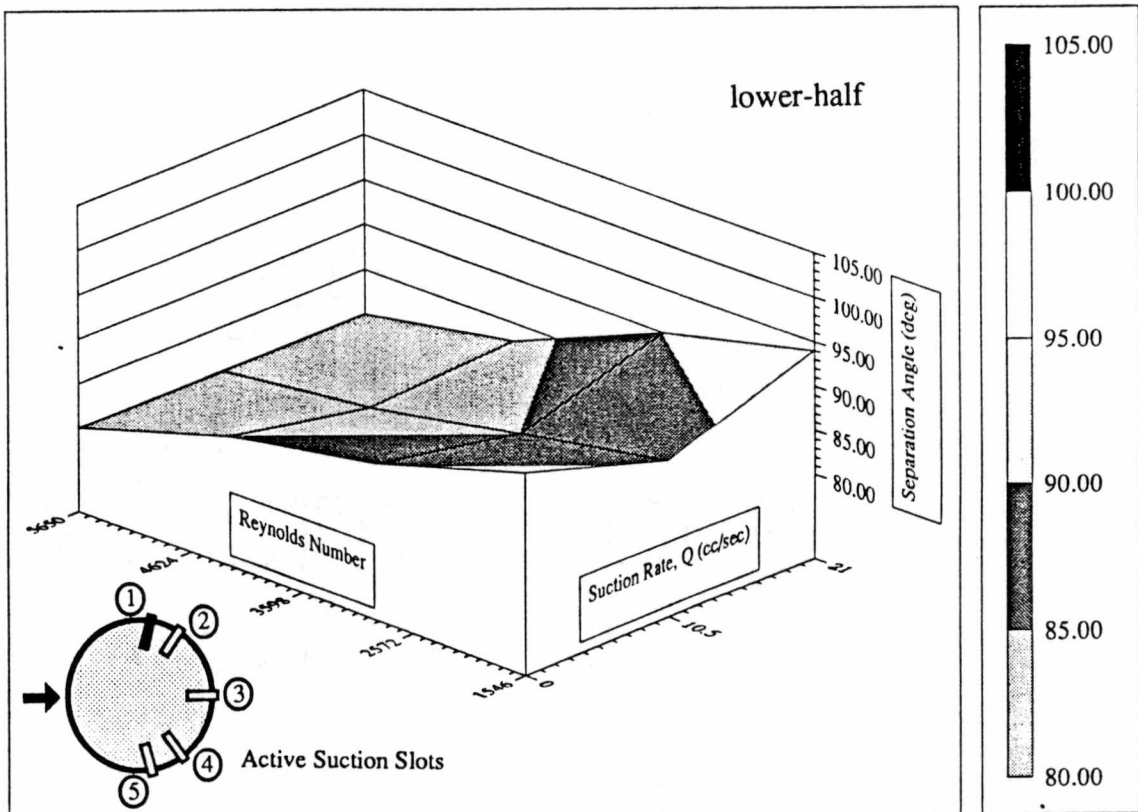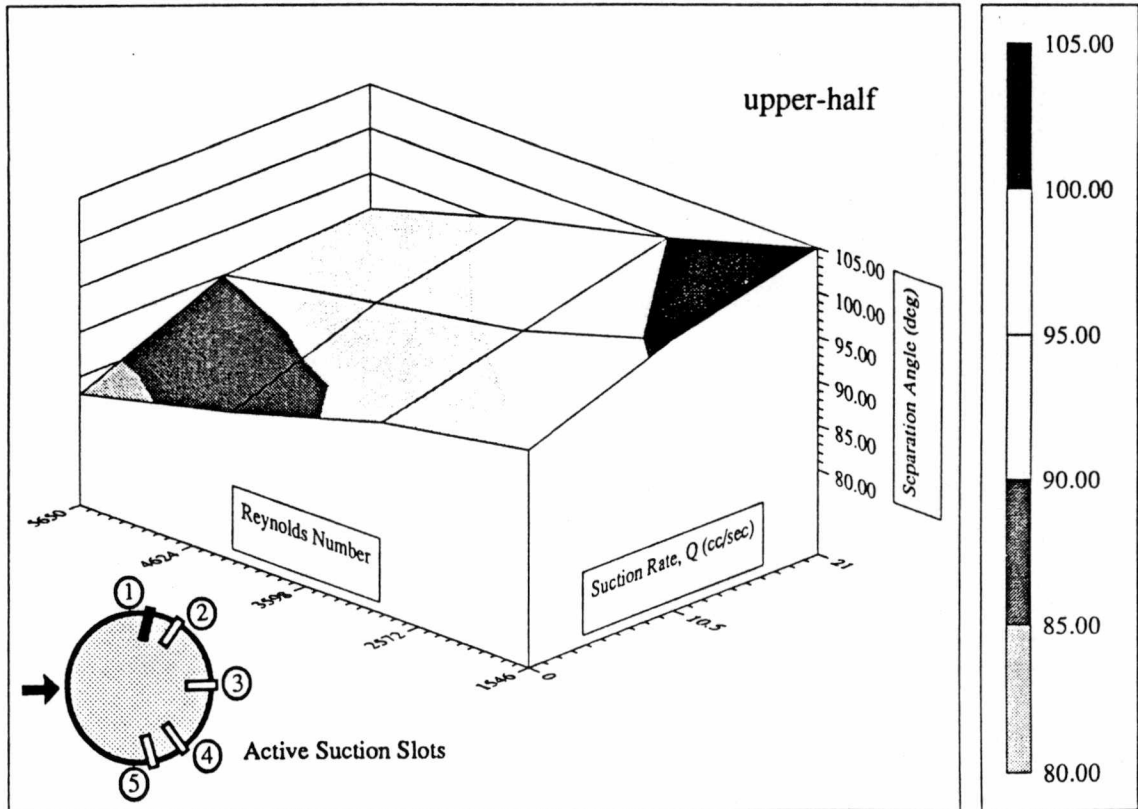
Figure 3.1 θ vs. Re_D and Q: suction through slot #1 only

45
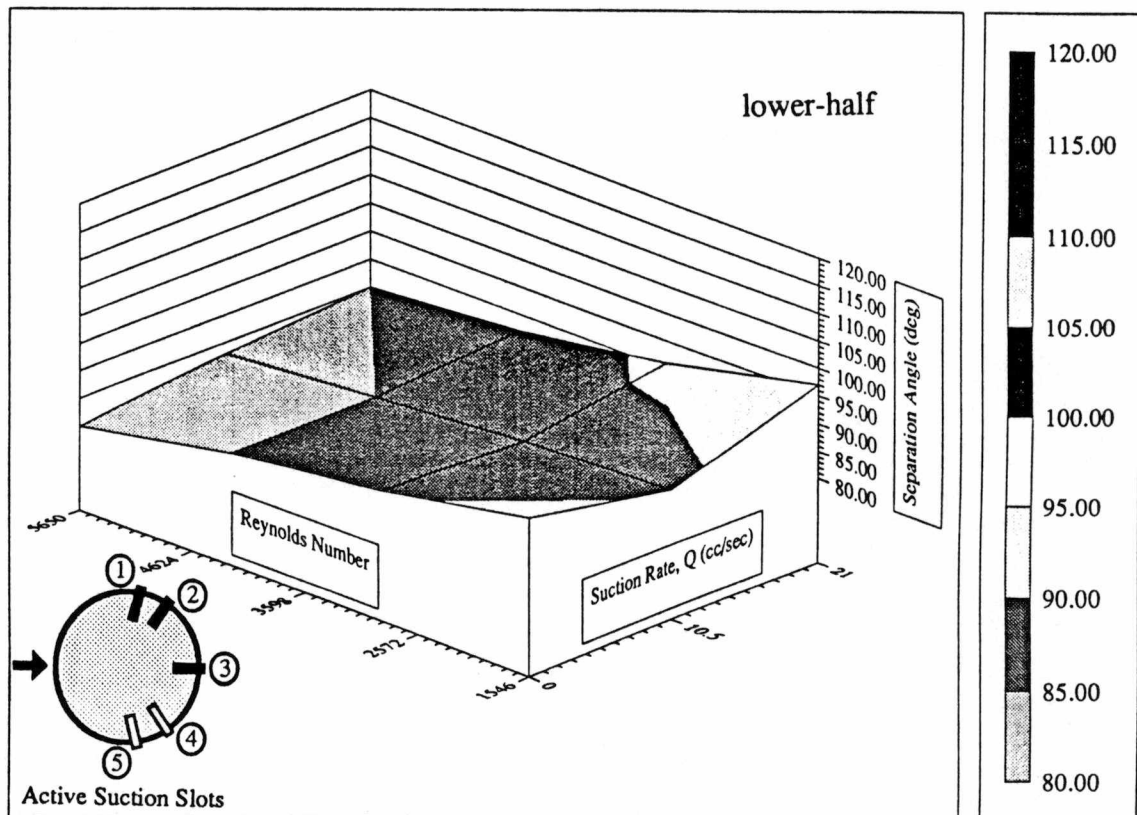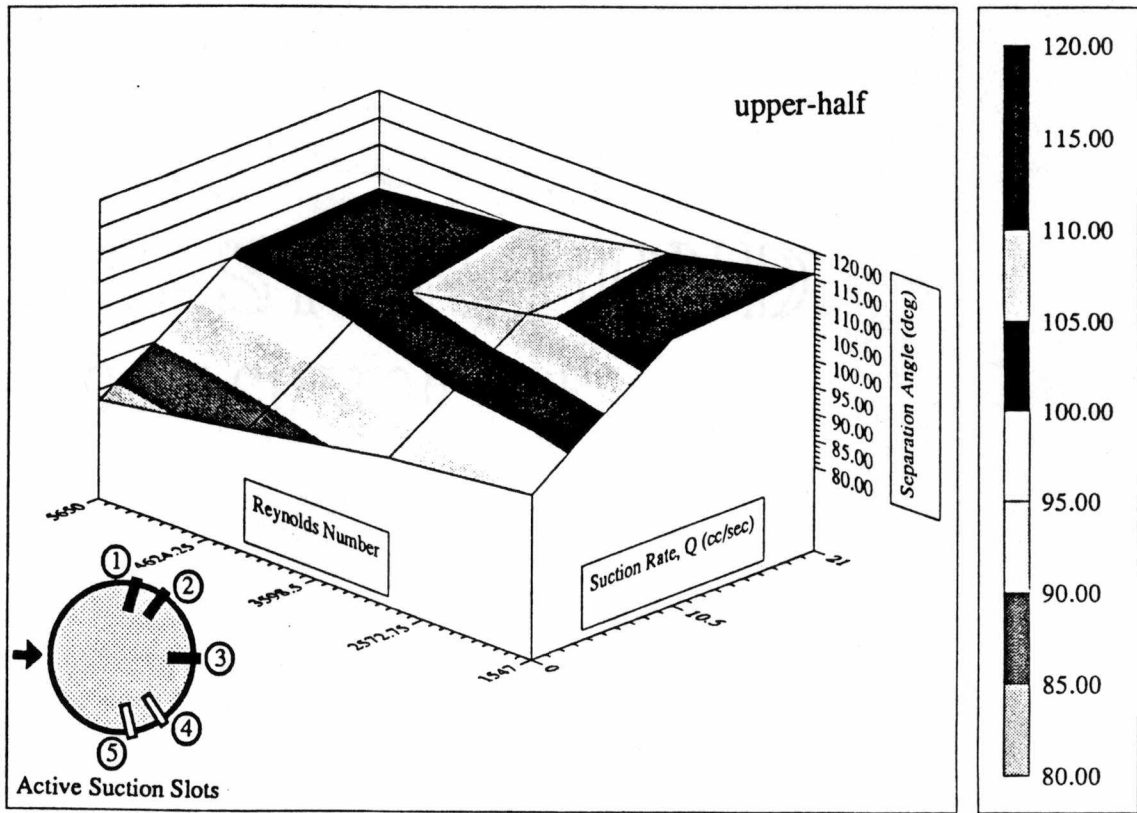
Figure 3.2 θ vs. Re_D and Q: suction through slots #1, 2, 3
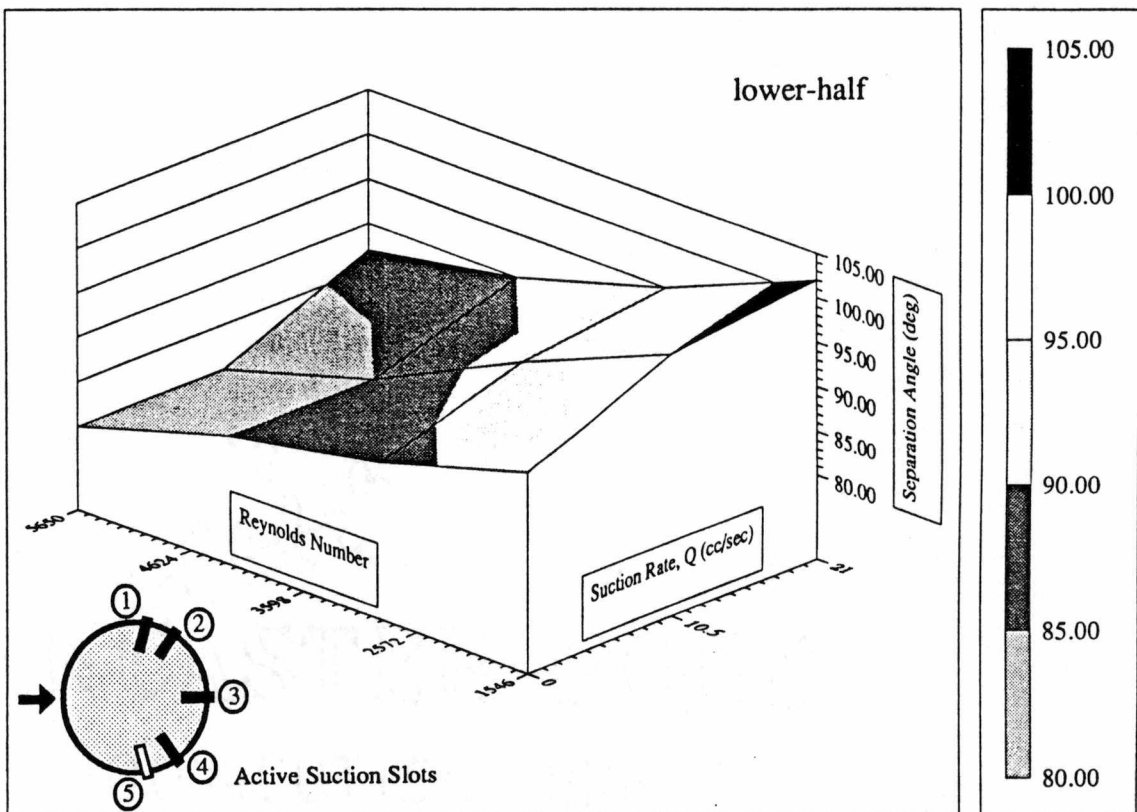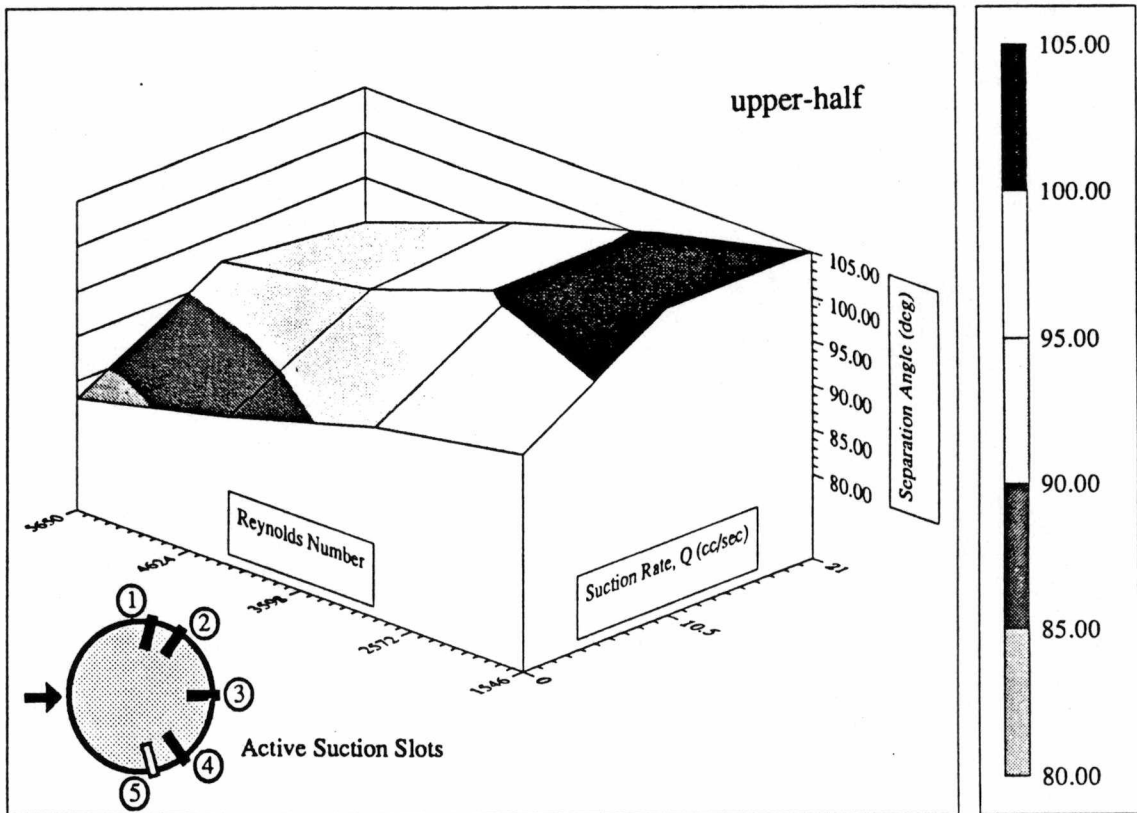
Figure 3.3 θ vs. Re_D and Q: suction through slots #1, 2, 3, 4
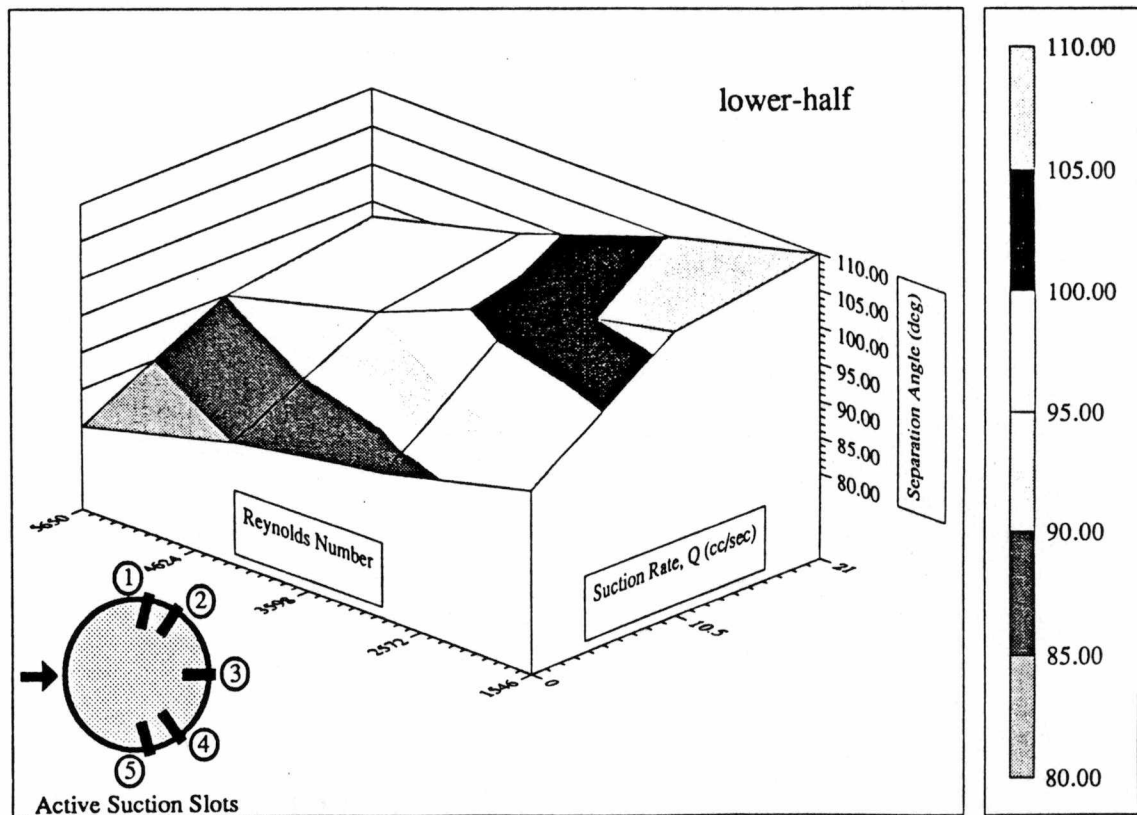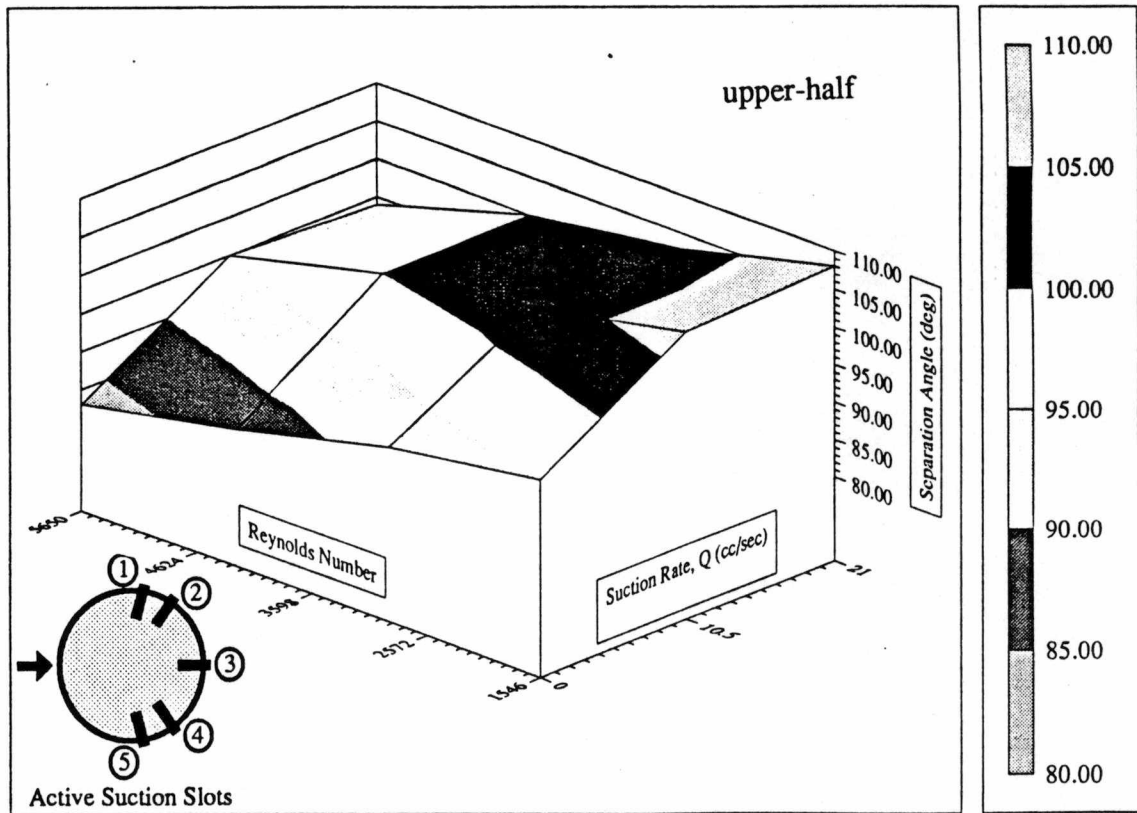
Figure 3.4 θ vs. Re$_D$ and Q: suction through slots #1, 2, 3, 4, 5
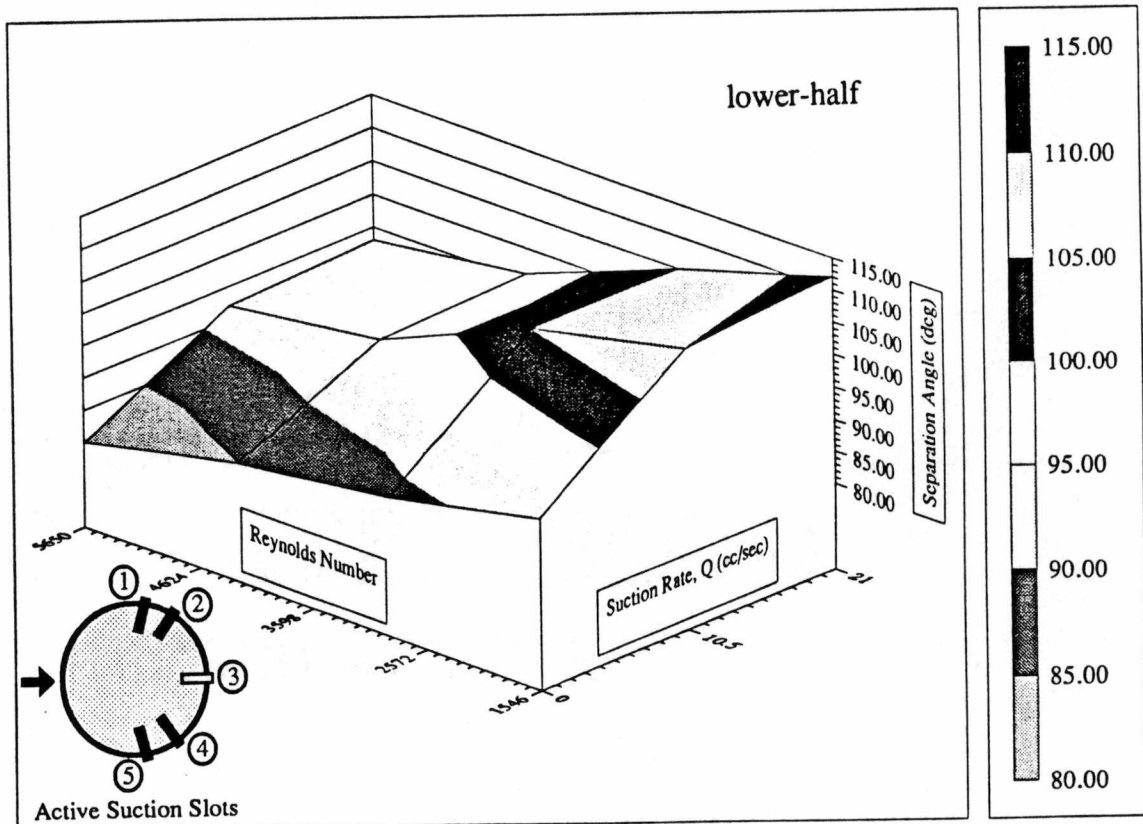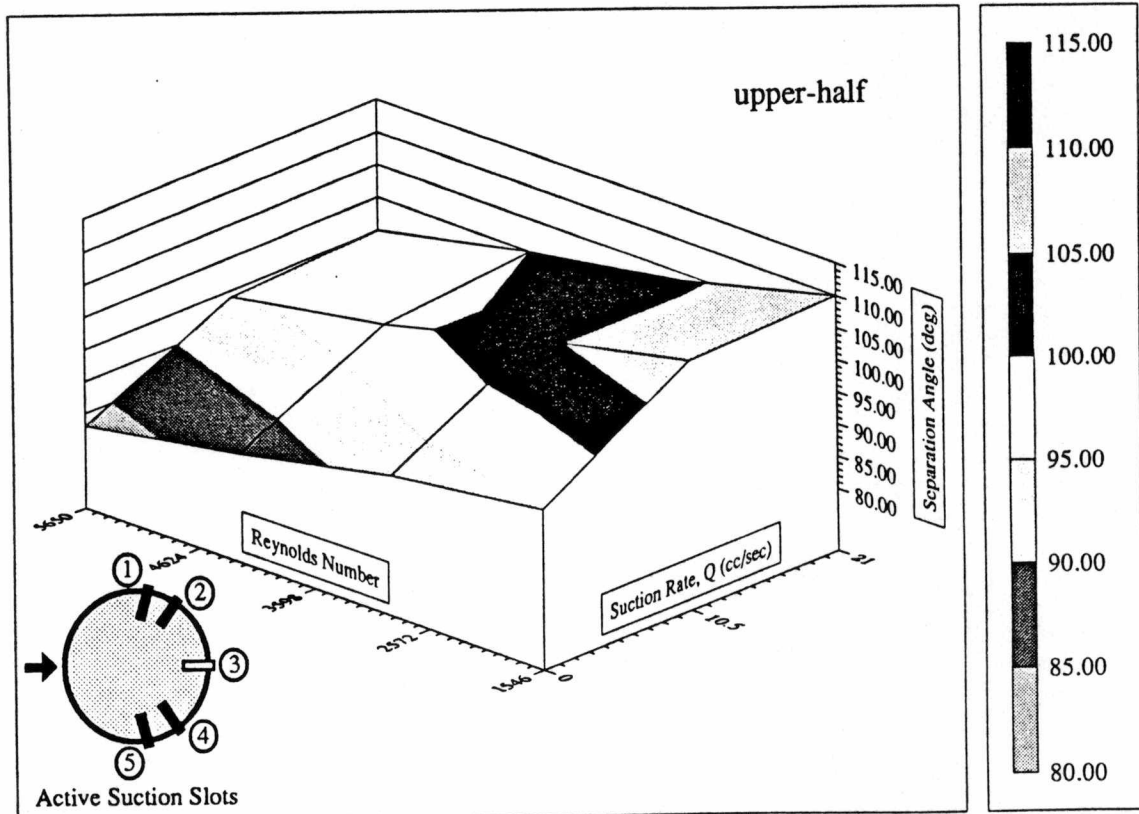
48

Figure 3.5 θ vs. Re$_D$ and Q: suction through slots #1, 2, 4, 5

49
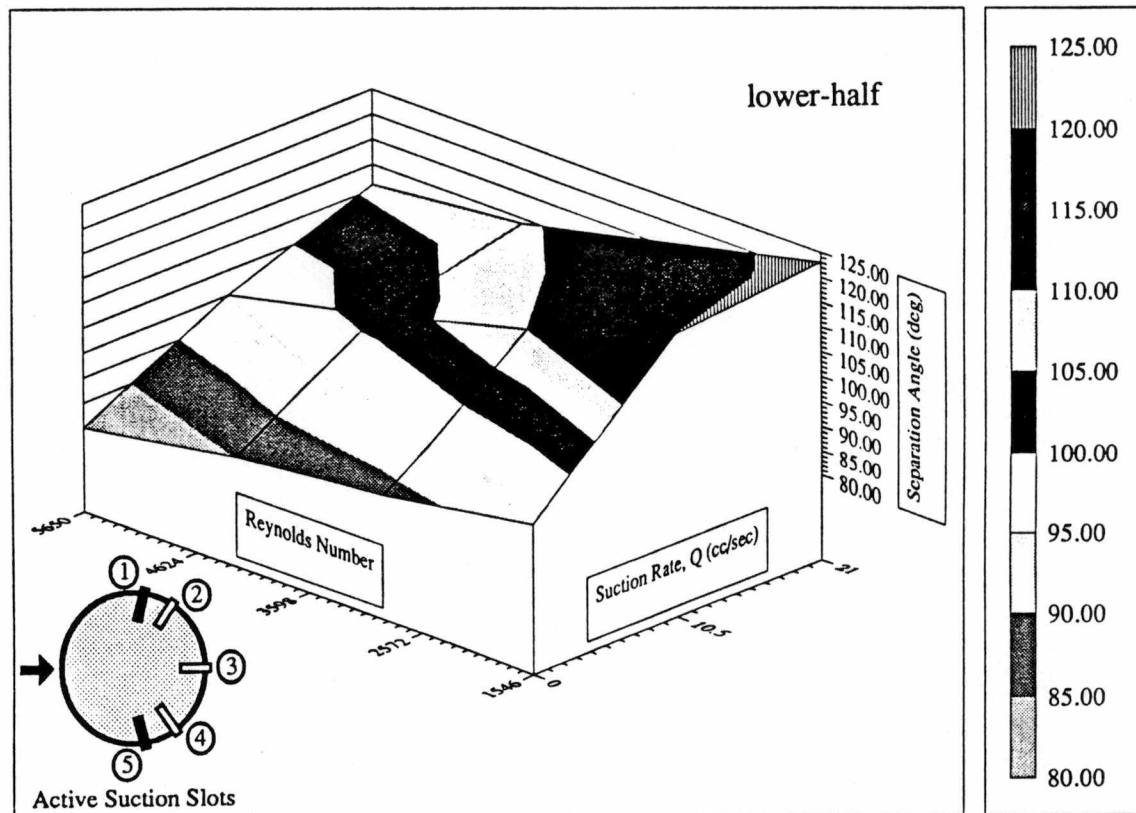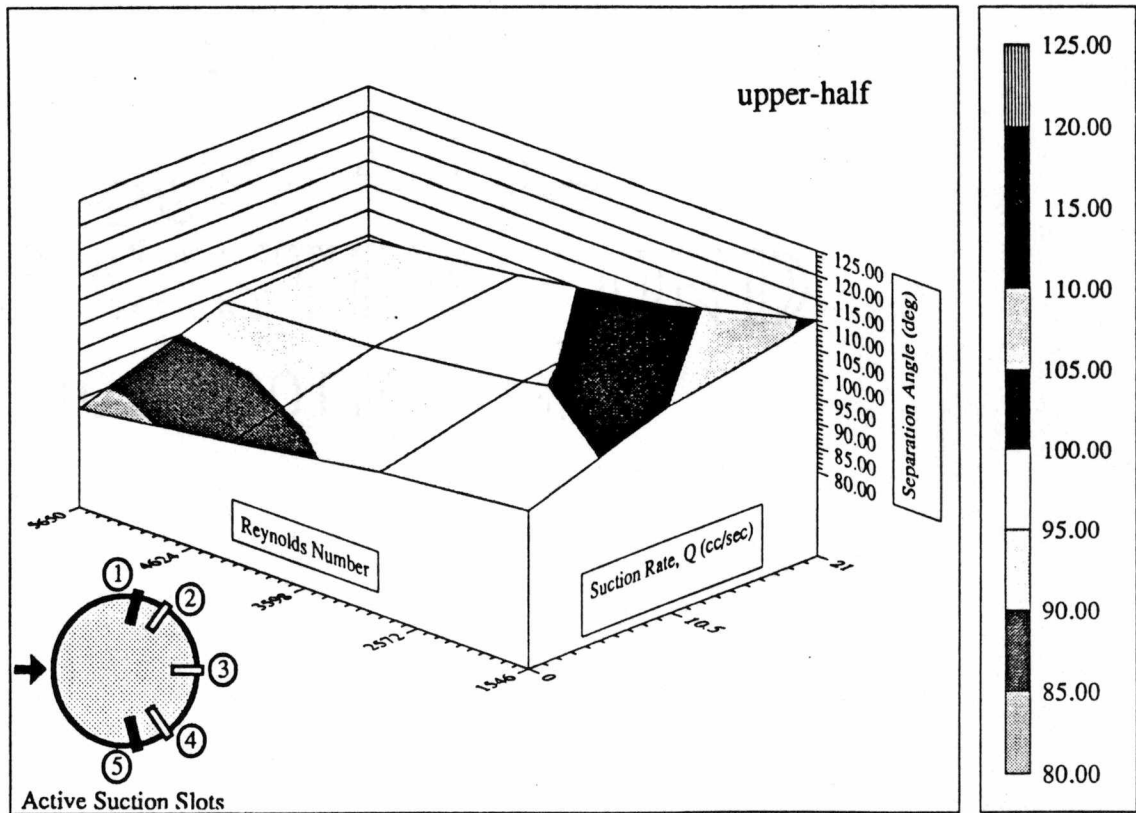
Figure 3.6 θ vs. Re_D and Q: suction through slots #1, 5

50

prolonged on the upper half because of suction. However, in the lower half prolongment of attached flow is not observed. In addition, the separation angle is observed to move forward promoting an early detachment of the flow (i.e. flow separates earlier on the lower half with non-symmetric suction on the upper half than, when there is no suction applied at all). The effect of this phenomenon on the flow field around the cylinder is schematically shown in Figure 3.7, where the general appearance of the flow field around both the upper and lower halves are shown for the cases without suction, and with suction only on the upper half. A clockwise shift of the stagnation point is observed for cases with suction only on the upper half (unsymmetrical suction). The promotion of flow attachment on the upper half to a greater degree, and the promotion of flow separation sooner on the lower half, due to suction only on the upper half is evident by the general downward shift in the z-plane (i.e. the separation angle, θ-plane) in Figures 3.1 and 3.3. In both figures it can be seen that the θ-plane is shifted downward for the lower half, indicating a general decrease in the value of θ, implying that separation occurs at a lower angle, whilst for the upper half the θ-plane is shifted upwards, indicating a general increase in θ, implying separation occurs at a larger angle. The effect of this unsymmetrical suction is greater when suction is applied through three slots (Figure 3.2) than when suction is applied through one slot (Figure 3.1). From Figures 3.1 and 3.2 it can be seen that on the upper half, for the case of suction through #1, 2, 3 slots, the θ-plane is, on the average, shifted upward everywhere by about 10° when compared to suction through slot #1; on the lower half, the difference in the downward shift of the θ-plane for suction through slots #1, and #1, 2, 3 is not as dramatic as on the upper half (i.e. Δθ is only around 4°). However, it is interesting to note that separation occurs at greater angles for the #1, 2, 3 case on the lower half than the #1 case. This probably is due to the greater influence slot #3 has on the lower half due to its geometric location, namely at 180°.

A detailed observation and study of the experimental data suggest that the variation of the separation angle, θ with both Reynolds number, Re and Suction Rate, Q is linear. Hence straight line curves were fitted for the experimental data of the various cases in all the two-dimensional plots that follow, for easier analysis and deductions of the results.

Two-dimensional plots of separation angle vs. Reynolds number for the same

51

No Suction
Applied

Flow
Direction

Stagnation
Point

Suction Applied
Only on Upper Half

Separation
Delayed

New Stagnation
Point

Flow
Direction

Movement of
Stagnation Point

Separation
Promoted
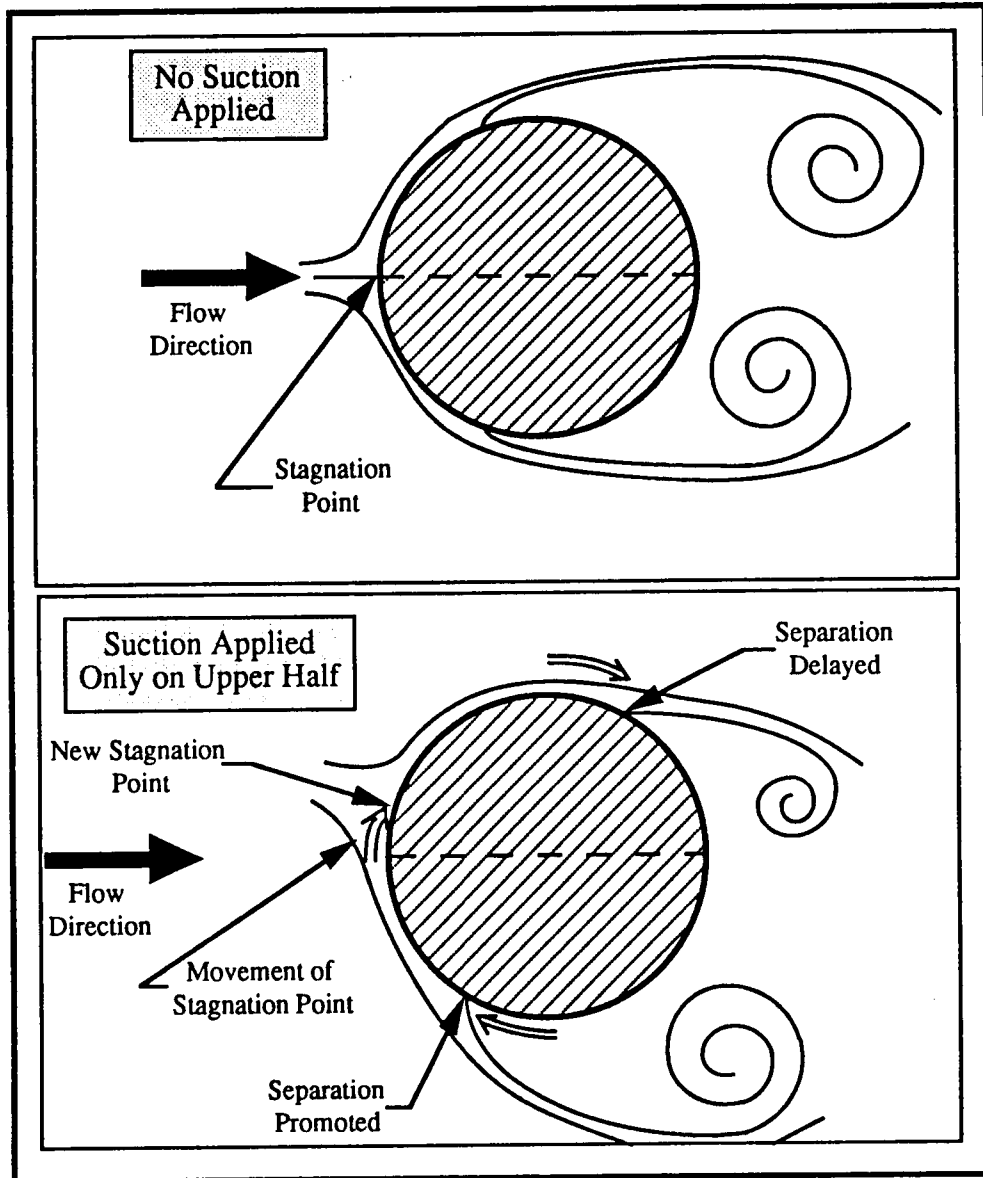
Figure 3.7 Schematic drawing of flow around cylinder showing
the effect on the flowfield with and without suction
applied only on the upper half

52

cases as above - suction applied through slots #1, and #1, 2, 3 are shown in Figure 3.8. The upper graph shows the variation for the case with Q = 10.5 cm^3/sec and the lower for Q = 21.0 cm^3/sec. These plots also indicate a general decrease in separation angle with increasing Reynolds number in a linear manner, with the slope of the plot for the various cases being approximately similar in value.

Here again, the effect of unsymmetrical suction can be clearly observed. For the case of suction through slots #1, 2, 3 with Q = 10.5 cm^3/sec, separation on the upper half is delayed to θ_u = 115° at Re = 1000, and to θ_u = 100° at Re = 6000, while separation on the lower half is promoted to θ_l = 89° at Re = 1000, and to θ_l = 84° at Re = 6000. For this case (lower half), for Reynolds numbers less than about 4000, separation occurs way before it does for the case with no suction.

For the case of suction through slot #1, Q = 10.5 cm^3/sec, the improvement in delaying the separation angle in the upper half is not as dramatic as the #1, 2, 3 case. However, the influential effect of unsymmetrical suction on the lower half is displayed well, in that separation, on the average, occurs before it does for the case with no suction (at Re = 1000, θ_l = 90° for suction through slot #1, θ_l = 77° for the case with no suction; at Re = 6000, θ_l = 77° for suction through slot #1, while, θ_l = 80° for the case with no suction).

The lower graph (Q = 21.0 cm^3/sec) demonstrates similar characteristics as the upper graph (Q = 21.0 cm^3/sec), however, for the former with suction through slots #1, 2, 3 separation does not occur before the 'no suction' case. This is due to the increased suction rate through hole #3 which now has an even greater influence on the lower half than with Q = 10.5 cm^3/sec.

Now, let us look at some case with *symmetrical* suction both on the lower and upper halves. Figures 3.4 and 3.5 are 3-D plots for the cases of suction through slots #1, 2, 3, 4, 5 and slots #1, 2, 4, 5. Figure 3.9 displays 2-D plots for the same cases at Q = 10.5, 21.0 cm^3/sec. It can be seen from Figures 3.4 and 3.5 that the variation of the separation angle with Reynolds number and Suction Rate, for both the upper and lower halves, is very similar to each other. For example, for the case of suction through slots #1, 2, 3, 4, 5, at Re = 1550, Q = 10.5 cm^3/sec, the separation angles are:
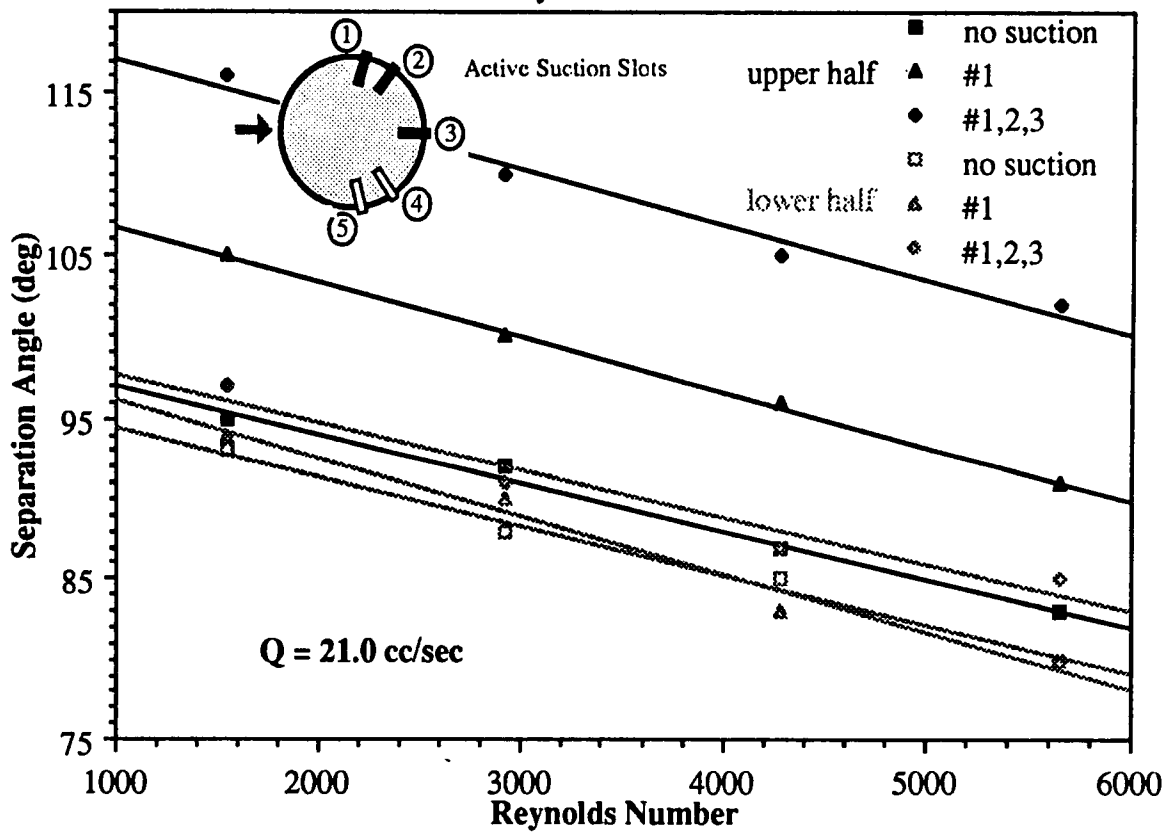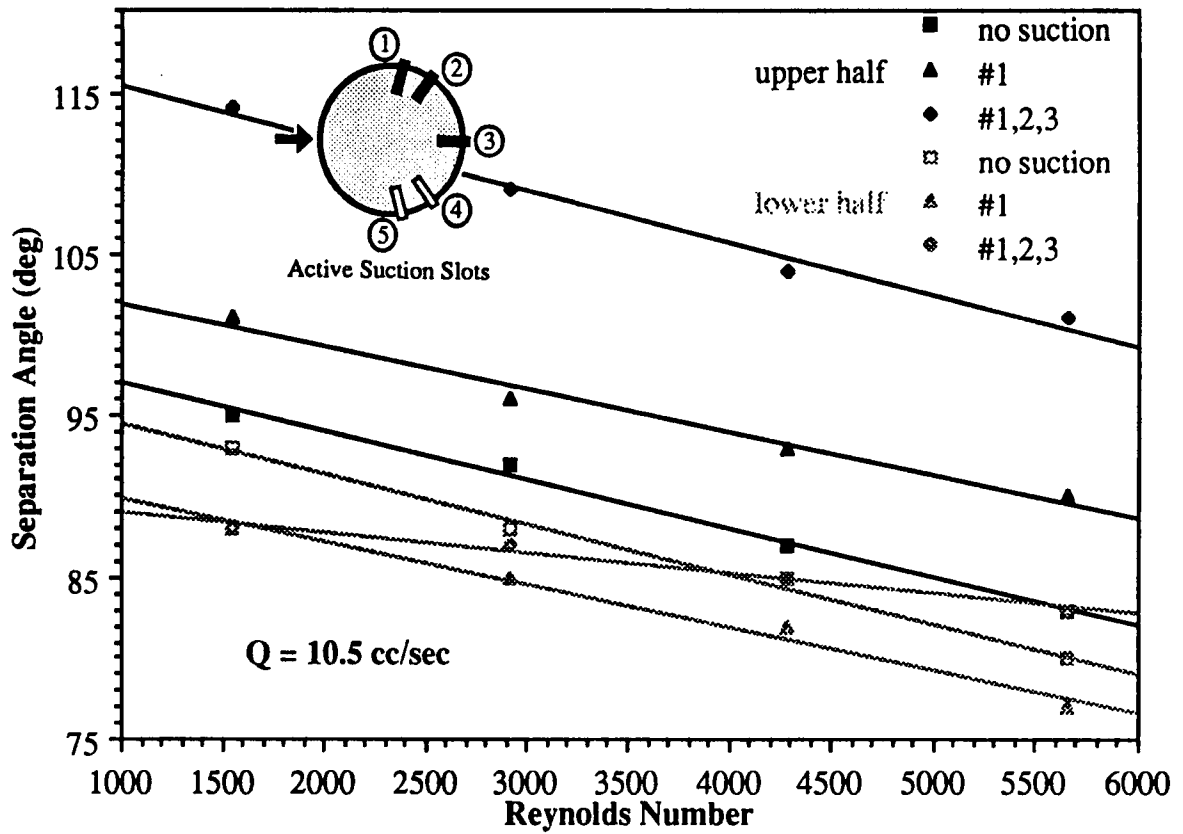
Figure 3.8 θ vs. Re$_D$ for suction through slots #1 and 1, 2, 3
at Q = 10.5 cc/sec and 21.0 cc/sec

54
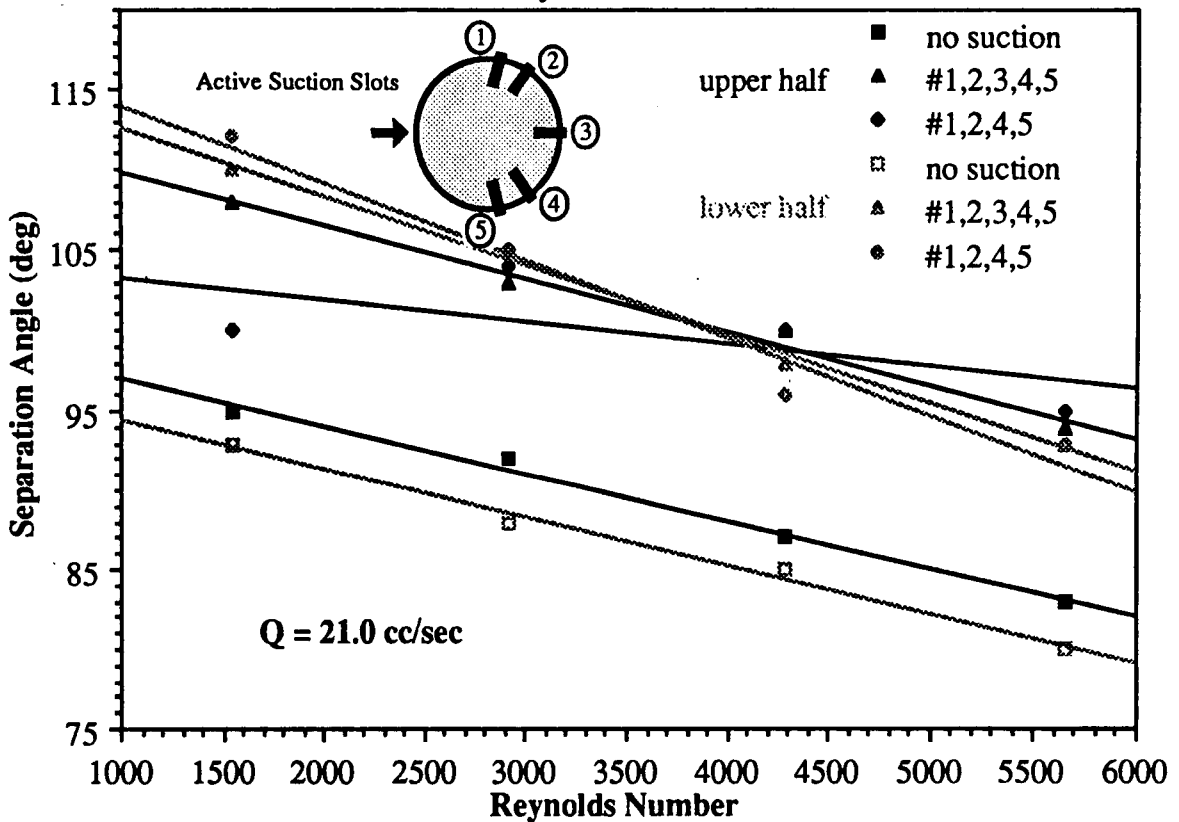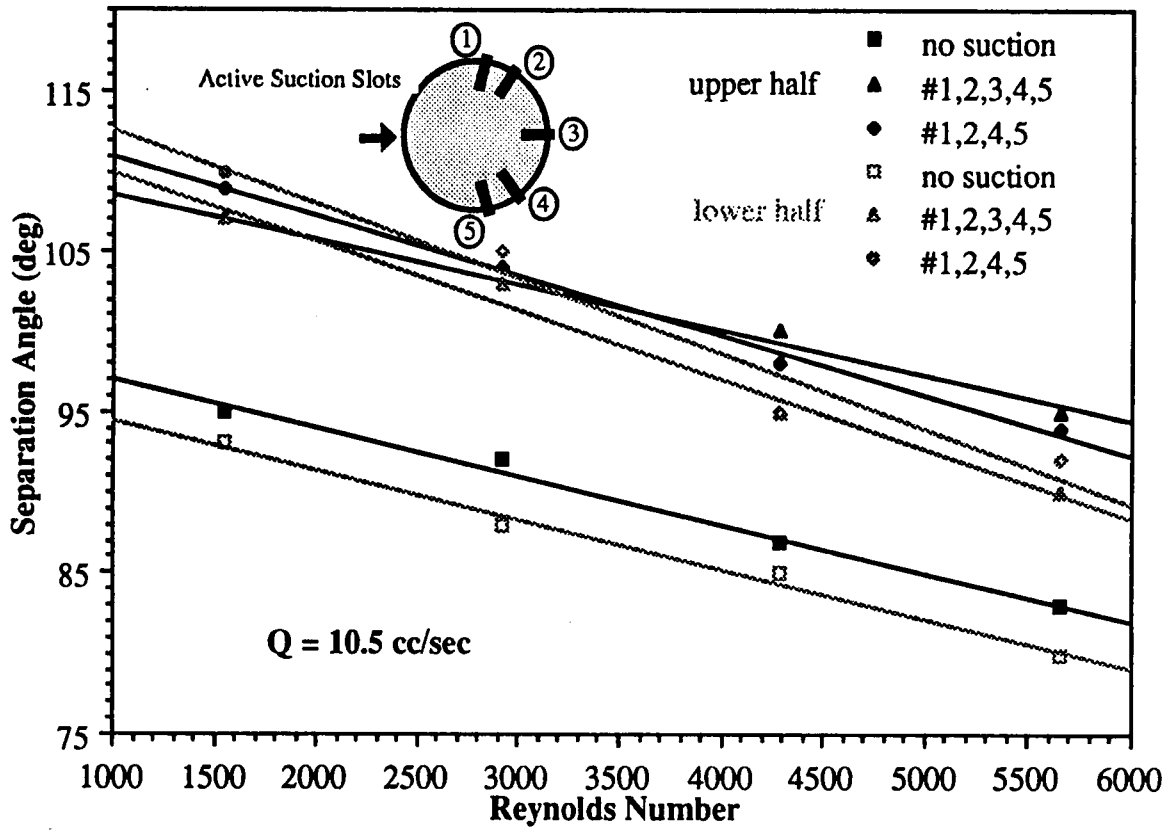
Figure 3.9   θ vs. Re_D for suction through slots #1, 2, 3, 4, 5 and
1, 2, 4, 5 at Q = 10.5 cc/sec and 21.0 cc/sec

$\theta_u = 107°$, $\theta_l = 108°$. At Re = 1546, Q = 21.0 cm³/sec: $\theta_u = 108°$, $\theta_l = 110°$. Similarly, considering the case of #1, 2, 4, 5, at Re = 1550, Q = 10.5 cm³/sec: $\theta_u = 110°$, $\theta_l = 111°$. For Re = 1550, Q = 21.0 cm³/sec: $\theta_u = 110°$, $\theta_l = 112°$. Further observation of Figures 3.4 and 3.5 reveals that the shape of the θ-plane in both the upper and lower half plots are very similar to each other, indicating, that due to symmetrical suction, flow separation occurs at approximately the same separation angles on both the upper and lower halves at the respective flow conditions (i.e. at the respective Reynolds number and suction rate). Although suction through slots #1, 2, 3 (unsymmetrical case) produced greater separation angles on the upper half than the case of #1, 2, 3, 4, 5 and #1, 2, 4, 5 (symmetrical cases), on the lower half case #1, 2, 3 could not deliver the same magnitude of flow attachment as discussed earlier. So, in essence, control of flow separation on both halves of the cylinder is better achieved by applying symmetrical suction (even though the extent of flow attachment is not as great as that achieved by unsymmetrical suction only on the half with suction).

In general, from Figures 3.4, 3.5, 3.9, it can be seen that there occurs a dramatic increase in separation angle from the 'no suction' case to the case with suction at Q = 10.5 cm³/sec. However, the increase in separation angle, from a suction rate of 10.5 cm³/sec to 21.0 cm³/sec is less substantial, and in fact is only a matter of a degree or two. This is an implication that increasing the suction rate indefinitely does not necessarily improve flow attachment, and that the effectiveness of flow control decreases with increasing suction rate.

Figure 3.10 illustrates the flowfield at $V_\infty = 11.75$ cm/sec and Re = 5650. The upper picture illustrates the case with no suction is applied, and the lower illustrates the case with suction applied through slots #1, 2, 4, 5 at Q = 21.0 cm³/sec and $C_Q = 0.0124$

Finally, comparing the cases of suction through slots #1, 2, 3, 4, 5 and slots #1, 2, 4, 5 (refer to Figures 3.4, 3.5, 3.9), it can be concluded that adding the extra slot, namely #5, in the case of the former does not contribute sufficiently to the effectiveness of flow control. That is, adding suction through slot #5 (located at θ = 180°), has very minimal influence on the prolongment of flow attachment. This is evident by comparing Figures 3.4 and 3.5 where the θ-planes are more or less at the same vertical locations as one another, indicating that separation, in general, for the two cases,
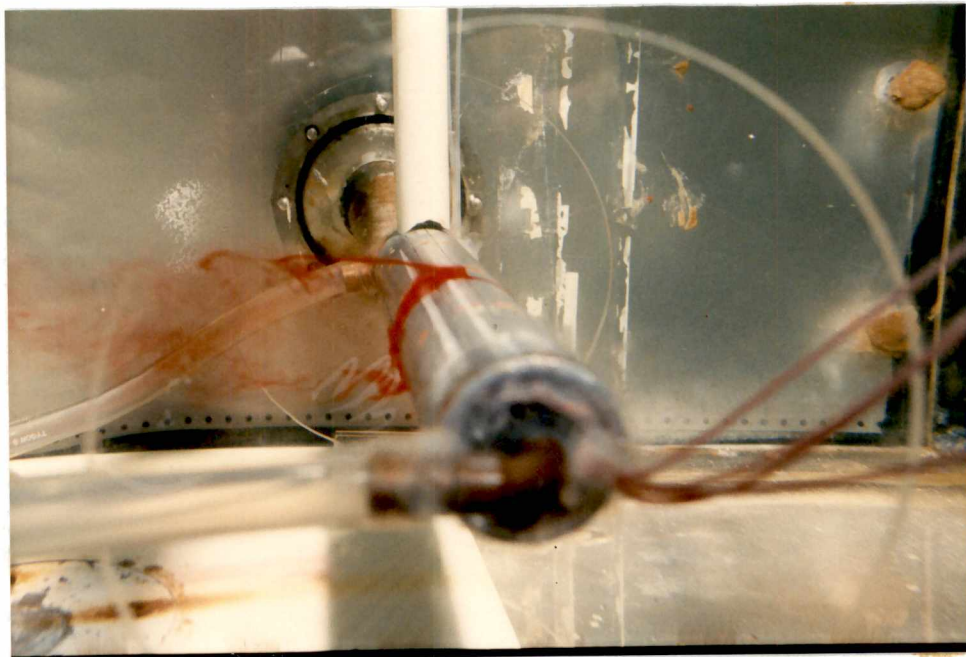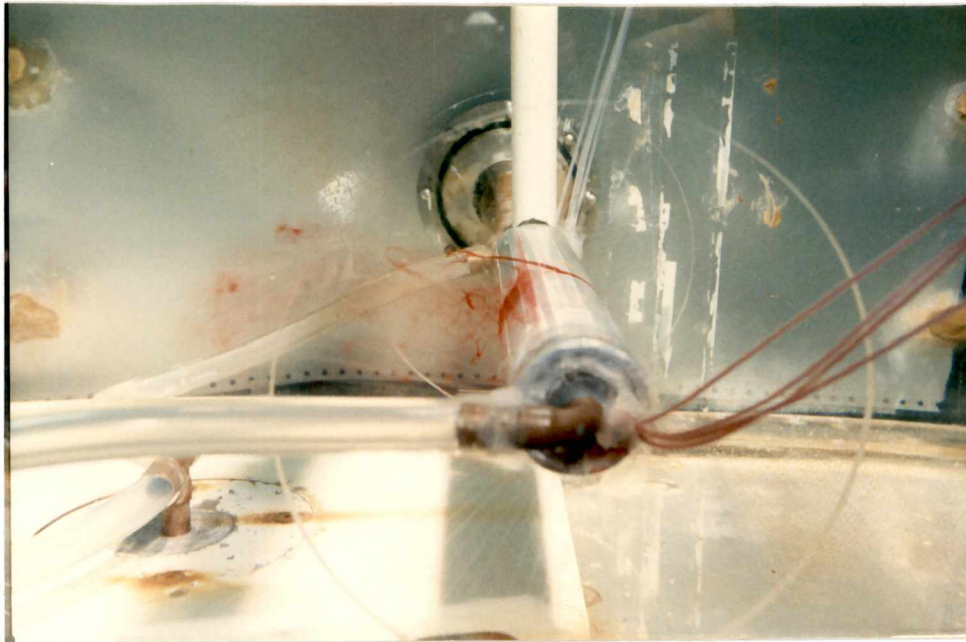
Figure 3.10 Flowfield without and with suction through slots #1, 2, 4, 5
at Q = 21.0 cc/sec and C_Q = 0.0124 (V_∞ = 11.75 cm/sec,
Re = 5650)

57

occurs at the same separation angles. In short then, suction through slots #1, 2, 4, 5 produced the same results as suction through slots #1, 2, 3, 4, 5 indicating that suction through slot #5 is redundant and can be avoided.

Figure 3.3 shows the 3-D variation (i.e. with Re and Q) of θ for the case of suction through slots #1, 2, 3, 4. Here again, the effect of unsymmetrical suction is visible. Although the difference in separation angle on the lower and upper halves is not as dramatic as for the case of suction through slot #1 (Figure 3.1) and slots #1, 2, 3 (Figure 3.2), the overall prolongment is not as good as case #1, 2, 4, 5 (Figure 3.5). For example, at Re = 1550, Q = 21.0 cm³/sec, θ is only between 102° - 105° for #1, 2, 3, 4, while for the #1, 2, 4, 5 case it is at the higher values of 110° - 112°. This result can also be seen in Figure 3.11 where the curves for the #1, 2, 4, 5 case are, in general, higher (i.e. greater θ's) than the curves for #1, 2, 3, 4.

From the analysis thusfar, the most effective flow control for the entire body (both upper and lower halves) is achieved by suction through slots #1, 2, 4, 5.

Figure 3.12 is a plot of separation angle vs. suction rate at Re = 1550, 5650 for the two non-symmetrical suction cases, #1 and #1, 2, 3. Here again, the phenomena described earlier is clearly seen, in that, although on the upper half separation is delayed considerably (dark lines), the lower half undergoes early separation (light lines). An interesting observation that is evident from these graphs is that on the upper half separation angle increases appreciably with increasing suction rate, whilst on the lower half the increase in separation angle with increase in suction rate is minimal. Furthermore, in the case of suction applied through slot #1 there is hardly any increase in separation angle at all, exhibiting a flat, horizontal line. This is again the result of unsymmetrical suction. The unsymmetrical suction only on the upper half induces the flow to stay attached to a greater degree as expected on the upper half, and also increasing the suction rate on the upper half causes the separation angle to increase noticeably. On the other hand, on the lower half since there is no suction applied, the flow separates much earlier, as expected, and even an increase in suction rate does not aide in prolonged attachment on the lower half.

In contrast, consider figure 3.13, which shows the variation of separation angle with suction rate for Re = 1550, 5650, only here, for the cases of symmetrical suction #1, 2, 3, 4, 5 and #1, 2, 4, 5, and for the case of near symmetrical suction #1, 2, 3, 4.

58
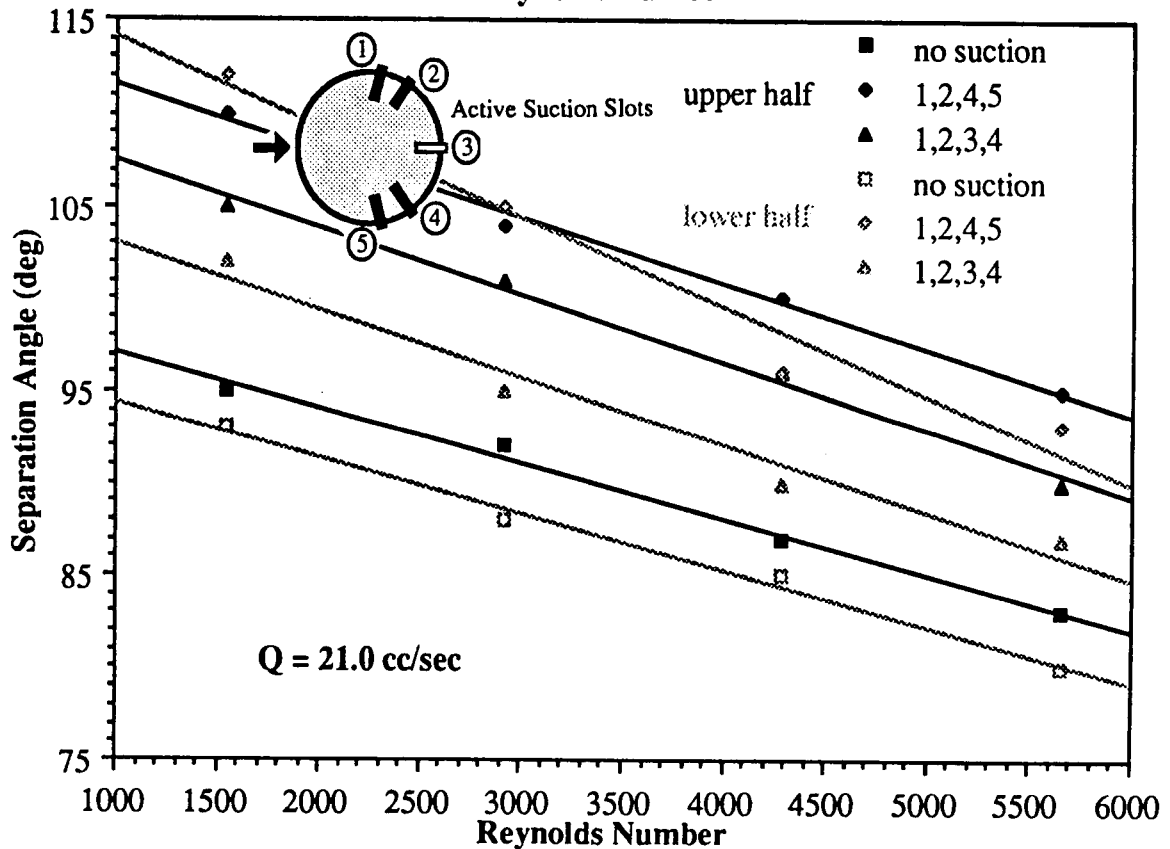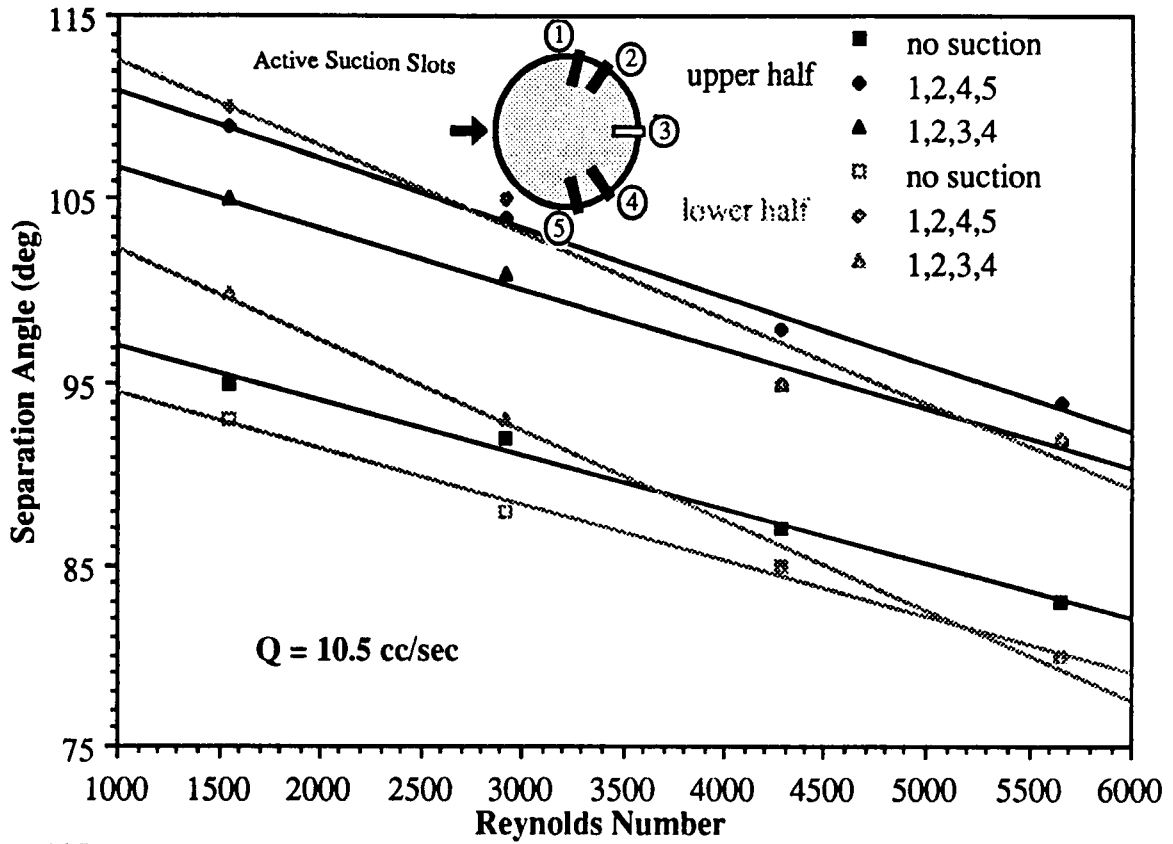
Figure 3.11 θ vs. Re$_D$ for suction through slots #1, 2, 3, 4 and
1, 2, 4, 5 at Q = 10.5 cc/sec and 21.0 cc/sec

59
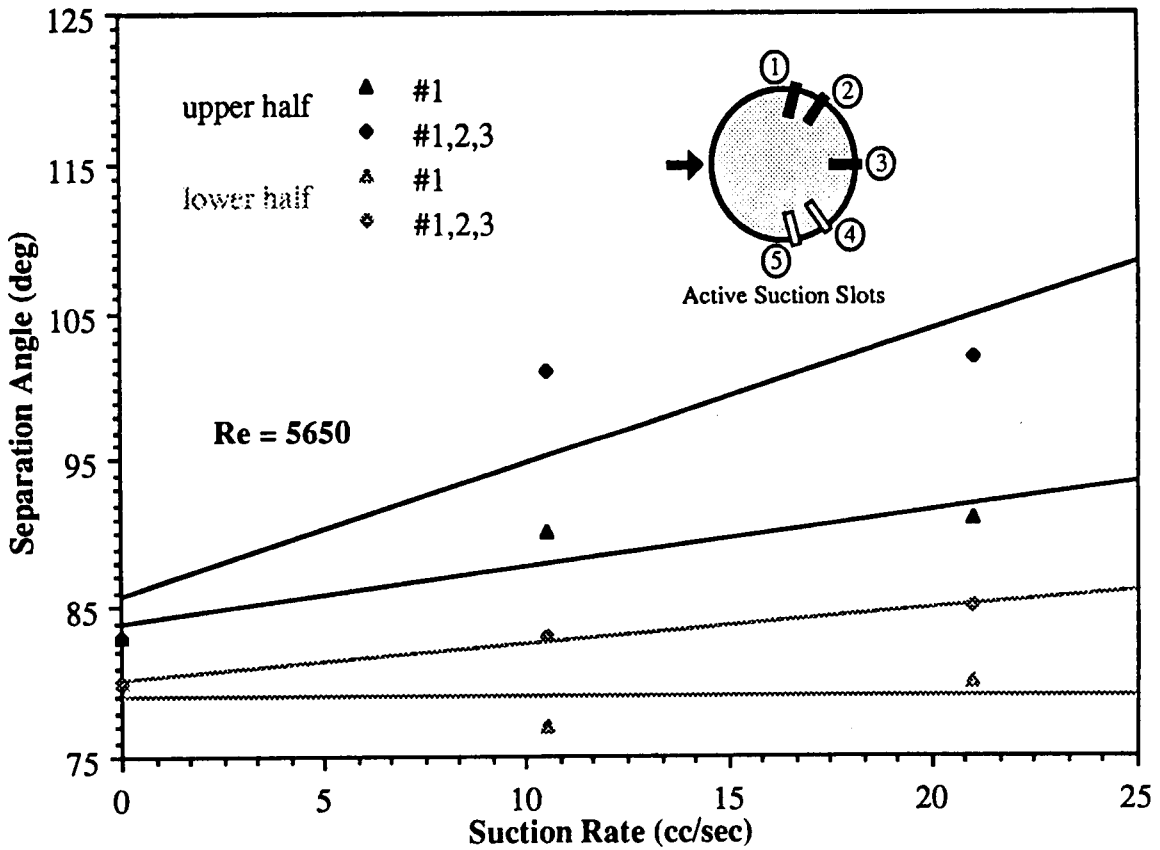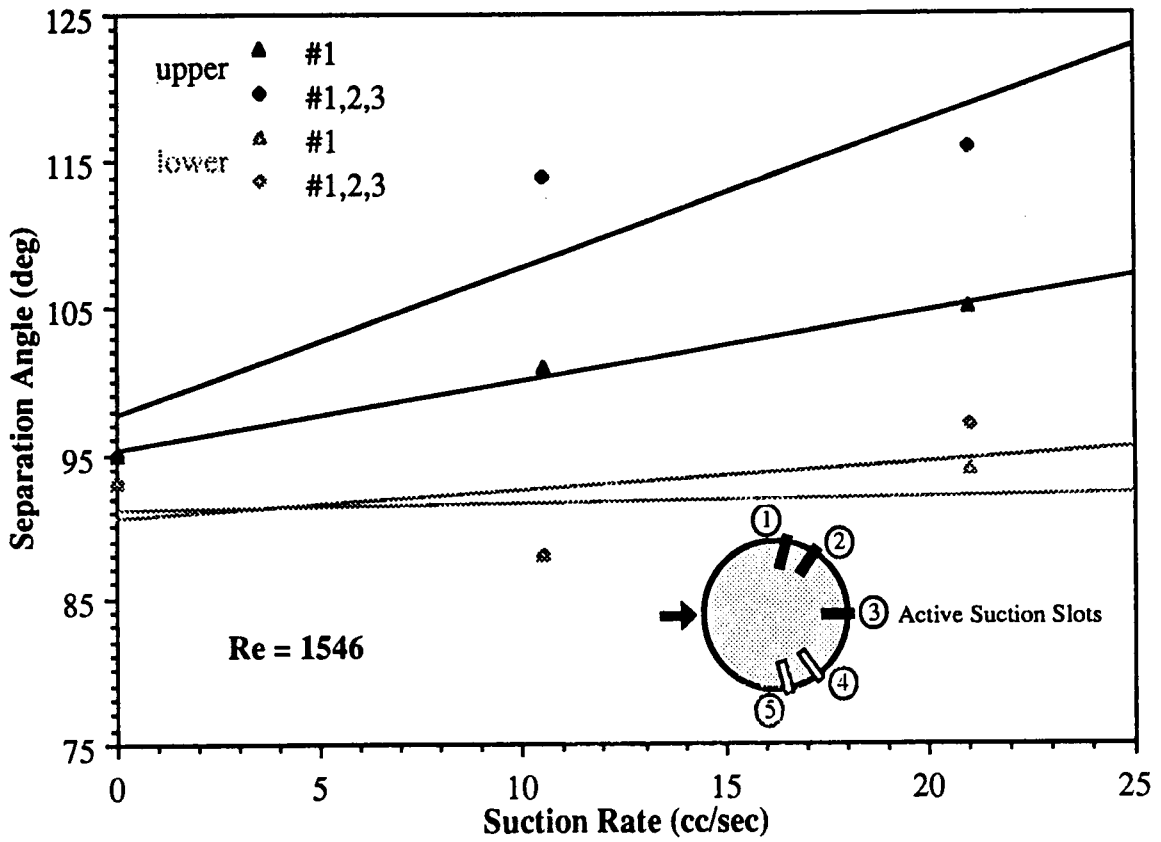
Figure 3.12   θ vs. Q for suction through slots #1 and 1, 2, 3
at Re_D = 1550 and 5650

60
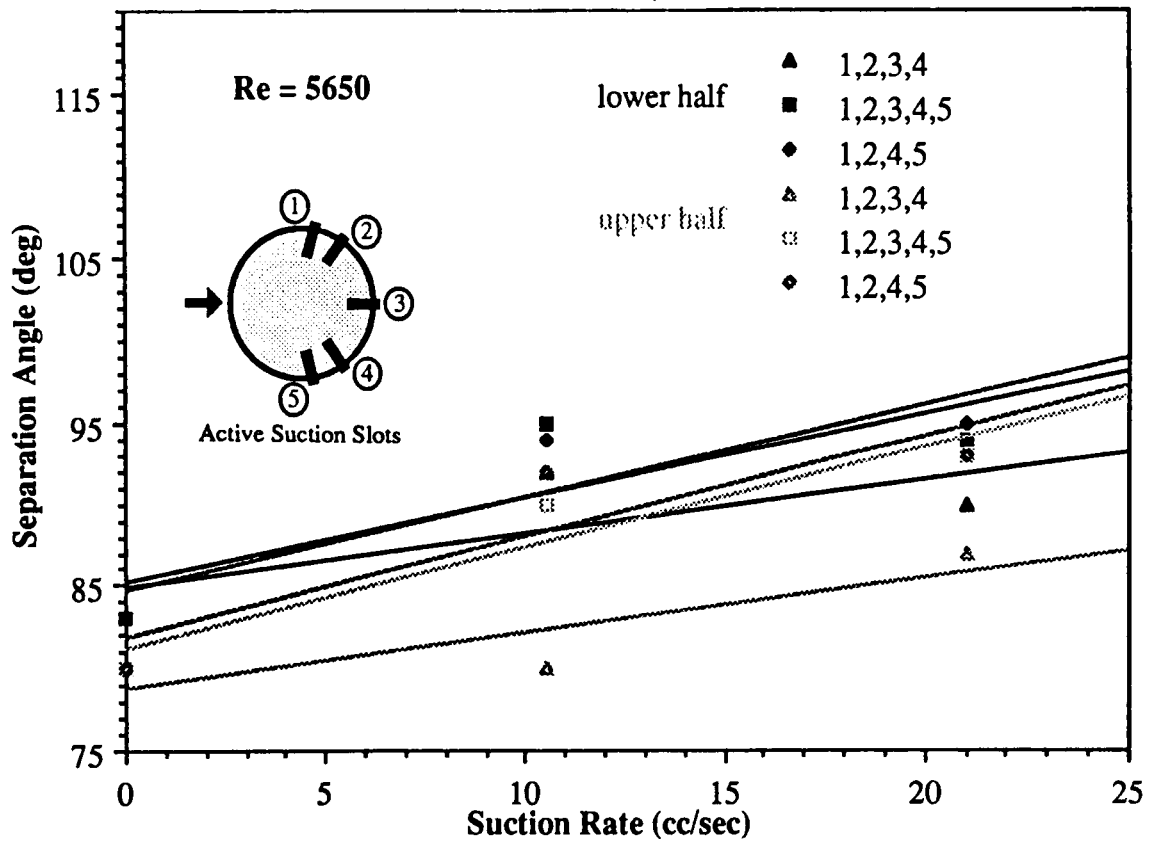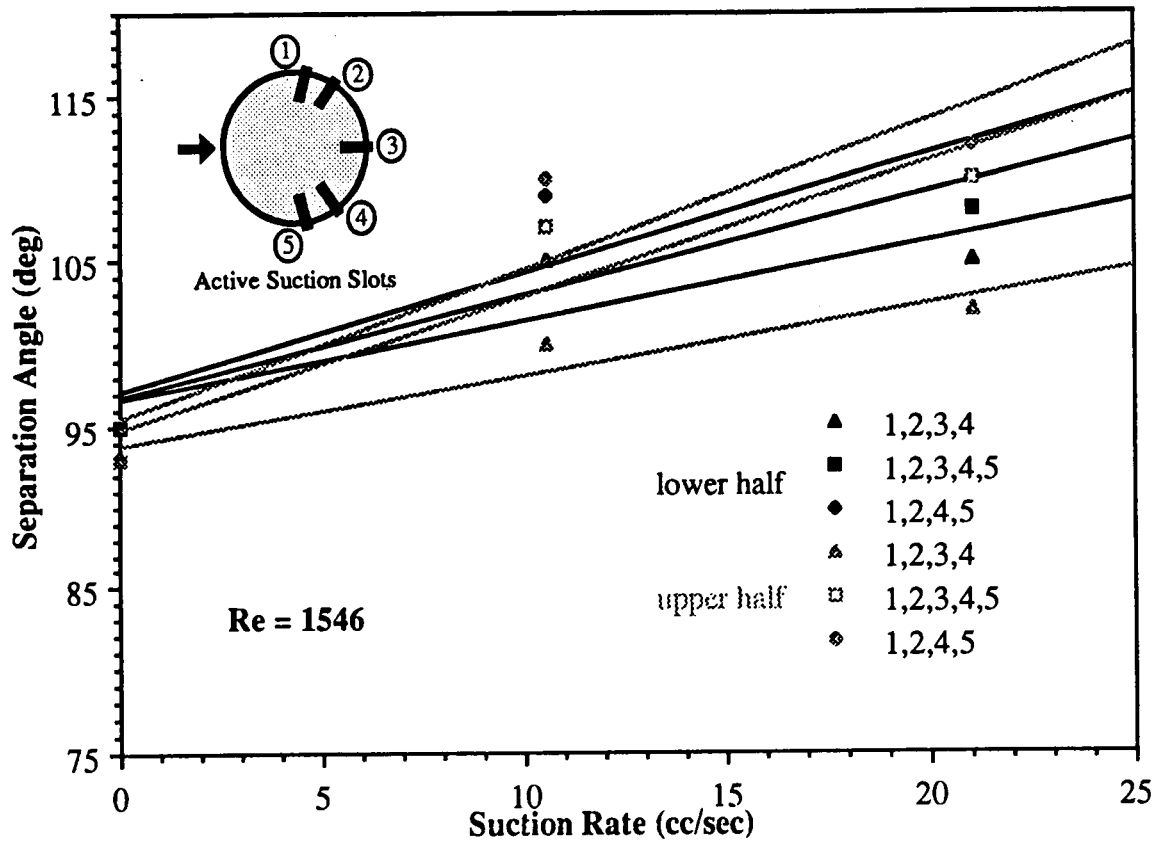
Figure 3.13 θ vs. Q for suction through slots #1, 2, 3, 4; 1, 2, 3, 4, 5
and 1, 2, 4, 5 at Re$_D$ = 1550 and 5650

Here all the plots for the various cases for the upper and lower halves are concentrated in a fairly narrow band spanning about 7°, depicting that separation occurs at approximately the same θ on both the upper and lower halves for these symmetrical cases. Also, unlike the unsymmetrical cases, the slope of the curves for the upper and lower halves for the symmetrical cases are approximately the same. The plots in Figure 3.13 for both the lower Reynolds number 1550 and the higher Reynolds number 5650 display the same characteristics, only for Re = 5650, the location of the entire structure of curves is moved downward, indicating, in general, earlier separation than the lower Reynolds number case.

Finally, Figure 3.14 indicates the variation of separation angle with suction rate at various Reynolds numbers, for the best overall case, namely suction applied through slots #1, 2, 4, 5. As expected, the separation angle increases with increasing suction rate, and the location of the plots are approximately similar for both upper and lower halves as should be for symmetrical suction case. Also evident is that the slopes for the various Reynolds number cases are approximately similar, and the plots are observed to move downward (in the direction of decreasing separation angle) with increasing Reynolds number, as pointed out earlier.

§ 3.2 BODY - FLAT PLATE JUNCTIONS

In this section, the results obtained from the cylinder - flat plate model and the streamlined body (namely, wing with NACA 0012-64 airfoil) - flat plate model are presented in the form of photographs and schematic drawings. These are accompanied by analyses of the results of utilizing the technique of suction for flow control.

§ 3.2.1 CYLINDER - FLAT PLATE JUNCTION

Tests with the cylinder - flat plate model were conducted at free-stream velocities ranging from V_∞= 3.22 cm/sec (1.27 in./sec) to 11.74 cm/sec (4.64 in./sec). The corresponding Reynolds numbers (based on the cylinder diameter) are Re_D = 3665 and Re_D = 13380. As illustrated in Figure 2.7, suction could be applied through a total of 12, 0.3175 cm (0.0125 in.) diameter holes, or any combination of selected holes ranging from 1 hole to a maximum of 12 holes. Table 3.5 tabulates the suction hole
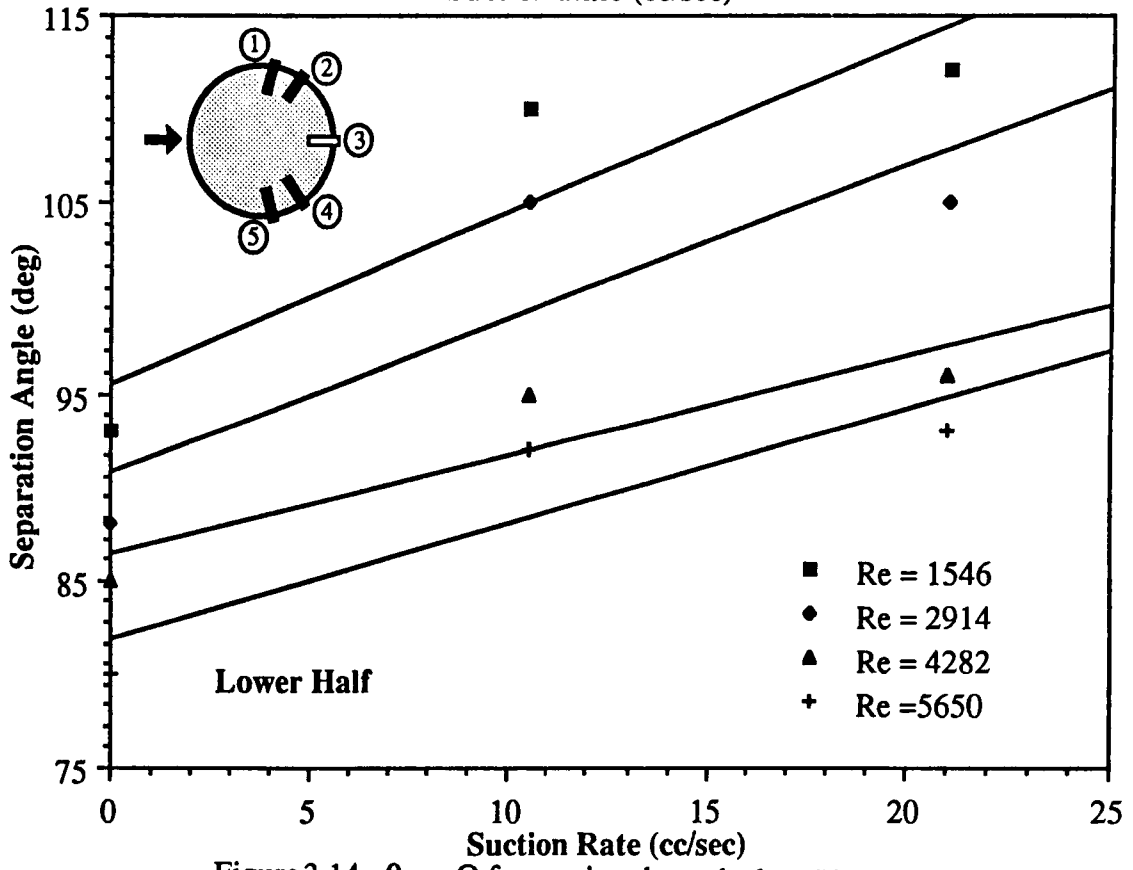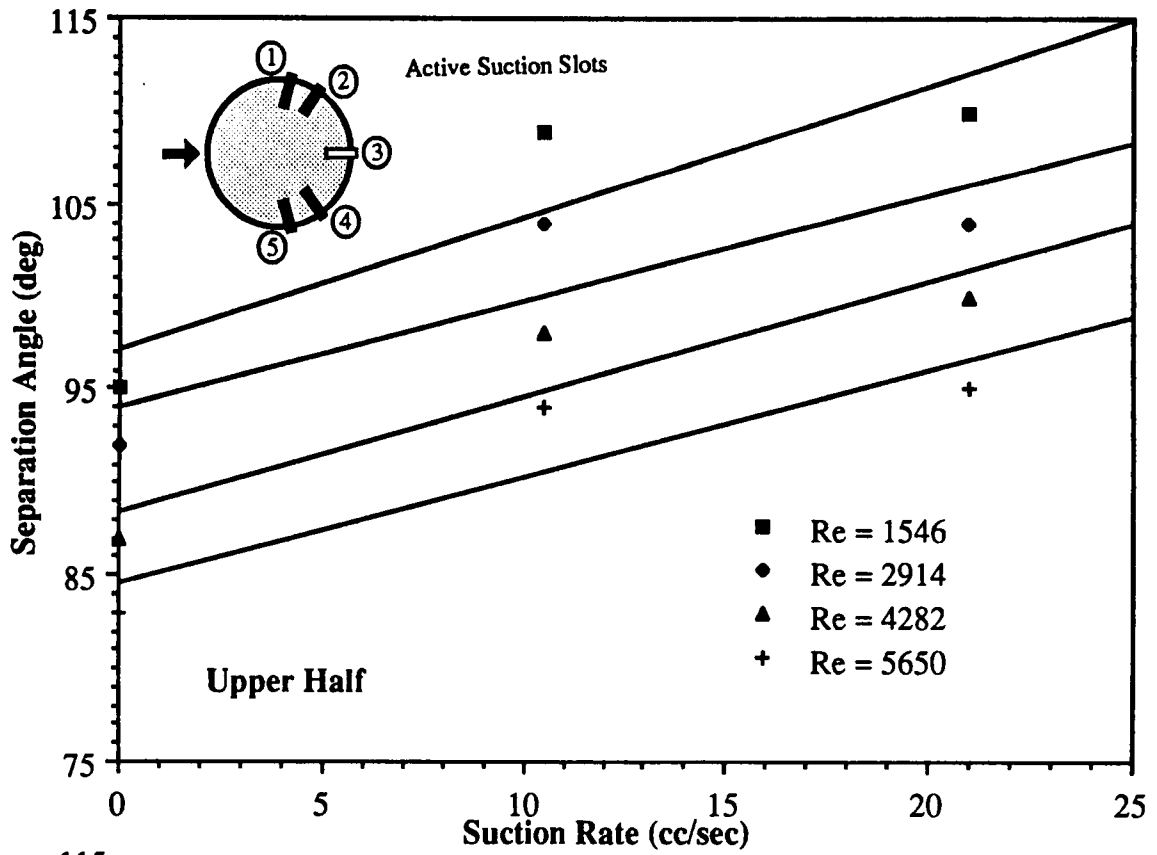
Figure 3.14   θ vs. Q for suction through slots #1, 2, 4, 5 at
Re_D = 1550, 2910 4280 and 5650

63

Table 3.5 Hole Reynolds numbers and suction velocities for various number of holes (cylinder - flat plate junction)

Total number of suction holes open	Suction Rate, $Q = 10.5$ cm^3/sec (0.64 in^3/sec)			Suction Rate, $Q = 21.0$ cm^3/sec (1.28 in^3/sec)		
	Suction hole Reynolds number, Re_s/hole	Suction Velocity, v_s/hole		Suction hole Reynolds number, Re_s/hole	Suction Velocity, v_s/hole	
		cm/sec	in./sec		cm/sec	in./sec
1	4190	132.6	52.2	8390	265.2	104.4
2	2100	66.3	26.1	4190	132.6	52.2
3	1400	44.2	17.4	2800	88.4	34.8
4	1050	33.1	13.0	2100	66.3	26.1
5	840	26.5	10.4	1680	53.0	20.9
6	700	22.1	8.7	1400	44.2	17.4
7	600	18.9	7.5	1200	37.9	14.9
8	525	16.6	6.5	1050	33.2	13.0
9	470	14.7	5.8	930	29.5	11.6
10	420	13.3	5.2	840	26.5	10.4
11	380	12.0	4.7	760	24.1	9.5
12	350	11.0	4.3	700	22.1	8.7

Reynolds number, Re_s/hole and suction velocity, v_s/hole, for the various number of holes utilized for suction, for total suction rates of $Q = 10.5$ cm^3/sec and $Q = 21.0$ cm^3/sec. It can be seen that for $Q = 10.5$ cm^3/sec, the suction velocity per hole ranges from a low of 11.1 cm/sec (4.3 in./sec) for the case of suction through 12 holes, to a high of 132.6 cm/sec (52.2 in./sec) for the case of suction through 1 hole. The suction hole Reynolds numbers per hole are: Re_s/hole = 350 (12 holes); Re_s/hole = 4190 (1 hole). For $Q = 21.0$ cm^3/sec, v_s/hole = 22.1 cm/sec (8.7 in./sec), Re_s/hole = 700 (for suction through 12 holes), and v_s/hole = 265.2 cm/sec (104.4 in./sec), Re_s/hole = 8390 (for suction through 1 hole).

Table 3.6 lists the suction coefficients, C_Q's at $Q = 10.5$ cm^3/sec and 21.0 cm^3/sec for the various free-stream velocities and Reynolds numbers. Suction coefficients range from a low of $C_Q = 0.0066$ for $Q = 10.5$ cm^3/sec at $V_\infty = 11.75$ cm/sec ($Re_D = 13380$) to a high of $C_Q = 0.0478$ for $Q = 21.0$ cm^3/sec at $V_\infty = 3.22$ ($Re_D = 3665$).

The left half of Figure 3.15 shows schematic sketches of the top and button views of the flowfield around the cylinder - flat plate junction at $V_\infty = 8.91$ cm/sec ($Re_D = 10140$). As shown in the figure, the flow separates from the flat plate ahead of the cylinder at approximately 5.25 cm ahead of the cylinder (i.e. approximately 0.46D, where D is the diameter of the cylinder), and as a result spirals into a vortex (this can be seen from the side view). As a result of the existence of a protuberance (cylinder) ahead, the flow, being incompressible, tends to go around the protuberance. This results in a horse-shoe vortex which spirals and travels around the cylinder and finally separates from the vicinity of the cylinder. Thereafter, the same system evolves into two wake vortices creating a Karmán vortex street. It was envisaged if the horse-shoe vortex system could be curtailed or at best eliminated by applying suction, the flow may be made to stay attached to the cylinder to a greater extent and thereby reducing the wake width. This would, of course means a reduction in form drag, which is highly desirable.

The main objective of this particular experiment was to curtail the horse-shoe vortex that forms just ahead of the cylinder - flat plate interface and just past the region of flow separation from the flat plate. This vortex travels around the cylinder preserving its spiral nature and eventually, after separating from the cylinder loses its three-dimensional nature and evolves into the well-known Karmán vortex street that forms at the wake of the cylinder. It was envisaged that if the horse-shoe vortex were

65

Table 3.6 Coefficient of suction for various velocities and Reynolds numbers for $Q = 10.5$ cm^3/sec, and $Q = 21.0$ cm^3/sec (cylinder - flat plate junction)

Free - Stream Velocity, V_∞		Reynold's Number, Re_D	Suction Coefficient, C_Q	
cm /sec	in. /sec		$Q = 10.5$ cm^3/ sec $= 0.64$ in.^{3} /sec	$Q = 21.0$ cm^3/ sec $= 1.28$ in.^{3} /sec
3.22	1.27	3665	0.0239	0.0478
6.06	2.39	6900	0.01275	0.0255
8.91	3.51	10140	0.0087	0.0174
11.75	4.62	13380	0.0066	0.0132

66
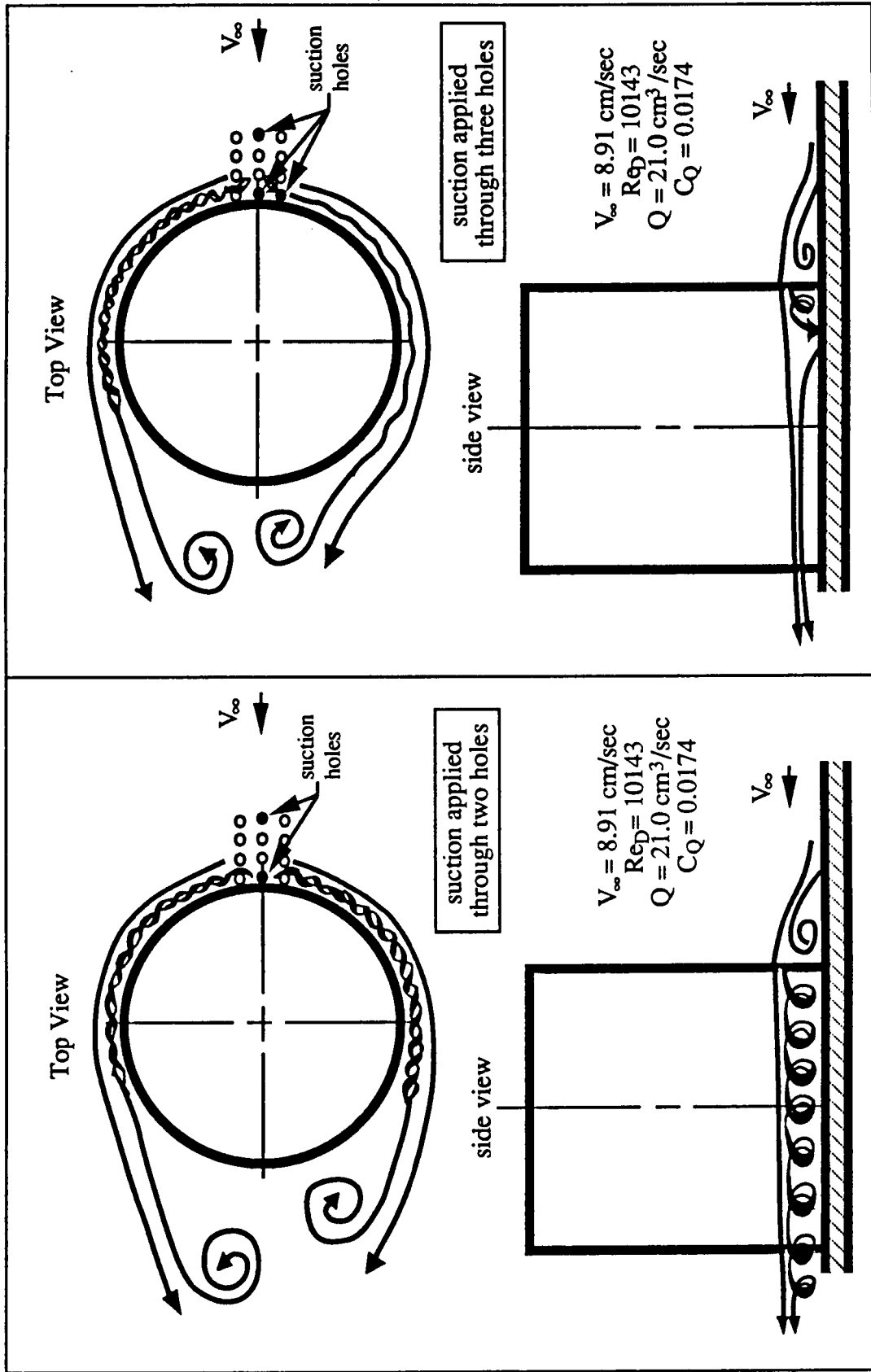
Figure 3.15   Schematic sketch of flowfield around cylinder - flat plate junction with no suction and with suction through one hole

to be curtailed or at best eliminated, a much smoother flow will result around the cylinder which would tend to stay attached to the cylinder to greater distances, and thereby produce a smaller wake. A smaller wake, of course, is desirable since it translates into a reduction in drag.

Hence, a series of three holes were fabricated on the flat plate at different diameters (refer to Figure 2.7), totaling 12 holes in all. The farthest diameter, which is at a distance of 5.25 cm from the cylinder is where separation is found to occur at a higher free-stream velocity of 11.74 cm/sec (Re_D = 13380), while the second farthest diameter from the cylinder, which is located at a distance of 3.5 cm from the cylinder, is where separation occurs at the lower free-stream velocity of 3.22 cm/sec (Re_D = 3665). A third series of holes were located at a distance of 1.75 cm from the cylinder. The distances between these three series of holes are all 1.75 cm. The fourth series of holes are situated immediately next to the cylinder. It was thought that if suction were applied at the separation point or at the vicinity, separation may be avoided or delayed and hence the horse-shoe vortex will be reduced in size, inducing a smaller wake.

The right half of Figure 3.15 shows the resulting flow with suction applied through one hole located at 5.25 cm (0.46D) from the cylinder, at V_∞ = 8.91 cm/sec (Re_D = 10140). The suction rate was kept at Q = 21.0 cm^3/sec resulting in a suction coefficient, C_Q = 0.0174. The suction hole Reynolds number, Re_S = 8390, and the suction hole velocity, v_s = 265.2 cm/sec (104.4 in./sec). Because of the application of suction, the separation point on the flat plate is delayed and flow separates further downstream closer to the cylinder - flat plate junction. The resulting spiraling vortex is found to be smaller in size. Accordingly, the spiraling horse-shoe vortex system itself is reduced in size. The system is also observed to stay closer to the cylinder for a greater distance before complete separation from the cylinder occurs. The above mentioned factors, namely an overall reduction in the size of the horse-shoe vortex system, and the tendency of the system to stay attached to the cylinder to a greater distance contributed to the smaller Karmán vortices and a smaller wake width, as can be seen in Figure 3.15.

Although suction through the first hole helped in reducing the size of the wake behind the cylinder, it failed to curtail the spiral vortex that forms above the flat plate as a result of separation. In essence, only the size of that spiraling vortex could be reduced, while the vortex itself moved closer to the cylinder - flat plate interface.

Suction through other center holes located closer to the cylinder also displayed similar results (i.e. the vortex moved even closer to the interface).

Hence, suction now was applied through the center hole located immediately next to the cylinder together with suction through the original hole (which, as mentioned earlier is located at the original point of flow separation). This resulted in a suction Reynolds number per hole, Re_S/hole = 4190 and the suction velocity per hole, v_s/hole = 132.6 cm/sec (52.2 in./sec). The suction rate was kept constant at Q = 21.0 cm^3/sec. The resulting flowfield sketch is shown in the left half of Figure 3.16. The size of the resulting horse-shoe vortex is reduced considerably. However, the spiraling characteristic of the system still prevailed inducing a horse-shoe vortex system that stayed closer to the cylinder to an even greater distance promoting a smaller wake.

Suction was now applied, in addition to the previous holes, through a side hole located immediately next to the cylinder as shown in the right half of Figure 3.16. The suction Reynolds number and velocities are: Re_S/hole = 2800; v_s/hole = 88.4 cm/sec (34.8 in./sec). Interestingly, even though on the side where suction was not applied the horse-shoe vortex continued to exist, on the side with suction, the little remains of the horse-shoe vortex system is almost eliminated. The spiraling nature, although very slightly prevalent, is now very much more relaxed and the resulting flowfield exhibits an almost 'non-spiral' motion as indicated in the figure. In addition, the flow stays attached to the cylinder to a much greater extent, and the resulting wake is considerably smaller. Also evident is the much smaller vortex that forms in the wake area, namely the initial vortex in the Karmán vortex street. Finally, the other 'side hole' immediately next to the cylinder was opened for suction. This, as expected, also almost eliminates the horse-shoe vortex on that side, and displays similar flow characteristics as the other side.

Figure 3.17 is an illustration of the top and bottom views of the flowfield with no suction applied, and Figure 3.18 shows the flowfield with suction applied through 3 holes at Q = 21.0 cm3/sec and C_Q = 0.0174. The flow velocity and Reynolds number in both Figures 3.17 and 3.18 are 8.91 cm/sec and 10140 respectively

Suction through more holes along the perimeter of the cylinder may totally eliminate the horse-shoe vortex and produce a non-spiraling flow pattern immediately next to the cylinder, which stays attached longer. This implies an even smaller wake and an even greater reduction in drag could be expected. However, due to the

Top View

suction hole

V_∞

suction applied through one hole

$V_\infty = 8.91$ cm/sec
$Re_D = 10143$
$Q = 21.0$ cm^3/sec
$C_Q = 0.0174$

side view

V_∞

Top View

V_∞

no suction applied

$V_\infty = 8.91$ cm/sec
$Re_D = 10143$
$Q = 21.0$ cm^3/sec
$C_Q = 0.0174$

side view

V_∞
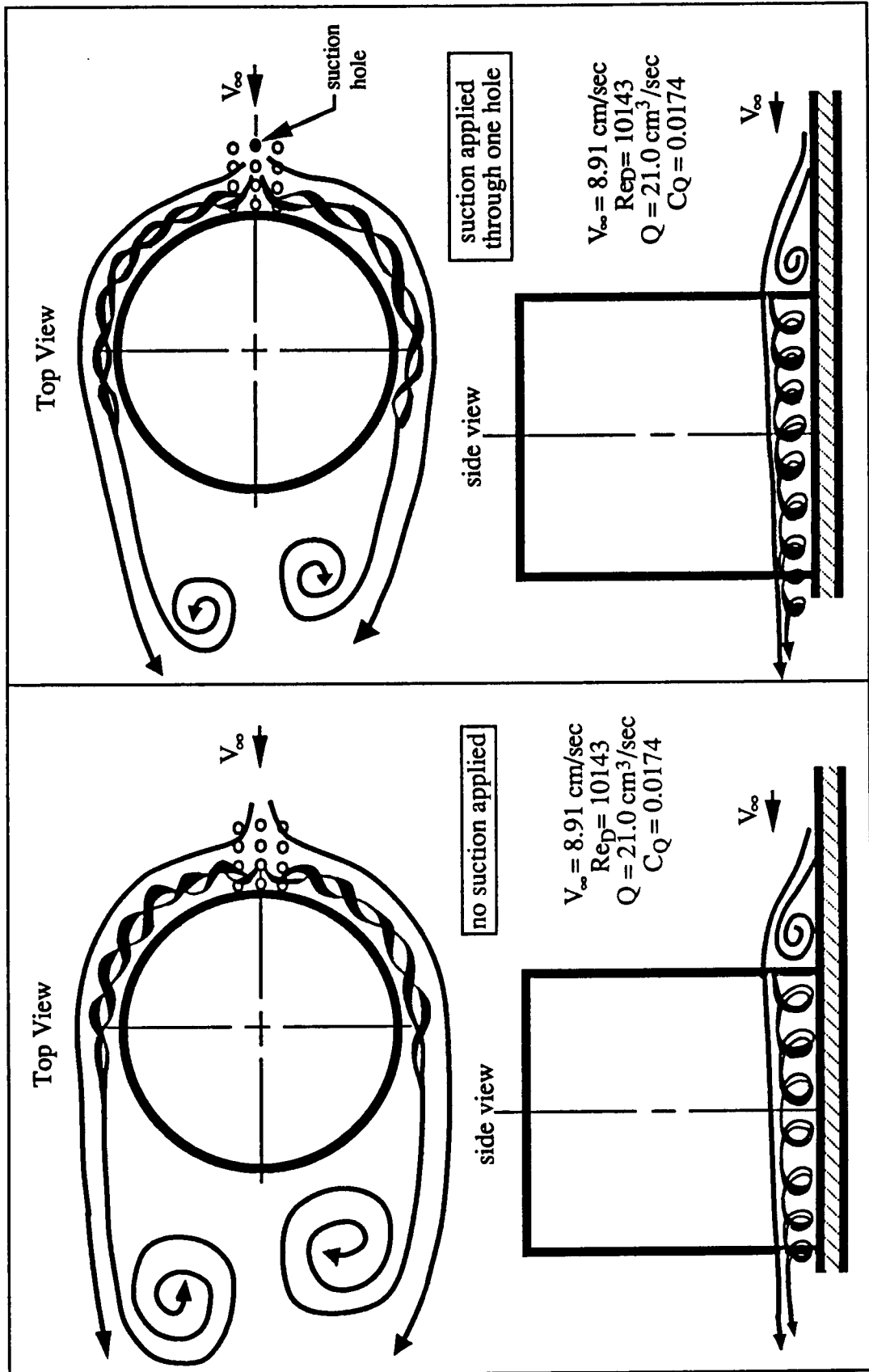
Figure 3.16 Schematic sketch of flowfield around cylinder - flat plate junction with suction through two and three holes

Figure 3.17 Top and bottom views of the flowfield with no
suction applied (V$_\infty$ = 8.91 cm/sec, Re = 10140
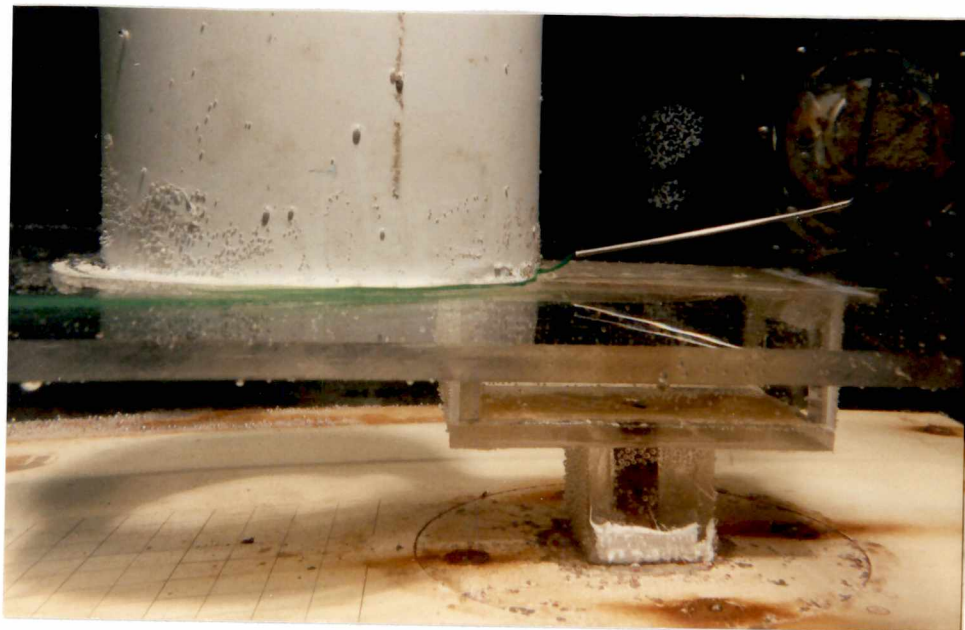
Figure 3.18 Top and bottom view s of the flowfield with suction
applied through 3 holes, Q = 21.0 cc/sec and
$C_Q = 0.0014$ (V_∞ = 8.91 cm/sec, Re = 10140)

72

limitation of the model, specifically lack of more suction holes along the perimeter of the cylinder, this is not experimentally verified. Nevertheless, suction through the three holes did indeed successfully curtail (or even nearly eliminated) the spiral nature of the system causing longer flow attachment and reduced wake size, with a suction rate of only 21.0 cm^3/sec inducing a suction coefficient of 0.0174.

Halving the suction rate to 10.5 cm^3/sec reduced the effectiveness with which the vortex system was curtailed. That is, with suction through the three holes as discussed above and with Q = 10.5 cm^3/sec, curtailment of the spiral nature of the vortex was not to the same extent as with Q = 21.0 cm^3/sec. Although the spirals appear relaxed when compared to the two-hole case (Q = 21.0 cm^3/sec), they are not as relaxed as the three hole case (Q = 21.0 cm^3/sec). In essence, then, the lower suction rate produced similar flow characteristics and patterns as the higher suction rate, only the effectiveness and magnitude of the results as pertinent to flow control (in this case, elimination of the horse-shoe vortex system) is not as promising as those resulting from the higher suction rate.

§ 3.2.2 STREAMLINED BODY - FLAT PLATE JUNCTION

Tests with this model were carried out at free-stream velocities of V_∞= 3.22 cm/sec (1.27 in./sec), 6.06 cm/sec (2.39 in./sec), 8.91 cm/sec (3.51 in.sec), and 11.75 cm/sec (4.62 in./sec). The corresponding Reynolds numbers based on the wing chord length, respectively are: Re_c = 5800, 10920, 16060, and 21180. Suction hole Reynolds numbers per hole, and suction velocities per hole are tabulated in Table 3.7, for suction holes ranging from 1 to 5. From Figure 2.9 it can be seen that a maximum of 5 holes can be utilized for suction at any one time. The suction Reynolds numbers per hole and the suction velocities per hole range respectively from a low of Re_s/hole = 840 and v_s/hole = 26.5 cm/sec (10.4 in./sec) at Q = 10.5 cm^3/sec to a high of Re_s/hole = 8390 and v_s/hole = 265.2 (104.4 in./sec) at Q = 21.0 cm^3/sec. Table 3.8 indicates suction coefficients, C_Q at the different free-stream velocities (and Reynolds numbers based on wing chord length). C_Q's range from a low of C_Q = 0.01045 at Q = 10.5 cm^3/sec, V_∞=11.75 to a high of C_Q = 0.0760 at Q = 21.0 cm^3/sec, V_∞= 3.22.

Tests were carried out with the model aligned with the on-coming flow (i.e. at side

73

Table 3.7 Hole Reynolds numbers and suction velocities for various number of holes (streamlined body - flat plate junction)

Total number of suction holes open	Suction Rate, Q = 10.5 cm^3/sec (0.64 in.^{3}/sec)			Suction Rate, Q = 21.0 cm^3/sec (1.28 in.^{3}/sec)		
	Suction hole Reynolds number, Re$_s$/hole	Suction Velocity, v$_s$/hole		Suction hole Reynolds number, Re$_s$/hole	Suction Velocity, v$_s$/hole	
		cm/sec	in./sec		cm/sec	in./sec
1	4190	132.6	52.2	8390	265.2	104.4
2	2100	66.3	26.1	4190	132.6	52.2
3	1400	44.2	17.4	2800	88.4	34.8
4	1050	33.1	13.0	2100	66.3	26.1
5	840	26.5	10.4	1680	53.0	20.9

Table 3.8 Coefficient of suction for various velocities and Reynolds numbers for $Q = 10.5$ cm^3/sec, and $Q = 21.0$ cm^3/sec (wing - flat plate junction)

Free - Stream Velocity, V_∞		Reynold's Number, Re_c	Suction Coefficient, C_Q	
cm /sec	in. /sec		$Q = 10.5$ cm^3/ sec $= 0.64$ in.^{3} /sec	$Q = 21.0$ cm^3/ sec $= 1.28$ in.^{3} /sec
3.22	1.27	5800	0.0380	0.0760
6.06	2.39	10920	0.0202	0.0404
8.91	3.51	16060	0.0137	0.0275
11.75	4.62	21180	0.0104	0.0209

75

slip angle, $\beta = 0°$), and at a side slip angle, $\beta = 6°$. At $\beta = 0°$, a total of four holes maybe utilized for suction, namely hole #1, #3, #4 and #5 (refer to Figure 2.9). At $\beta = 6°$, all five holes maybe utilized, namely #1, #2, #3, #4, #5.

At $\beta = 0°$, with no suction applied, the flowfield exhibits a pattern much like the one generated by the cylinder - flat plate junction, with the size of the vortices created being much smaller. The on-coming flow separates from the flat plate very close to the wing - flat plate interface (approximately 1 cm from the interface, or at 0.055c measured from the leading edge, where c is the wing chord length). The separated flow evolves into a reasonably small spiral vortex (visible diameter, $d \approx 1$ cm). This vortex is much smaller in size when compared to the vortex generated in the cylinder - flat plate case. Much like the cylinder - flat plate case, the vortex spirals and travels around the wing and separates almost immediately (at approximately 5 - 10% chord length measured from the leading edge). The spiraling nature of the flow persists until about 90% chord, after which, the spiraling effect dissipates and the usual trailing-edge vortices are observed. Obviously, this is due to the streamlined nature of the wing. Figure 3.19 shows the top and side views of the flowfield at $\beta = 0°$, $V_\infty = 8.91$ cm/sec (3.51 in./sec), $Re_C = 16060$, with no suction applied.

At $\beta = 6°$, much the same flowfield as the $\beta = 0°$ case is observed, except now the size of the vortex that forms when the flow separates from the flat plate is larger in size. This vortex tends to travel down the right half of the wing (looking from top, refer to Figure 2.9), while on the left half the flow is much 'calmer' or smoother, displaying no signs of the spiral nature. Also evident is that the flow around the right half almost immediately separates from the wing (at approximately 5% c from the leading edge), while the flow around the left half stays attached for a longer distance (approximately 20% c measured from the leading edge). Figure 3.20 shows the side and top views of the flowfield at $\beta = 6°$, $V_\infty = 8.91$ cm/sec, $Re_C = 16060$, with no suction applied.

The main objective was to kill or partially eliminate the spiral vortex that forms ahead of the wing flat plate junction, thereby prompting prolonged attached flow as the flow travels around the wing curvature. Initially, suction was applied through hole #4 at a suction rate, $Q = 21.0$ cm^3/sec resulting in a suction coefficient, $C_Q = 0.0275$. The suction Reynolds number, $Re_S = 8390$ and the suction velocity, $v_s = 265.2$ cm/sec
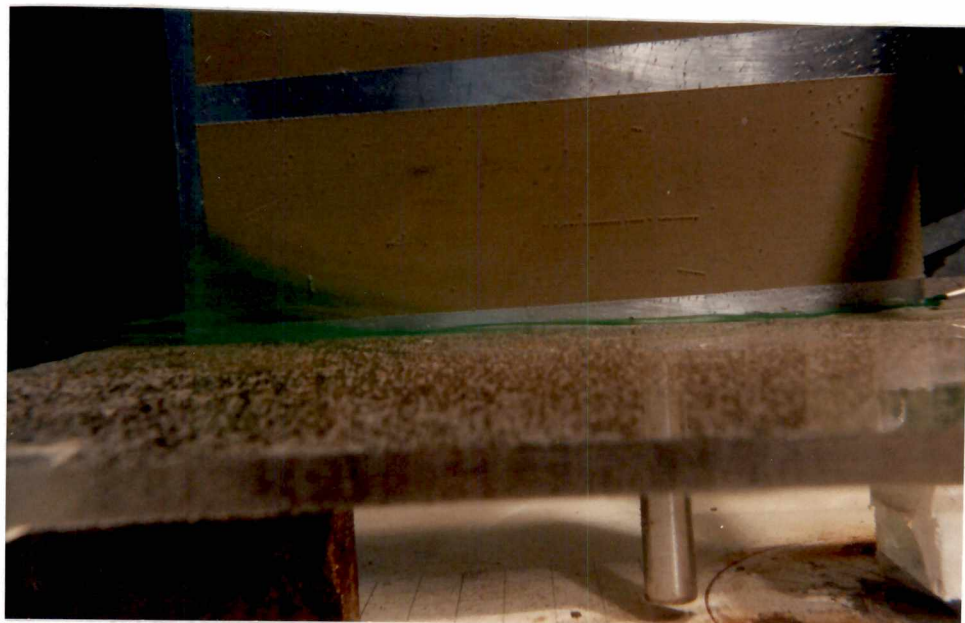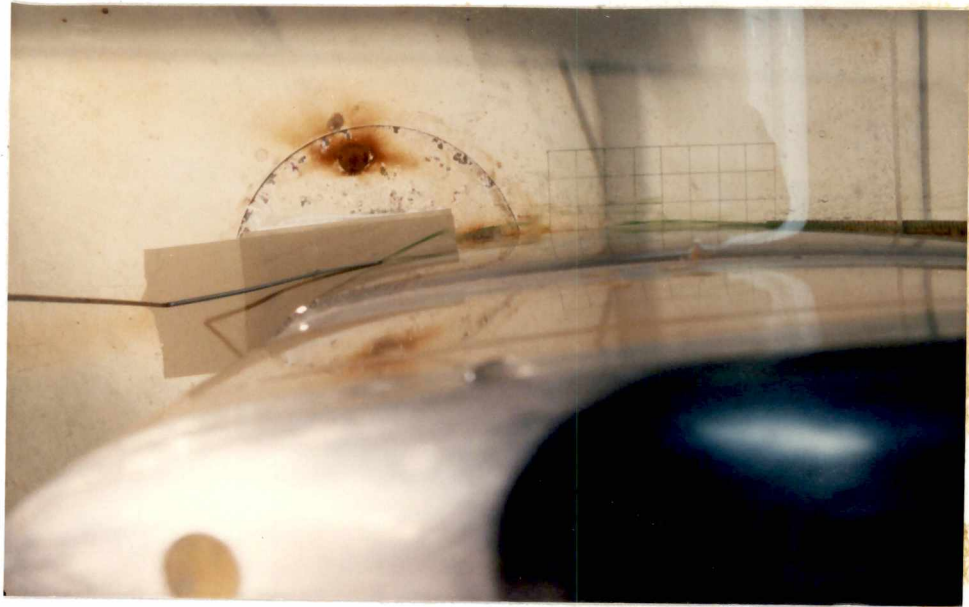
Figure 3.19 Top and bottom views of the flowfield with no
suction applied for $\beta = 0°$ ($V_\infty = 8.91$ cm/sec
Re = 16060

77
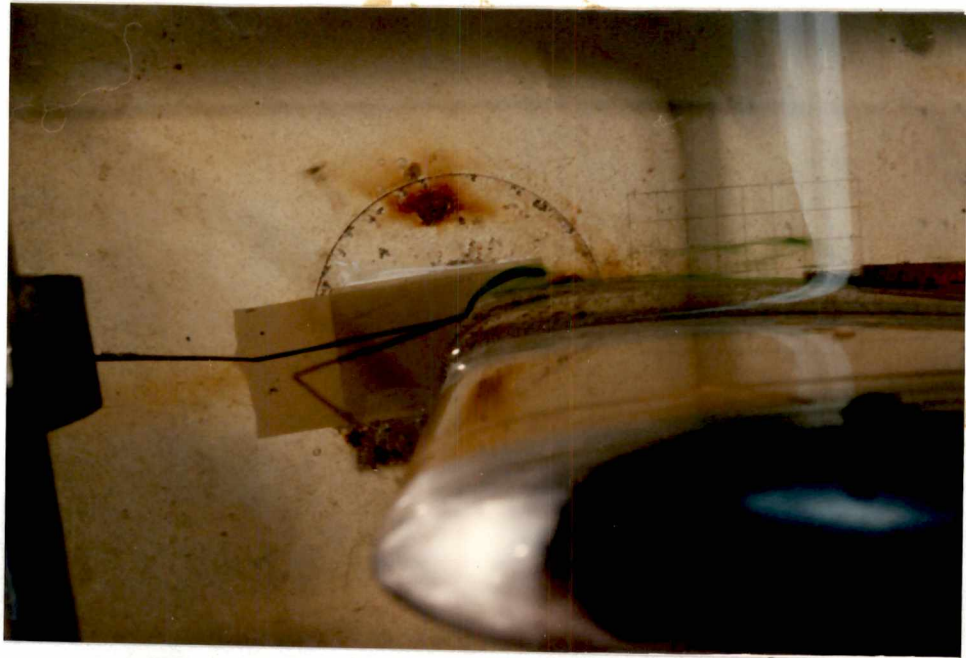
Figure 3.20 Top and bottom views of the flowfield with no
suction applied for $\beta = 6°$ ($V_\infty = 8.91$ cm/sec,
Re = 16060)

78

(104.4 in./sec). The flow now stays attached longer than the case without suction and the sporadic spiraling nature of the flow is reduced. Also the flow is more organized and less 'spiral-like' when compared to the 'no suction' case. At $\beta = 6°$, with #4 hole open for suction (with the same conditions), and appreciable improvement in the flowfield is not visible.

Next, suction was applied through two holes, #1 and #4, at $Q = 21.0$ cm^3/sec (C_Q = 0.0275). The resulting suction hole Reynolds number per hole and suction hole velocity per hole are respectively 4200 and 132.6 cm/sec (52.2 in./sec). The flow now is observed to stay attached to the wing to a much greater distance and the flow is very much more organized. However, for the $\beta = 6°$ case with the same conditions and suction through holes #1 and #4, the effects are not as dramatic. Not only does the flow separates well in advance when compared to the $\beta = 0°$ case, but it is also much more disorganized.

Since suction through holes #1 and #4 at $\beta = 6°$ did not produce highly effective results as desired (i.e. flow attachment was not prolonged to a greater distance nor was the flow more organized), suction was applied through three additional holes, namely #2, #3 and #5. Again the suction rate was kept a constant ($Q = 21.0$ cm^3/sec; C_Q = 0.0275) and the suction Reynolds number and velocity per hole are as follows: Re_s/hole = 2100; v_s/hole = 66.3 cm/sec (26.1 in./sec). It is evident that the flow now stays attached to the wing upto approximately 80 - 90% C and that the flowfield is much 'calmer' or smoother displaying very much more regularity. Again, compared to the 'two-hole' suction case (#1 and #4), a much more organized flow field is visible. The top and bottom views of the flowfield for the above conditions are illustrated in Figure 3.21.

Finally, for the $\beta = 0°$ case, suction was applied through four holes, namely #1, #3, #4 and #5. The top and bottom views of the resulting flowfield is shown in Figure 3.22. The flow velocity and Reynolds number respectively are 8.91 cm/sec and 16060. The suction rate is 21.0 cm^3/sec and the suction coefficient is 0.0275. From the top view it is evident that nearly full-chord attached flow is achieved (upto approximately 95% chord) and the flowfield is extremely organized. Again, in the side view the regularity of flow is further illustrated.
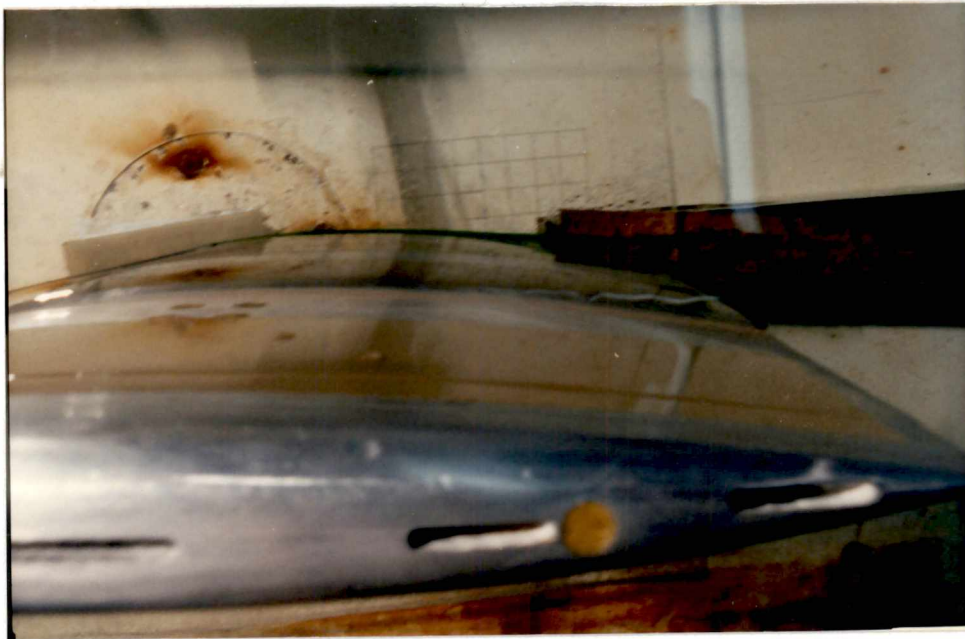
Figure 3.21 Views of the flowfield with suction applied through 4 holes
Q = 21.0 cc/sec and C_Q = 0.0275, at β = 6° (V_∞ = 8.91 cm/sec,
Re = 16060)

80
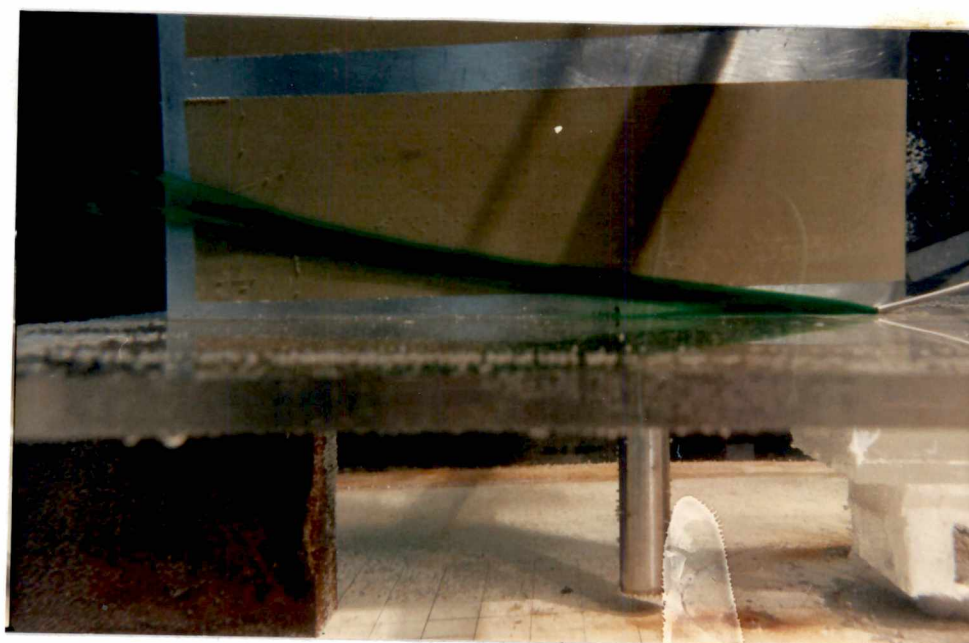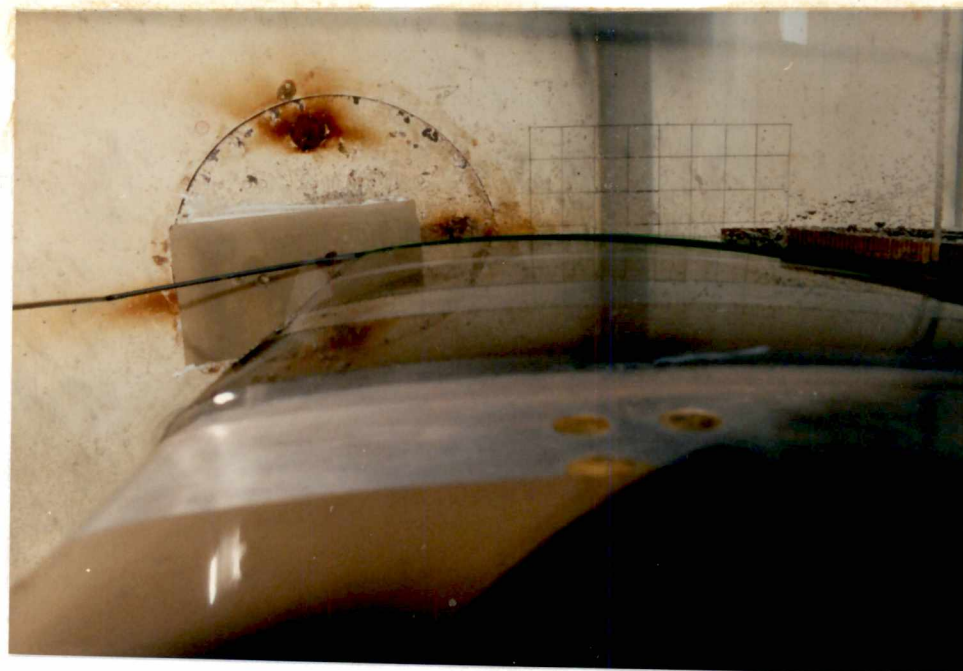
Figure 3.22 Views of the flowfield with suction applied through 5 holes
Q = 21.0 cc/sec and C_Q = 0.0275, β = 0° (V_∞ = 8.91 cm/sec,
Re = 16060

The structure of the flowfield is found to be insensitive to change in free-stream velocity in the range that experiments were conducted in, namely V_∞ = 3.22 cm/sec (1.27 in./sec, Re_C = 5080) to V_∞ = 11.75 cm/sec (4.62 in./sec, Re_C = 21180).

The flowfield is more receptive to changes in suction rates. The lower suction rate, Q = 10.5 cm^3/sec produced less effective results. In other words, the level of flow control achieved was not as impressive as in the case of Q = 21.0 cm^3/sec.

§ 3.3 WING AT VERY HIGH ANGLES OF ATTACK

The swept-forward wing model is contoured with a NACA 0012-64 airfoil giving it a thickness-to-chord ratio, t/c = 0.12, with a chord length, c = 16.2 cm (6.38 in.). The model was tested at the following free-stream velocities and corresponding Reynolds numbers based on wing chord length: V_∞ = 3.22 cm/sec (1.27 in./sec), 6.06 cm/sec (2.39 in./sec), 8.91 cm/sec (3.51 in./sec), 11.75 cm/sec (4.02 in./sec); Re_c = 5190, 9770, 14370, 18950. The model was tested at two high angles of attack, namely 30° and 40°. These angles of attack are well above the 'stall angle of attack' for this airfoil, and full-chord reversed or separated flow is observed on the entire wing surface, except for a small region near the nose of the wing at approximately 80-90% span towards the tip, just ahead of a vortex system that forms in the vicinity. The nature of this vortex, together with the flow field pattern around this vortex with and without suction will be discussed later in this section. The flowfield with no suction applied respectively at 30° and 40°, at Q = 21.0 cm^3/sec and C_Q = 0.0096 and 0.0075 respectively are illustrated in Figure 3.23. The flow velocity and Reynolds number are respectively 8.91 cm/sec and 14370.

Suction could be applied through any combinations of holes ranging from 1 to 37. Table 3.9 outlines the suction hole Reynolds number per hole and the suction velocity per hole for different number of hole used, for suction rates of Q = 10.5 cm^3/sec and Q = 21.0 cm^3/sec. Here the range of Re_s/hole is from 221 at Q = 10.5 cm^3/sec for 37 holes to 16380 at Q = 21.0 cm^3/sec for 1 hole. Suction coefficients for various free-stream velocities and Reynolds numbers are tabulated in Table 3.10. Suction coefficients range from C_Q = 0.0037 at Q = 10.5 cm^3/sec, V_∞ = 11.74 to C_Q = 0.0142 at Q = 21.0 cm^3/sec, V_∞ = 3.22, at α = 30°. For α = 40°, the range is: C_Q = 0.00285

82
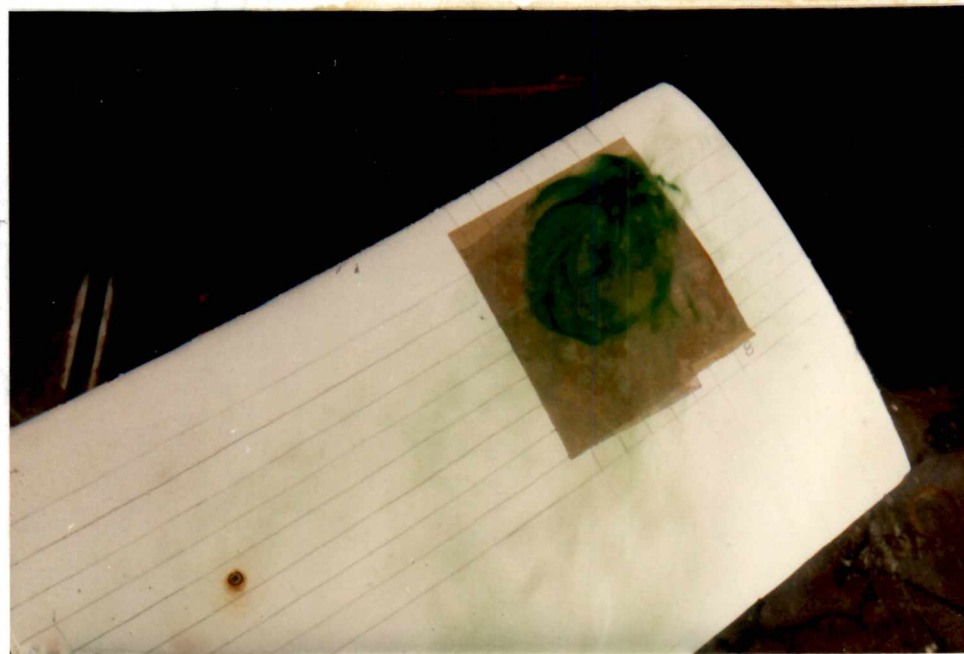
Figure 3.23 Views of flowfield with no suction applied at
α = 30° (top picture), 40° (bottom picture)
(V_∞ = 8.91 cm/sec, Re = 14370)

83

Table 3.9   Hole Reynolds numbers and suction velocities for various number of holes (swept - forward wing)

Total number of suction holes open	Suction Rate, Q = 10.5 cm^3/sec (0.64 in.^{3}/sec)			Suction Rate, Q = 21.0 cm^3/sec (1.28 in.^{3}/sec)		
	Suction hole Reynolds number, Re_s/hole	Suction Velocity, v_s/hole		Suction hole Reynolds number, Re_s/hole	Suction Velocity, v_s/hole	
		cm/sec	in./sec		cm/sec	in./sec
1	8190	132.6	52.2	16380	265.2	104.4
2	4000	66.3	26.1	8190	132.6	52.2
3	2730	44.2	17.4	5460	88.4	34.8
4	2050	33.1	13.1	4100	66.3	26.1
5	1640	26.5	10.4	3280	53.1	20.9
6	1365	22.1	8.7	2730	44.2	17.4
7	1170	18.9	7.4	2340	37.9	14.9
8	1020	16.6	6.5	2050	33.1	13.1
9	910	14.7	5.8	1820	29.5	11.6
10	820	13.3	5.2	1640	26.5	10.4

Table 3.10 Coefficient of suction for various velocities and Reynolds numbers for Q = 10.5 cm^3/sec, and Q = 21.0 cm^3/sec (swept - forward wing)

Free - Stream Velocity, V$_\infty$		Reynold's Number, Re$_c$	Suction Coefficient, C$_Q$			
			Q = 10.5 cm^3/ sec = 0.64 in.^{3}/sec		Q = 21.0 cm^3/ sec = 1.28 in.^{3}/sec	
cm /sec	in. /sec		AOA = 30°	AOA = 40°	AOA = 30°	AOA = 40°
3.22	1.27	5190	0.0215	0.0104	0.0430	0.0207
6.06	2.39	9770	0.0071	0.0055	0.0142	0.0110
8.91	3.51	14370	0.0048	0.0038	0.0096	0.0075
11.75	4.62	18950	0.0037	0.0028	0.0073	0.0057

85

at $Q = 10.5$ cm^3/sec, $V_\infty = 11.75$, and $C_Q = 0.0110$ at $Q = 21.0$ cm^3/sec, $V_\infty = 3.22$ cm/sec.

At an angle of attack, $\alpha = 40°$, the NACA 0012-64 is completely stalled and reversed flow is observed everywhere on the wing. The narrow region (the width equaling about 0.2C) is located to the right (or towards the wingtip in the spanwise direction) of a large horn vortex (visible diameter, $d \approx 0.3c$) and is centered at approximately 80% span and 30% chord, and to the left (towards the wing root in the spanwise direction) of a system of much smaller 'wingtip vortices' that form at the proximity of the wingtip. A schematic sketch showing the skin friction lines of the flow field at $\alpha = 40°$, $V_\infty = 8.91$ cm/sec (Re = 14370) is illustrated in Figure 3.24. (This schematic was sketched based on freezing certain frames of a video-taped sequence of the experiments, where continuous dye injection through a 'rake' of dye injection probes was utilized for flow visualization. Schematics of this nature that are referred to later on in this section were sketched in a similar fashion.) The susceptibility of the movement of the large vortex due to change in free-stream velocity (in the range in which tests were conducted, namely between $V_\infty = 3.22$ -11.75 cm/sec) is very minimal. With change in velocity the vortex moves very little and any movement is constrained to within an area that is small in size compared to the wing planform area. Here, the system of suction holes (described in § 2.3.4) were located encompassing the location of this horn vortex at $\alpha = 40°$. It was envisaged that if this detrimental vortex can be curtailed or reduced in size, flow reversal may be minimized and favorable flow could be obtained at least partially on the wing.

Figure 3.25 is a sketch of the flowfield at a freestream velocity of 8.91 cm/sec and at a Reynolds number of 14370, with suction through one hole at a suction rate of 21.0 cm^3/sec and a suction coefficient, $C_Q = 0.0075$. The suction hole is located (centered) at a distance of 2.22 cm from the wing leading edge and at a distance of 4.13 cm from the wing tip. The suction hole Reynolds number is $Re_S = 16380$ and the suction velocity is $v_s = 265.2$ cm/sec (104.4 in./sec). With the application of suction through this hole, the size of the vortex reduces approximately to that where the visible diameter, $d \approx 0.15c$. The vortex is also observed to move in the spanwise direction, towards the root of the wing. The movement of the center of this vortex is approximately 0.1 of the total span (i.e. the vortex which originally formed at 80% span, now moves to the 70% span location). The chordwise movement of the vortex is minimal. It is seen that the vortex moves slightly towards the wing leading edge
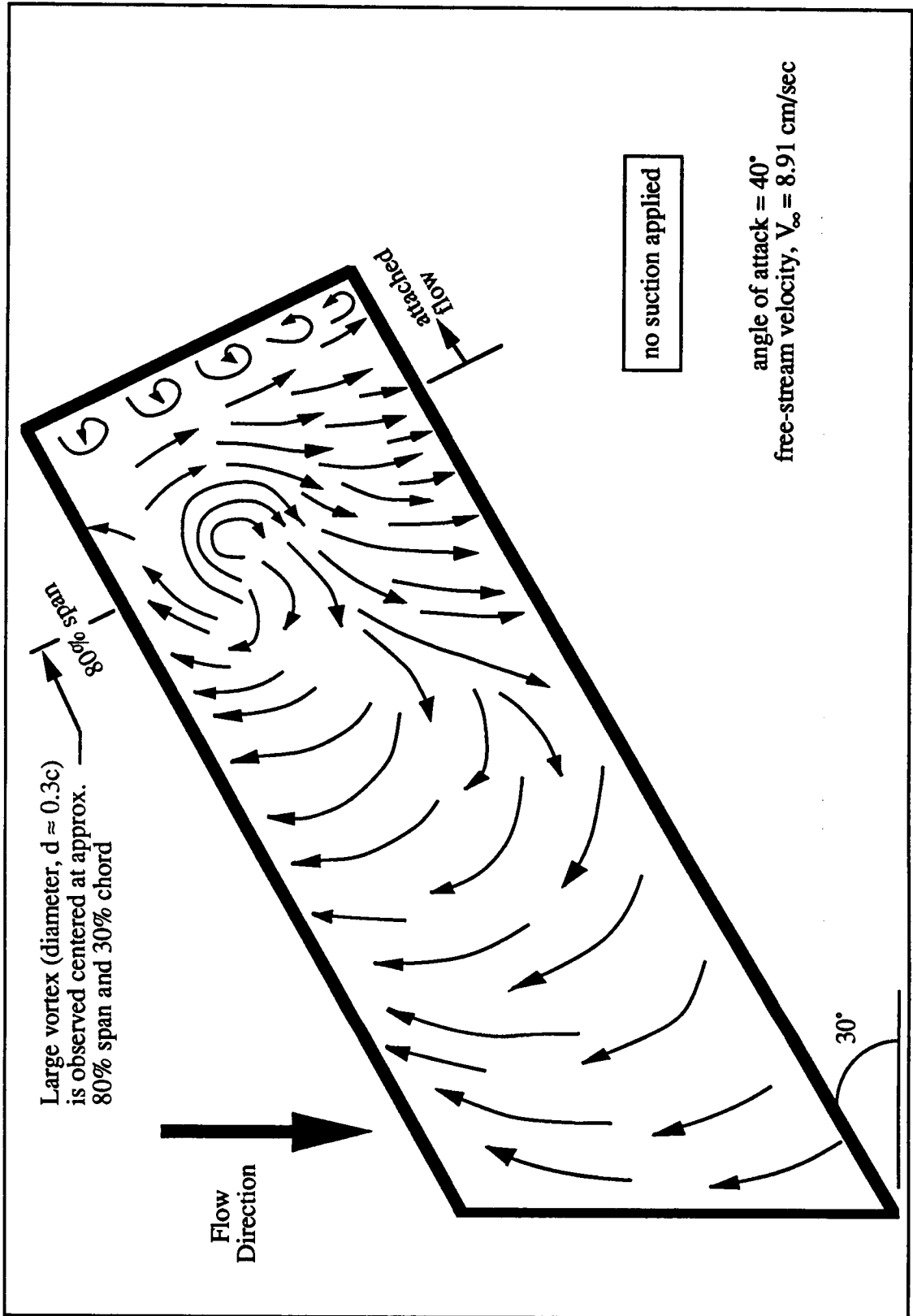
Figure 3.24 Schematic showing skin friction lines on wing at AOA = 40° and V∞ = 8.91 cm/sec, with no suction applied
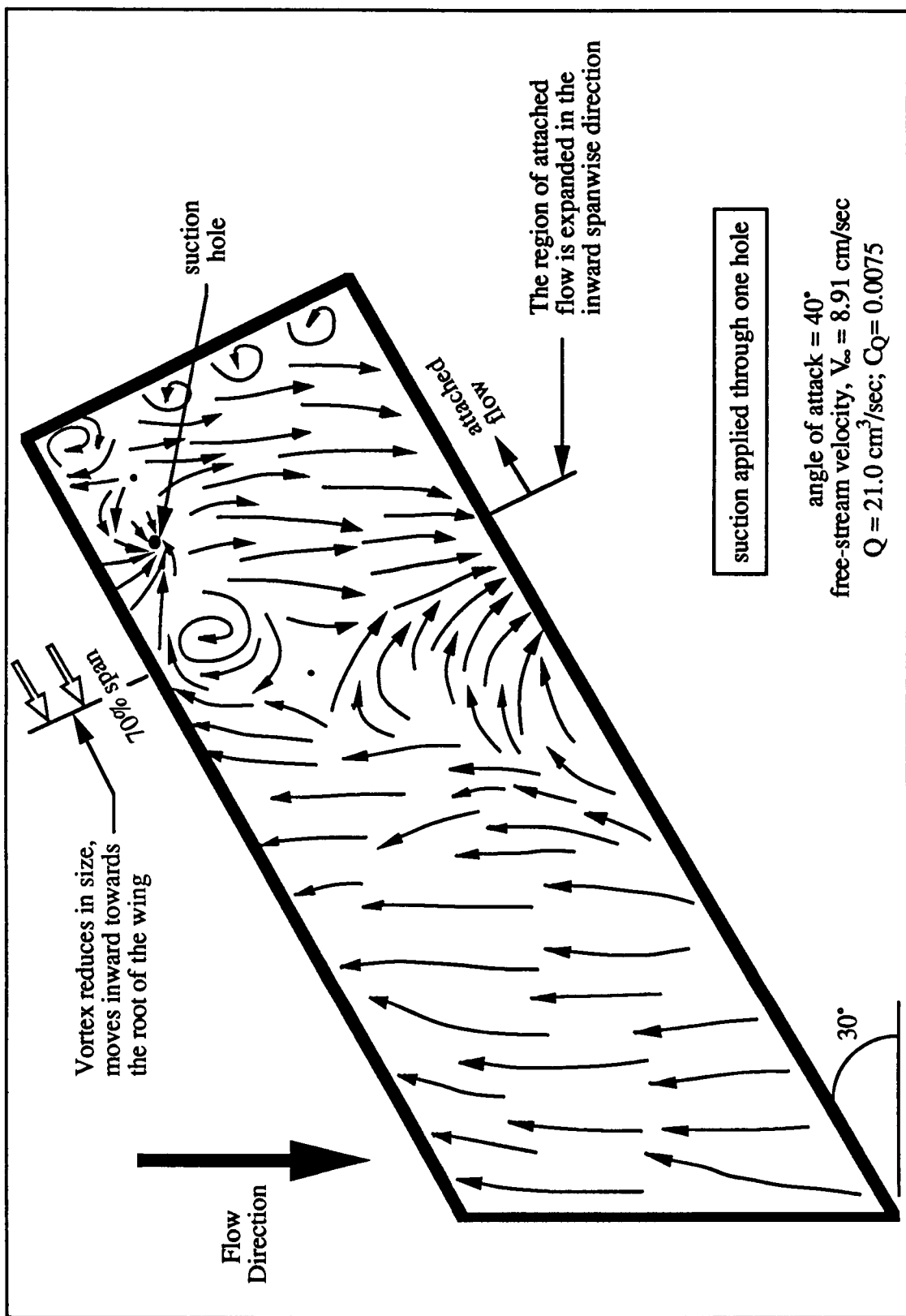
Figure 3.25 Schematic showing skin friction lines on wing at AOA = 40° and V_∞ = 8.91 cm/sec, suction through one hole

with suction, when compared to its original location without suction. This shift of the vortex from 80% to 70% span also expands the region of attached flow. As is evident in Figure 3.25, this vortex whose sense of rotation is in the clockwise direction. Hence, (looking from top) the direction of the flow induced by the vortex to the right of the vortex, is in the direction of the on-coming flow, while the flow to the left of the vortex (which is also partially induced by the presence of the vortex) is opposite to the direction of the on-coming flow (causing of course a 'flow reversal' situation). Hence the movement of the vortex from right to left (i.e. from closer to the tip of the wing towards the root) results in the region of attached flow being expanded also towards the left (or towards the root).

Next, another hole was opened for suction, which is located directly below (in the chordwise sense towards the trailing edge) the first hole. This did not result in any significant movement of the vortex. However, the region of attached flow was slightly expanded not in the spanwise direction, but rather in the chordwise direction (more closer to the trailing edge). Therefore, the next logical step seemed to be to open suction holes that are to the left (towards the root) of the original hole, in anticipation of a further rootward movement of the vortex, while opening holes towards the trailing edge would prove to serve no purpose and hence be redundant.

Now, four holes were utilized, the two additional holes being located directly to the left of the original holes. The consequent flowfield that results is shown in Figure 3.26. The velocity of the flow within each of the suction hole is v_s/hole = 252.8 cm/sec (99.5 in./sec), and the Reynolds number within each of the hole is Re_s/hole = 4095. It can be seen that the location of the vortex, now, is moved to 65% span and reduced in size slightly. As a result the region of attached flow is further expanded to upto approximately 55% span.

Finally, Figure 3.27 shows the flowfield scenario with suction through 5 holes. The suction hole quantities are as follows: Re_s/hole = 3280; v_s = 202.3 cm/sec (79.6 in./sec). Again, the 5th hole is located to the left of the existing holes. As expected, the vortex further moves towards the root of the wing to approximately 60% span, resulting in attached flow to as far as about 45-50% span.

The flowfield at α = 30° and 40°, with 4 holes open and with a suction rate of 21.0 cm³/sec and at a suction coefficient of 0.0038 and 0.0075 respectively at the above angles is illustrated in Figure 3.28. The flow velocity and Reynolds number are

89
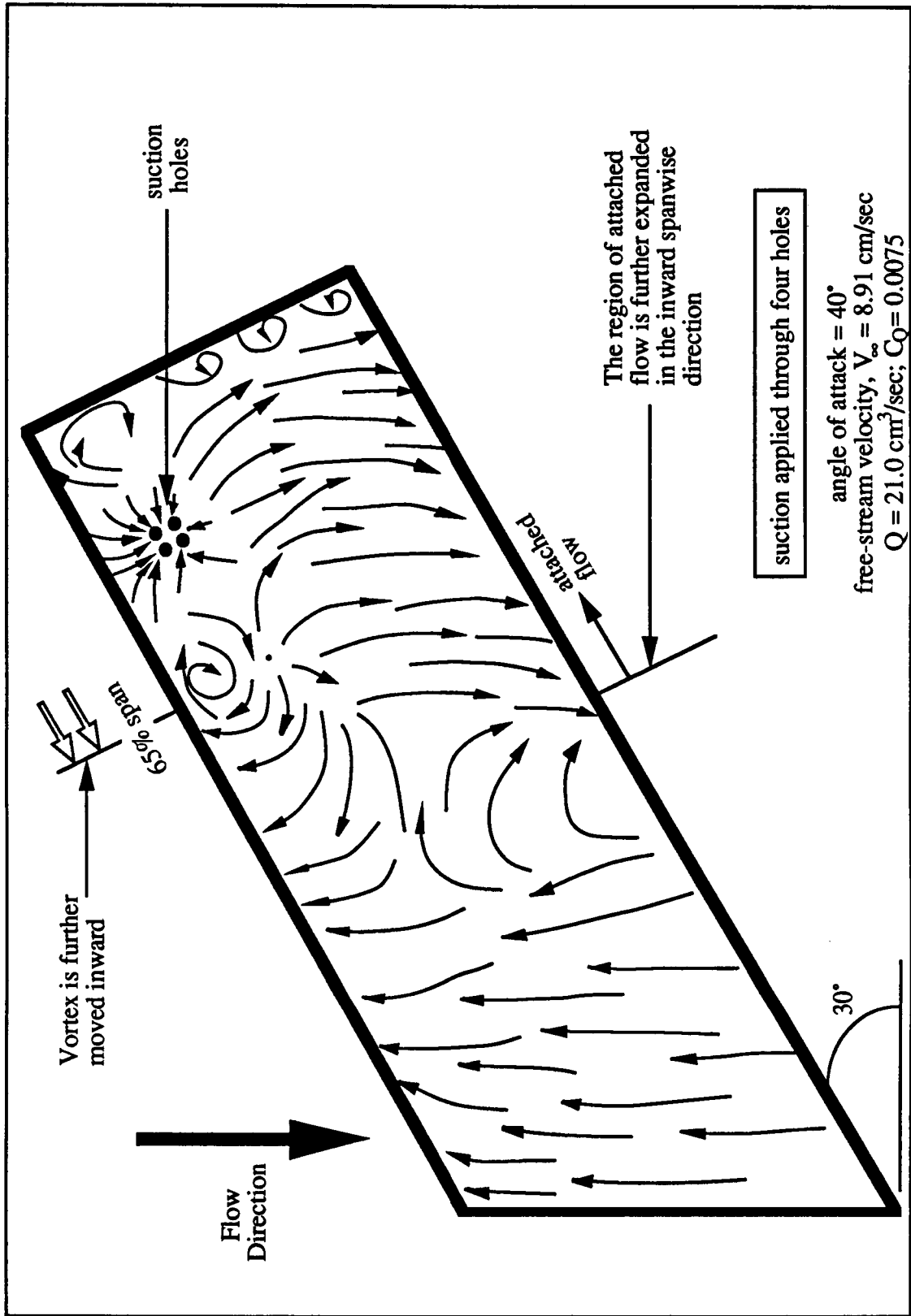
Figure 3.26 Schematic showing skin friction lines on wing at AOA = 40° and V∞ = 8.91 cm/sec, suction through four holes
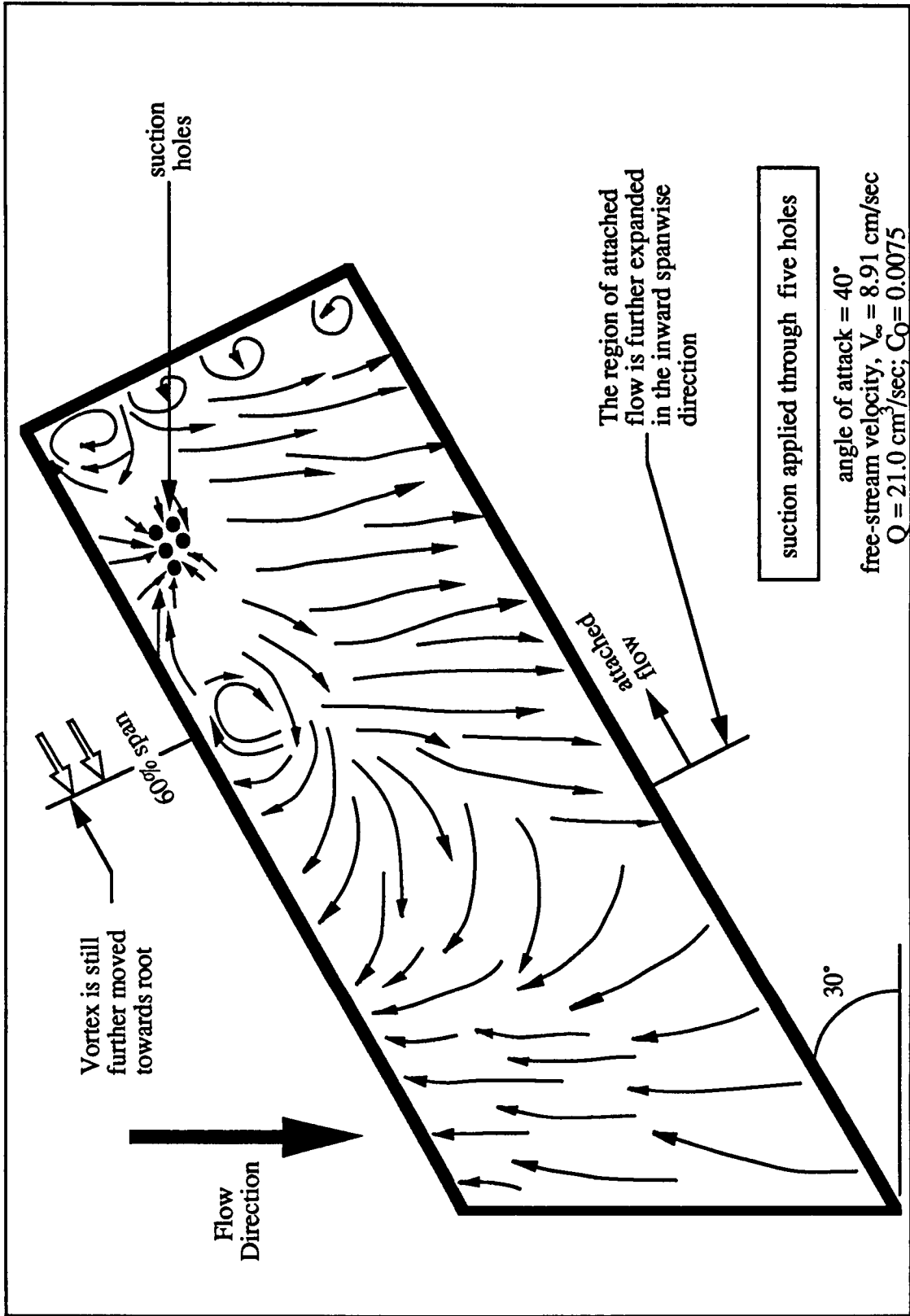
Figure 3.27 Schematic showing skin friction lines on wing at AOA = 40° and V∞ = 8.91 cm/sec, suction through five holes
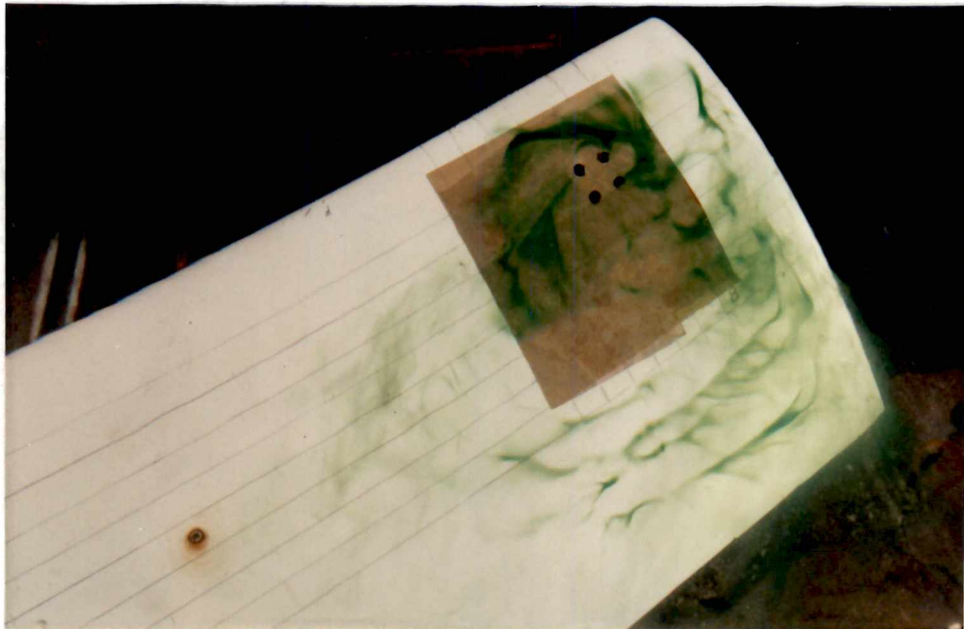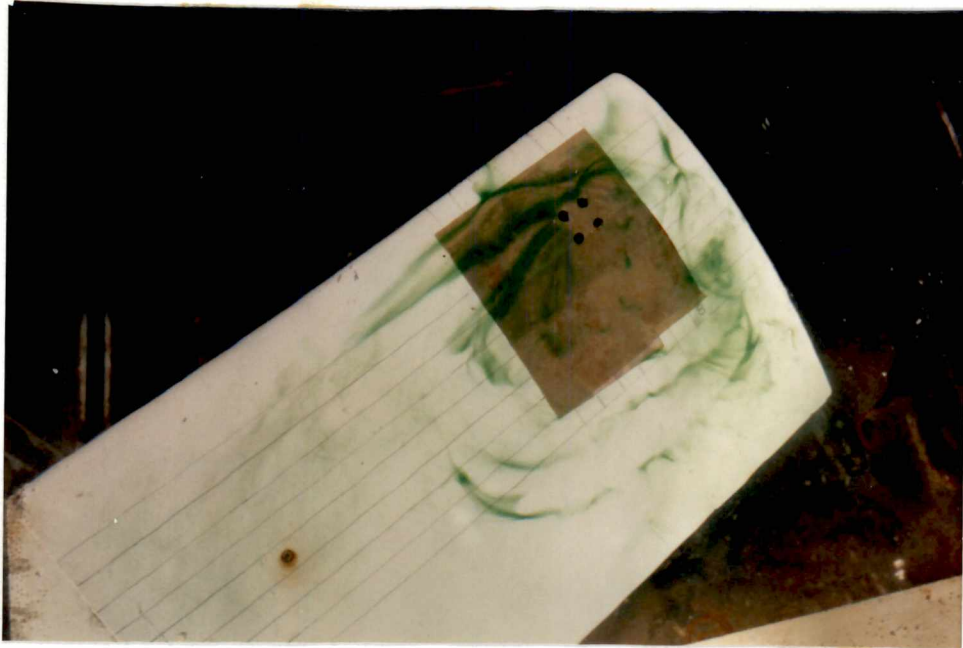
Figure 3.28 Flowfield with suction applied through 4 holes at
$\alpha = 30°$ (top picture), $40°$ (bottom picture),
$Q = 21.0$ cc/sec, $C_Q = 0.0075, 0.0038$
($V_\infty = 8.91$ cm/sec, Re = 14370)

92

respectively 8.91 cm/sec and 14370.

Further tests were conducted by including more suction holes located below the existing ones (i.e. towards the trailing edge). However, as mentioned before, the contribution to maintain attached flow is minimal. As the number of holes were increased in the chordwise direction towards the trailing edge, a redundancy in the effectiveness in the utilization of holes was clearly evident, as these extra holes did not promote any further favorable effect on the flowfield. On the other hand, as seen in Figures 3.25, 3.26 and 3.27, it is very clearly evident that the expansion of suction holes in the spanwise direction towards the root, prompts the vortex to move in that direction, and as a result expands the area of attached flow. Due to the limitations of the model design (i.e. suction holes were concentrated only around the initial location of the vortex), tests were not performed with further increase in suction holes towards the root. However, it is clearly evident that an expansion of suction holes towards the root will indeed expand the area of attached flow and perhaps even confine the vortex only to a region very close to the root and thereby inducing nearly full-chord and full-span attached flow.

The sensitivity of the location of the vortex with change in angle of attack, is observed to be minimal. At $\alpha = 30°$, the vortex was found to form at approximately the same location as that for $\alpha = 40°$. At $\alpha = 30°$, the vortex also exhibits similar movements in location (i.e. the distances and location that the vortex traverses with the application of suction through the various holes) as that of the $\alpha = 40°$ case. The pattern and tendency of the vortex movement for both $\alpha = 30°, 40°$ are essentially similar.

CHAPTER IV
CONCLUSIONS AND RECOMMENDATIONS

In this chapter, a summary of this study is presented followed by a short comparison with theoretical prediction. § 4.3 lists the conclusions drawn from the study. The final section is devoted to some recommendations for future study.

§ 4.1 SUMMARY OF STUDY

In the case of the cylinder, suction was applied through slots of 0.127 cm width and 29.2 cm length, located at 95°, 120°, 180°, -120°, and -95°. Various combination of slots were used for suction, specifically #1; #1, 2, 3; #1, 2, 3, 4; #1, 2, 3, 4, 5; #1, 2, 4, 5; and #1, 5. Tests were carried out at free-stream velocities of 3.22 cm/sec, 6.06 cm/sec, 8.91 cm/sec, and 11.75 cm/sec. The corresponding Reynolds numbers based on cylinder diameters are 1550, 2910, 4280, and 5650. Experiments were performed at a suction rate of 10.5 cm^3/sec and 21.0 cm^3/sec. At a total suction rate of 10.5 cm^3/sec, the coefficient of suction varied from 0.0062 to 0.0226, and at a rate of 21.0 cm^3/sec, the suction coefficient varied from 0.0124 to 0.0452. In general, the separation angle increases with increasing suction rate and decreasing Reynolds number (or free-stream velocity) in a linear manner. Even though unsymmetric suction produces remarkable delay in separation on the half where suction is applied, it actually worsens flow attachment on the half without suction. The most favorable results that equally benefit both halves of the cylinder (i.e. considering the entire cylinder as one entity, and not separate parts) are produced by application of symmetric suction. Utilizing slot #5 (which belongs to neither the upper nor the lower half and is located at 180°) together with slots #1, 2, 4, 5 proved to be redundant, and does not contribute towards further prolongment of attached flow.

For the cylinder - flat plate configuration, suction was applied through various combinations of holes, ranging from a single hole to a maximum of twelve holes of diameter 3.175 in. Suction rates of 10.5 cm^3/sec and 21.0 cm^3/sec were employed giving rise to suction coefficients that varied from 0.0066 to 0.0478. The range of free-stream velocities and the corresponding Reynolds numbers based on cylinder diameter were from 3.22 cm/sec to 11.75 cm/s and from 3665 to 13380. With suction applied through the three holes immediately adjacent to the cylinder and the farthest

94

center hole at a distance of 5.25 cm ahead of the cylinder (at a distance of 0.46D), The horse-shoe vortex is almost completely eliminated and the flow is found to stay attached to the cylinder to a greater distance, and consequently a smaller wake is generated. Suction through any of the 'side hole' farther from the cylinder does not produce any significant improvement in the flowfield and hence maybe considered redundant.

For the streamlined body - flat plate model, tests were carried out at side slip angles of 0° and 6°. The free-stream velocities ranged from 3.22 cm/sec to 11.75 cm/sec. The range of Reynolds numbers based on the wing chord ranged from 5800 to 21180. Suction was applied at rates of 10.5 cm³/sec and 21.0 cm³/sec. The suction coefficients ranged from 0.0104 to 0.0760. At $\beta = 0°$, with suction through holes #1, 3, 4, 5, nearly full-chord attached flow (upto approximately 0.95 c) is achieved quite easily. At $\beta = 6°$, with suction applied through holes #1, 2, 3, 4, flow attachment upto 80% chord is easily achieved.

In the case of the swept-forward wing, velocities were varied from 3.22 to 11.75 cm/sec, and the Reynolds numbers based on chord length were varied from 5190 to 18950. Suction coefficients ranged from 0.0028 to 0.0430 at suction rates of 10.5 and 21.0 cm³/sec. The models were tested at angles of attack of 30° and 40°. With suction applied through merely five holes the 'horn' vortex is moved to a location at about 60% span, and the size is reduced to approximately half as that without application of suction. The region of attached flow is expanded to about 45 -50% span and nearly full-chord.

§ 4.2 COMPARISON WITH PRINCIPLES

In general, the results from all the experiments agreed with predictions as governed by the principles that were based on the physics of the flow. The application of discrete, controlled suction, applied only at certain locations, proved to be very effective in achieving favorable and reasonable flow control.

The principles on which the discrete suction technique was based are essentially two-folded. First, wherever possible suction was applied only at local regions where separation was found to occur, and through the application of suction separation was

95

delayed to another region. Suction then was applied again at the new region of separation, in which case separation was further delayed, and so on. Second, suction was applied at locations in the vicinity of vortices or vortex systems that are a consequence of reversed, detached flow. Through the application of suction, these vortices were curtailed.

In the case of a very blunt body such as the cylinder model, suction was applied through a set of slots located (on both halves of the cylinder) in the proximity of the region where separation was found to occur. This essentially sucked the separating streamlines (volume of mass) and hence flow was made to stay attached longer, until the flow once again separated at a distance away from the original separation point. This illustrates that suction applied at only crucial points is very effective in delaying separation. Consider the case where suction, in addition to strategically located slots #1, 2, 4 and 5, is applied through slot #3, located at $\theta = 180°$. This (i.e. suction through all five slots) did not establish any appreciable improvement in the delay of separation when compared to suction through only slots #1, 2, 4, and 5. This is obviously due to the fact that slot #3 (located at $\theta = 180°$) was situated at a point where flow separation did not take place and was at a point the flow has long been separated.

In the cases of the body - flat plate junction configurations, again, the same principles were followed and found to be effective in achieving proper flow control. In these cases, again suction was applied at the point of separation on the flat plate. Even though this did not completely prevent separation from occurring, the separation vortex was considerably reduced in size. Next, suction was applied in the path of the horse-shoe vortex tube that follows the contour of the particular body. This application, in the case of the cylinder - flat plate junction configuration, almost totally alleviated the horse-shoe vortex, and in the case of the streamlined body - flat plate junction configuration, completely alleviated the horse-shoe vortex. Here again, the prediction that applying suction at irrelevant points does not contribute towards achieving effective flow control is established. This is evident by the results obtained when suction was applied through hole located at regions other than where separation occurred, in which cases, no improvements in the flow patterns were observed.

Consider the case of a wing (in this study, the swept-forward wing) at high angle of attack with massive flow separation on the lee-side surface. Suction was originally applied at the core of the 'horn' vortex that formed on the wing which was a consequence of reversed flow in the entire region away from the wing-tip. Although

the vortex could not be totally eliminated, it was appreciably reduced in size and the location of the vortex was moved towards the root of the wing. This reulted in an expanded region of attached flow. Further suction near the new location of the vortex further moved the vortex towards the root. It is conceivable to design a procedure that will follow the vortex shifting. This is done by continuously applying suction, so as to further reduce the adverse pressure gradient and to alter the flow pattern. This may totally alleviate the 'horn' vortex. Due to time and budgetary constraints, this point has not been pursued to its completion.

The above experiments demonstrate that the theoretical principles indeed work well in curtailing the flow separation or minimizing its detrimental effects by applying very localized slot or hole suctions.

§ 4.3 CONCLUSIONS

For the cylinder

(1) In general, the separation angle reduced with increase in free-stream velocity and Reynolds number, i.e. at lower speeds and Reynolds numbers the flow stayed attached on the cylinder to a greater distance. The variation of separation angle with velocity and Reynolds number is found to be linear.

(2) In general, with the application of suction, the separation angle increased. The separation angle also increased with increasing suction coefficients. The suction coefficients reduced with increasing Reynolds numbers. The increase in separation angle with suction rate of 0 to 10.5 cm^3/sec is more effective than the increase from 10.5 cm^3/sec to 21.0 cm^3/sec.

(3) Symmetric suction produced better results on both halves of the cylinder.

For the cylinder - flat plate junction

(1) Flow is observed to separate from the flat plate ahead of the cylinder - flat plate interface. The distance varies with varying Reynolds number and free-stream velocity

and is between 0.4D and 0.5D (where D is the cylinder diameter) for Reynolds numbers between 3665 and 13380.

(2)   The best results were obtained when simultaneous suction was applied through a hole located at the separation point and through holes immediately adjacent to the cylinder. The resulting flowfield is one in which the size of the initial horse-shoe vortex evolving into one of a 'string-like' nature, where the spiraling effect is almost eliminated. The flow is also observed to stay attached to the cylinder longer, and hence separation is delayed, causing a smaller wake, approximately half the size of the wake with no suction applied.

(3)   Doubling the suction rate did not provide significant increase in the effectiveness of flow control, and it is observed that the flow is insensitive or non-responsive to any further increase in suction rates.

(4)   Flow speed (and Reynolds number) are more crucial to the final form of the flowfield. With increase in Reynolds number, the size of the initial vortex is observed to increase and the spiraling nature of the subsequent vortex tube is intensified. Flow separation from the cylinder is also observed to occur much sooner.

For the streamlined body - flat plate junction

(1)   With suction applied through one hole alone, located at the proximity of the separation point on the flat plate, the spiraling nature of the horse-shoe vortex was nearly completely eliminated.

(2)   Further suction through holes located immediately next to the wing and along the contour of the wing, attached flow was observed upto 80 - 85% chord for $\beta = 6°$. At $\beta = 0°$, attached flow was observed upto 95% chord. The wake at the wing trailing edge - flat plate interface was almost nonexistent.

For the wing at high angles of attack

(1) Application of suction through a hole located close to the core of the large clockwise-rotating 'horn' vortex ($d \approx 0.3c$) observed in the vicinity of 80% span and 30% chord, reduced the size of the vortex and moved it towards the wing root. Simultaneous suction through the original hole and through holes adjacent to the

original hole and along the direction of the wing span towards the root, further moved the vortex towards the root. As a result of this movement, attached, non-reversed flow was observed to the right of the vortex extending all along the chord.

(2) Angles of attack and Reynolds numbers were the more dominant factors governing flow separation. Increasing the suction rate at the same location did not significantly increase the effectiveness which indicates that the location should be varied as the vortex shifts towards the root. A change in angle of attack, though did not move the vortex significantly, slightly altered the size of the vortex.

Overall remarks compared with other researchers:

It is difficult to compare directly the present study with others due to differences in geometries, flow conditions, etc. Nevertheless, it might be informative to list them all so that a general 'overview' may be realized. This outline is given in Figure 4.1. It can be seen through rough comparisons that the present proposed technique is superior than the others, including a severe case of lee-side separation control at much higher angles of attack studied by others.

§ 4.4 RECOMMENDATIONS

In the case of the cylinder, separation angle is found to be more sensitive to change in Reynolds number and hence it is worthwhile to spend more time experimenting into this aspect of the study. Flow Reynolds numbers could be extended to a broader regime and the effects observed. Due to a steady decrease in the separation angle with increasing Reynolds number, it may require more slots spaced closer together.

In the case of the cylinder - flat plate junction, since utilizing the 'side holes' located in the immediate vicinity of the cylinder resulted in a significant change in the flowfield, future tests should include more suction holes on the flat plate all along the contour of the cylinder and a broader Reynolds number range.

In the case of the streamlined body - flat plate junction, since very favorable results were obtained within the range of suction rates used, further experimentation with this configuration is not needed unless orders of change in Reynolds numbers are

99

Current Research	Previous Research
Medium: Water Free-stream Velocity: $V_\infty = 3.22 - 11.75$ cm/sec $= (1.27 - 4.62$ in./sec) Reynolds Number: $Re_D = 1546 - 5650$ Suction Slot Velocity: $v_s = 0.6 - 6.0$ cm/sec $= (0.22 - 2.22$ in./sec) Suction Slot Reynolds Number: $Re_s = 7.59 - 75.90$ Suction Coefficient: $C_Q = 0.0062 - 0.0452$ • Non-reversed full-chord attached flow was achieved upto 45%-50% span.	<u>Phenninger (1949)</u> - 17% thick airfoil - Suction slots along the chordwise direction - unswept wing, zero angle of attack $Re_D = 2.5 \times 10^6$ **Medium: Air** $C_Q = 0.0014 - 0.0018$ • Full-chord laminar boundary layer on both surfaces <u>Braslow, Burrows, Tetervin, and Visconti (1951)</u> - NACA 64A010, chord length = 3 ft. - Suction through porous surface centered at midspan and covers the entire chord - Unswept wing, zero angle of attack $Re_D = 19.8 \times 10^6$ **Medium: Air** $C_Q = 0.012$ $v_s = 6$ in./sec • Full-chord laminar flow <u>Poppleton (1955)</u> - 40° sweepback wing, zero angle of attack - Continuous and slot suction in the nose region $Re_D = 1.3 \times 10^6$ $C_Q = 0.0037$ (continuous suction) **Medium: Air** $C_Q = 0.009$ (slot suction) • Full-chord laminar flow was not achieved

Figure 4.1 Comparison of current research with previous research (flow parameters and other details) for the wing model

Current Research	Previous Research
Medium: Water Free-stream Velocity: V_∞ = 3.22 - 11.75 cm/sec = (1.27 - 4.62 in./sec) Reynolds Number: Re_D = 1546 - 5650 Suction Slot Velocity: v_s = 0.6 - 6.0 cm/sec = (0.22 - 2.22 in./sec) Suction Slot Reynolds Number: Re_s = 7.59 - 75.90 Suction Coefficient: C_Q = 0.0062 - 0.0452 • Non-reversed full-chord attached flow was achieved upto 45%-50% span.	<u>Gregory and Walker (1955)</u> - NACA 63A009 - Unswept wing, AOA = 14° - Distributed suction over entire chord area Re_D = 3.5 X 10^6 **Medium: Air** C_Q = 0.0023 • Separation was avoided at AOA = 14° <u>Gross (1962)</u> - 4% thick airfoil, 17 ft. chord - 100 suction slots (all along chord) - straight wing, zero angle of attack Re_D = 26 X 10^6 **Medium: Air** C_Q = 0.0013 <u>Pfenninger, et al. (19550)</u> - F - 94 aircraft (flight tests) - Tapered wing, NACA 65-213, unswept, AOA = 0° - slot suction between 41.5%c and 94%c 12 slot case: Re_D = 25 X 10^6 69 slot case: Re_ℓ = 36 X 10^6 C_Q = 0.00034 C_Q = 0.0029 • Full-chord laminar flow **Medium: Air**

Figure 4.1 (Cont.) Comparison of current research with previous research (flow parameters and other details) for the wing model

101

considered. Even at an increased free-stream velocity, the flow should be very controllable, and should not pose difficulty in curtailing any of the prevailing vortices. Experimentation with a thicker airfoil might be of interest. Configurations with higher side-slip angles may be more interesting. Evident from the current tests, flow control may be achieved with relative ease where streamlined bodies are involved.

In the case of the swept-forward wing, future experiments should include suction applied through holes located all along the span at approximately 20% chord. This may move the vortex completely to the root of the wing and attached flow may be established to the most part of the span.

In this study, the concept of applying suction intelligently and achieving better results of flow control has been experimentally verified. The study serves as a foundation for further detailed studies that would allow for more quantitative answers to practical engineering problems.

BIBLIOGRAPHY

BIBLIOGRAPHY

1. Bacon, J. W. Jr., Tucker, V. L., and Pfenninger, W., "Experiments on a 30° swept, 12% thick symmetrical laminar suction wing in the 5- by 7-ft. University of Michigan Tunnel", Report No. BLC-93, Northrop Aircraft, Inc., February 1957.

2. Betz, A., "History of boundary layer control in Germany", Boundary Layer and Flow Control (edited by Lachmann, G. V.), Pergamon Press, Ltd., 1961.

3. Braslow, A. L., Visconti, F., and Burrows, D. L., "Priliminary wind tunnel investigation of the effect of area suction on the laminar boundary layer over an NACA 64A010 airfoil", NACA RM L7L15, 1948.

4. Braslow, A. L., Burrows, D. L., Tetervin, N., and Visconti, F., "Experimental and theoretical study of area suction for the control of laminar boundary layer on a NACA 64 010 airfoil:, NACA Report No. 1025, 1951.

5. Burrows, D. L., and Schwartzberg, M. A., "Experimental investigation of an NACA 64A0101 airfoil section with 41 suction slots on each surface for control of laminar boundary layer", NACA TN 2644, 1952.

6. Bushnell, D.M., and Tuttle, M.H., "Survey of Bibliography on Attainment of Laminar Fow Control in Air using Presure Gradient and Suction", NASA Reference Publication 1035, September, 1979.

7. Carlson, J. C., Phenninger, W., and Bacon, J. W., Jr., "Low drag boundary layer suction experiment using a 33° swept 15% thick laminar suction wing with suction slots normaal to leading edge", NOR-64-281 Northrop Corporation, November 1964.

8. Carmichael, B. H., and Raspet, A., "Flight observations of suction stabilized boundary layers", Aeronautical Engineering, Volume 13, No. 2, pp. 36 - 41 February, 1954.

9. Chang, Paul K., "Control of Flow Separation: Energy Conservation, Operational Efficiency, and Saftey", Hemisphere Publishing Corporation, 1976.

10. Floryan, Jerzy M. and Saric, William S., "Effects of suction on Gortler Instability of boundary layers", AIAA Journal, Volume 21, pp. 1635 - 1639, 1983.

11. Goldsmith, J., and Meyer, W. A., "Preliminary experiments on laminar boundary layer suction through circular holes at high Reynolds numbers and low turbulence", Report No. BLC-23, Northrop Aircraft, Inc., December, 1953.

12. Goldsmith, J., "Experiments with laminar boundary layer suction through rows of closely spaced circular holes at high Reynolds numbers and low turbulence", Report No. BLC-36, Northrop Aircraft, Inc., March 1954.

13. Goldsmith, J., "Additional experiments on laminar boundary layer suction through holes at high Reynolds numbers and low turbulence", Report No. BLC-28, Northrop Aircraft, Inc., February 1954.

14. Goldsmih, J., "Critical suction quantities and pumping losses associated with laminar boundary layer suction through rows of closely spaced holes", Report No. BLC-72, Northrop Aircraft, Inc., February 1955.

15. Goldsmith, J., "Investigation of the flow in a tube with laminar suction through 80 rows of closely spaced holes", Report No. BLC-86, Northrop Aircraft, Inc., March 1956.

16. Goldsmith, J., and Meyer, W. A., "Laminar flow experiments in the inlet length of a 2-in. tube at high Reynolds numbers and small external disturbances with boundary layer suction through hole", Summary of Boundary Layer Control Research, WADC Technical Report 56-111, U. S. Air Force, pp. 8 - 10, 18 - 19, 32 - 38, April 1957.

17. Goldstien, S., "Low drag and suction airfoils", Journal of Aeronautical Sciences, Volume 15, No. 189, 1948.

18. Goldstein, S., "Theoretical methods for the design of airfoils specially suited for slot suction", Journal of Aeronautical Sciences, Volume 15, No. 189, 1948.

19. Gregory, N., and Walker, S., "Wind tunnel test on the NACA 63 009 airfoil with distributed suction over the nose", British ARC, R & M No. 2900, 1955.

20. Gross, L, W., "Investigation of a laminar suction modified Sears-Haack body of revolution in the Norair 7- by 10-ft. wind tunnel", Summar of Boundary Layer Control Research, Volume I, pp. 155 - 165, U. S. Air Force, March 1964.

21. Gross, L. W., "Investigation of a laminar suction body of revolution having a cylindrical center section in the Norair 7 by 10 wind tunnel", NOR-64-116, Northrop Corporation, May 1964.

22. Groth, E. E., "Calculation of boundary layer with continuous suction around a body of revolution of fineness ratio 8", Report No. BLC-5, Northrop Aircraft, Inc., August 1953.

23. Groth, E. E., "Low speed wind tunnel experiments on a body of revolution with low drag boundary layer suction", Report No. NAI-58-335, Northrop Aircraft, Inc., may 1958.

24. Head, M. R., and Johnson, D., "Flight experiments on boundary layer control for low drag", British ARC, R & M No. 3025, March 1955.

25. Holstein, H., "Messungen zur laminarhaltung der grenzschicht durch absaugung an einen trag flügel", Bericht s10, L.G.L., Preisausschreiben, pp. 17 - 27, 1940.

26. Kay, J. M., "Boundary layer flow along a flat plate with uniform suction", British ARC, R & M No. 2628, 1953.

27. Keeble, T. S., "Flight tests of the suction wing glider", Report No. A.71, Aeronautical Research Laboratory (Melbourne), May 1951.

28. Kosin, R. E., "Laminar flow control by suction as applied to the X-21A airplane", AIAA Paper No. 64-284 (1st AIAA Anual Meeting, Washington, D. C.), 1964.

29. Kozlov, L. F., and Tsyganyuk, A. I., "Drag on bodies of revolution with boundary layer suction", Fluid Mechanics - Soviet Res., Volume 5, No. 1, pp. 136 - 139, January - February 1976.

30. Lachmann, G. V., "Boundary Layer and Flow Control - Principles and Application", Volumes I, II, Pergamon Press, Ltd., 1961.

31. Landeryou, R. R., and Porter, P. G., "Further tests of a laminar flow swept wing boundary layer control by suction", Report No.192, College of Aeronautics, Cranfield, U.K., May 1966.

32. Lighthill, M. J., "A theoretical discussion of wings with leading edge suction", British ARC, R & M, No. 2162, 1945.

33. Lighthill, M. J., "Laminar Boundary Layers", ed. L. Rosenhead, pp 46 - 13, Oxford University Press, 1963.

34. Liu, M. J., and Su, W. H., "Some developments in vortex moyion research", Acta Aero. Astro. Sinica, Vol. 6,1, 1985.

35. Loftin, L. K., Jr., and Burrows, D. L.,"Investigations relating to the extension of laminar flow by means of boundary layer suction through slots", NACA TN 1961, 1949.

36. Loftin, L. K., Jr., and Burrows, D. L., "Further laminar flow experiments in a 40-ft. long 2-in. diameter tube", Report No. AM-133, Northrop Aircraft, Inc., February 20, 1951.

37. Loftin, L. K. Jr., and Horton, E. A., "Experimental investigation of Boundary layer suction through slots to obtain extensive laminar boundary layers on a 15% thick airfoil section at high Reynolds numbers", NACA RM L52D02, 1952.

38. McCormick, B. W., "An experimental study of drag reduction by suction through circumferential slots on a bouyantly propelled axisymmetric body", Naval Hydrodynamics - Ship motions and drag reductions, ARC-112, Office of Naval Research, Department of Navy, pp. 1001 - 1015

39. Meyer, W. A., "Smoke observations of the laminar flow in an 8-in. tube with suction through holes", Summary of Laminar Boundary Layer Control Research, WADC Technical Report No. 56-111, U. S. Air Force, pp. 10 - 12, 18 - 19, 39 - 41, April 1957.

40. Moss, G. S., "Low speed wind tunnel tests with suction slots on a wing of 45° seepback", Unpublished M.O.S (British Ministry of Supplies) Paper, 1947.

41. Pankhurst, R. C., and Gregory, N., "Power requirements for distributed suction", British ARC, Current Paper 82, 1948.

42. Pankhurst, R. C., and Thwaites, B., " Experiments on the flow past a porous circular cylinder fitted with a Thwaites flap", British ARC, R & M No. 2787, 1950.

43. Pearce, W. E., "Progress at Douglas on laminar flow control applied to commercial transport aircraft", AIAA Report No. ICAS-82-1.5.3, pp. 811 - 817, 1982.

44. Phenninger, W., "Investigations on drag reduction of wings, in particular by means of boundary layer suction", NACA TM 1181, 1947.

45. Phenninger, W., "Experiments on a laminar suction airfoil of 17% thickness", Journal of Aeronautical Sciences, Volume 16, No. 4, April 1949.

46. Phenninger, W., "Experiments with laminar flow in a 2-in. diameter, 40-ft. long tube at high Reynolds numbers", Report No. AM-128, Northrop Aircraft, Inc., December 20, 1950.

47. Phenninger, W., "Boundary layer suction experiments with laminar flow in a tube at high Reynolds numbers with one suction slot", Report No. AM-134, Northrop Aircraft, Inc., February 20, 1951.

48. Phenninger, W., "Experiments with laminar boundary layer suction in a tube at high Reynolds numbers with 8 suction slots", Report No. AM-141, Northrop Aircraft, Inc., May 1951.

49. Phenninger, W., "Experiments with a 15% thick slotted laminar suction wing model in the NACA, Langley Field, low turbulence wind tunnel", Technical Report 5982, U. S. Air Force, April 1953.

50. Phenninger, W., and Meyer, W. A., "Transition experiments in the inlet length of a 1-in. I.D. tube at high Reynolds numbers and low turbulence", Report No. BLC-24, Northrop Aircraft, Inc., November, 1953.

51. Phenninger, W., Moness, E., and Sipe, O. E., Jr., "Investigation of laminar flow in a tube at high Reynolds numbers and low turbulence with boundary layer suction through 80 slots", Report No. BLC-53, Northrop Aircraft, Inc., July 1954.

52. Phenninger, W., Groth, E. E., Carmichael, B. H., and Whites, R. C., "Low drag boundary layer suction experiment in flight on the wing glove of a F-94A airplane", NAI-55-458, Northrop Aircraft, Inc., April 1955.

53. Phenninger, W., Gross, L., and Bacon, J. W. Jr., "Experiments on a 30° swept 12% thick symmetrical laminar suction wing in the 5-ft. by 7-ft. Michigan tunnel", Report No. BLC-93, Northrop Aircrat, Inc., February 1957.

54. Phenninger, W., Meyer, W. A., Moness, E., and Sipe, O. E., Jr., "Laminar flow experiments in the inlet length of a 2-in. tube at high Reynolds numbers and small external disturbances with boundary layer suction through 80 slots", Summary of Laminar Boundary Layer Control Research, WADC Technical Report No. 56-111, U. S. Air Force, pp. 2 - 8, 18, 20 - 29, April 1957.

107

55.   Phenninger, W., and Gault, D. E., "Experimental investigation of a 30° swept 12% laminar suction wing in NASA Ames 12-ft. presure wind tunnel", Report No. NOR-60-108 Northrop Corporation, October 1961.

56.   Poppleton, E. D., "Boundary layer control for high lift by suction at the leading edge of a 40° swept-back wing", British ARC, R & M No. 2897, 1951.

57.   Prandtl, L., "Uber Flüssigkeitsbewegung bei sehr kleiner reibung", Verh.d.III. Intern. Mathem. Kongresses, Heidelburg, 1904. (Neudruck in Prandtl-Betz, Vier Abhandlungen zul Hydro- und Aerodynamik, Göttingen, 1927.), Auslieferung durch springer.

58.   Reed, H. L., and Nayfeh, A. H., "Stability of flow over plates with porous suction strips", AIAA Paper No. 81-1280 (AIAA 14th Fluid and Plasma Dynamics Conference, Paulo Alto, California), 1981.

59.   Reynolds, G. A., and Saric, W. S., "Experiments on the stability of the flat-plate boundary layer with suction", AIAA Paper No. 82-1026 (AIAA/ASME 3rd Joint Thermophysiscs, Fluids, Plasma and Heat Transfer Conference, Saint Louis, Missouri), 1982.

60.   Saric, William S., "Laminar flow control with suction: Theory and experiment", AGARD Report No. AGARD-R-723 (Drag Prediction and Reduction), 1985.

61.   Saric, W. S., and Reed, H. L., "Effect of suction and blowing on boundary-layer transition", AIAA Paper No. 83-0043 (AIAA 21st Aerospace Sciences Meeting, Reno, Nevada), 1983.

62.   Schlichting, Herman, "Boundary Layer Theory" (Translated by Kestin, J), 6th edition, McGraw Hill, Inc., 1968.

63.   Schlichting, Herman and, Truckenbrodt, Erich, "Aerodynamics of the Airplane" (Translation of "Aerodynamik des Fluzeuges" by Ramm, Heinrich J.), McGraw Hill, Inc., 1979

64.   Shi, Z., "A Study of Jets in Crossflow and its Application on Wingtip Blowing", PhD. Dissertation, The University of Tennessee, Knoxville, May 1990.

65.   Smith, A. M. O., and Brazier, J. G., "Wind tunnel tests on a 6-ft. chord model of the DESA-2 laminar suction airfoil", Report No. ES 17129, Douglas Aircraft Company, Inc., March 9, 1953.

66.   Stark, W. W., "Laminar flow control summary flight test report - Laminar flow control airplane demonstration program", NOR-61-134, Northrop Corporation, April 1964.

67.   Thelander, J. A., Allen, J. B., and Welge, H.R., "Aerodynamic development of laminar flow control on swept wings using   distributed suction through porous surfaces", AIAA Paper No. 82-40894 (Aircraft Systems Technology Conference Proceedings, volume 1, pp. 182 - 189), 1982.

68.   Thomas, A. S. W. and, Cornelius, K. C., "Investigation of a laminar boundary layer suction slot", AIAA Journal, Volume 20, pp. 790 - 796, 1981.

69.   Van Ingen, J. L., "Theoretical and experimental investigation of incompressible laminar boundary layers with and without suction", Report No. VTH-124, Department of Aeromautical Engineering, Technological University of Delft, October 1965.

70.   Williams, John, "A brief history on British research on boundary layer control for high lift", Boundary Layer and Flow Control (edited by Lacmann, G.V.), Pergamon Press, Ltd., 1961.

71.   Wu, J. Z., Wu, J. M., and Wu, C. J., "A general three dimensional viscous compressible theory on the interaction of solid body and vorticity-dilation field", UTSI Report 87/03 (see also Fluid Dynamics Research, Vol. 3, Nos. 1-4, pp. 202-208), 1987.

72.   Wu, J. Z., Gu, J. W., and Wu, J. M., "Steady three-dimensional fluid particle-separation from arbitrary smooth surface and formation of free vortex layers", Z. Flugwiss Weltraum Forsch, Vol 12, pp. 89-98 (see also AIAA Paper No. 87-2348-CP), 1988.

73.   Wu, J. Z. and Wu, J. M., "Guiding Principles for Vortex Flow Control", AIAA Paper No. 91-0617, 1991.

74.   Zalovcik, J. A., Wetmore, J. W., and Van Doenoff, A. E., "Flight investigations of boundary layer control by suction slots on an NACA 35-215 low darg airfoil at high Reynolds numbers", NACA WR L-521, 1944

75.   Zozulya, V. B., and Cheranovskiy, O. R., "Control of laminar flow past a wing in free flight" Fluid Mechanics, Soviet Res., Volume 2, No. 5, September - October, 1973.

APPENDIX

In this section, a chronological summary of all major previous research conducted in the area of boundary layer control by application of suction, both continuous and distributed, through porous surfaces, perforated surfaces, holes, and slots are presented in tabular form.

Time Period	Investigator(s)	Facility/ Airplane	Configuration	Results	Comments
1904	Prandtl	Göttingen	Cylinder with one suction slot on the upper surface at $90° >$ theta $> 180°$	Flow stayed attached to the cylinder without separation to a greater degree on the upper half (where the suction slot was located) when compared to the flow in the lower half which separated from the cylinder much earlier. (Visual study - Still photographs)	Conceptually showed that suction can be utilized as an effective means of boundary layer flow control
late 1920's - early 1930's	Schrenk	Aerodynam-ische Versu-chsanstalt at Göttingen	Two experimental aircraft were built in the late 1930's and tested with one suction slot located on the wing just ahead of the flap	Full-chord laminar flow was achieved over the entire flap, when the flap was deflected	Exstensive experim-ental research with the objective of ach-ieving increased lift
1940 - 1948	Holstein		- 15% thick airfoil with Karman-Trefftzt airfoil with rounded edge flaps. - NACA 0012-64 wing with slot suction - Flat plate with suction through perfor-ated surface	Full-chord laminar flow was achieved upto Re = 3.2×10^6	Tunnel turbulence was not low. Problems with roughness sensi-tivity resulted in 'oversuction'.
1944	Goldstein	National Physics Laboratory (NPL)	Wing with 30% thick airfoil designed for slot suction near the rear of the wing and ahead of the flap	Partial laminar flow was achieved over the flap with suction, at a flap deflection of $16°$. $C_{L(max)}$ = 4 - 5 were attained.	The suction quantity required to maintain a particular lift decrea-ced with increasing flap deflection
1944-1947	Zalovcik, Wetmore, and Van Doenoff	Douglas B-18 aircraft	Wing glove outside of slip-stream with NACA 35-215 airfoil with, (a) 9 slots (b) 17 slots spaced at a distance of 5%chord from each other	Laminar flow upto 45% chord was ach-ieved upto Re = 13×10^6, C_L = 0.35; Re = 30.8×10^6, C_L = 0.19. Transition moved from 40% chord to 45% chord for the 9-slot case	'Oversuction' resulted in the 17-slot case

Time Period	Investigator(s)	Facility/ Airplane	Configuration	Results	Comments
1945	Goldstein and Lighthill	NPL	Two 8.5% airfoils designed specially for nose slot-suction: (a) Lighthill airfoil with sharp l.e. and slot located at l.e. (b) Glauert airfoil with rounded l.e. and slot at 0.005% chord	Suction requirements were unduly high for practical application	Stalling incidence angle and $C_{L(max)}$ increased steadily with increasing suction
1947	Moss	Royal Aircraft Establishment (RAE)	14% thick, highly tapered, 45° sweep-back wing with aspect ratio of 4.5. Suction applied through spanwise and chordwise slots	Gains due to suction were disappointing	Spanwise slots were found to be more effective than chordwise slots
1947-1949	Pfenninger	7 X 10 ft. wind tunnel at the Federal Inst. of Technology, Zurich	Wing with a 17% thick laminar airfoil, with several suction slot geometries	Full-chord laminar b.l. on both surfaces at Re = 2.5 X 10^6, with C_Q = 0.0014 - 0.0018. At Re = 2.4 X 10^6, $C_{D(min)}$ = 0.0023 compared to $C_{D(min)}$ = 0.0048 at Re = 2 X 10^6	Tunnel turbulence was in the order of 0.4%
1948	Pankhurst	NPL	Wing with 8% thick airfoil and large nose radius. Suction through porous surface with constant resistance over nose	Partial laminar flow was maintained over the wing	
1948-1951	Braslow, Burrows, Visconti, Tetervin, and Albert		Wing with NACA 64 A010 airfoil with suction applied through porous surface	Full-chord laminar flow was attained upto Re = 20 X 10^6 . 38% increase in total (wake + suction) drag was achieved when compared to the same wing with no suction	Minimum C_Q required for full-chord laminar flow decreased with increasing Re. C_Q was in the same order as theoretical results
1949	Loftin and Burrows		Several airfoil sections including NACA 18-212, NACA 0007-34, NACA 27-215	Laminar flow was increased to as much as 52% chord at Re 2.5 X 10^6	Tunnel turbulence level varied from 0.02% to 0.2%

Time Period	Investigator(s)	Facility/ Airplane	Configuration	Results	Comments
1950-1951	Phenninger	Northrop Norair wind tunnel	2 in. diameter, 40 in long tube (no suction was applied in this case, refer to cases below for with suction)	Transition was observed to occur at Re = 19 X 10^6. Momentum thickness Reynolds number at transition = 2900	
1950's	Pankhurst and Thwaites		Wholly porous cylinder of 3 in. diameter and flap of length 1/8 in.	At a flap deflection of 60°, and $C_Q\sqrt{Re}$ = 35 (at Re = 0.1 X 10^6), circulatory flows were realized with $C_{L(max)}$ = 9	The suction quantity decreased slightly with increasing deflection angle
1951	Poppleton		Untapered 10% thick wing with 40° sweep-back and aspect ratio 4.6. Slot suction was applied at x/c = 0.025. Slot width-to-chord ratio, w/c = 0.0023	Increased maximum lift with suction compared to the 'no suction' case. Improved longitudinal stability right upto stall	
1951	Phenninger	Northrop Norair wind tunnel	2 in. diameter tubes of length 20 ft. and 40 ft. with 8 suction slots (only one slot was used in this particular test)	Suction through slot destabilized the flow without favorable presure gradient immediately downstream of the slot	
1951	Phenninger	Northrop Norair wind tunnel	2 in. diameter tube of length 20 ft. and 8 suction slots (all 8 slots were used)	Whole-tube laminar flow was maintained upto Re = 14.7 X 10^6	
1951	Unpublished work at R.A.E. (refer to reference 68)	R.A.E.	Untapered, 10% thick wing with 40° sweep and aspect ratio 4.6. Suction applied through porous surface	Optimum extent of porous area for suction was found to be in the first 2.5%c of the upper surface of the wing nose, with 1.5 times suction at the outboard section of the span as the inboard section	
1951	Keeble	D.H.G.2 Glider	Modified GLAS II, designed for separation control by applying suction. Un-swept tapered wing of chord 8 ft.	At speeds upto 180 ft./sec, transition was delayed upto x/c = 0.63	Boundary layer was evidently tripped by slot
1951	Loftin and Horton	3 X 7.5 ft. Langley TDT	15% thick airfoil with 17 slots on upper, 13 slots on lower surface (40%-100% c)	Full-chord laminar flow was achieved upto Re = 17 X 10^6	

Time Period	Investigator(s)	Facility/Airplane	Configuration	Results	Comments
1951	Braslow, Burrows, Tetervin, and Visconti	Langley low turbulence presure tunnel	Wing with NACA 64 A010 airfoil with chord length 3 ft. Suction applied through porous surface of 13 in. length, centered at mid-span	At a suction velocity, v_s = 0.5 ft/sec (induced by a suction of 1.84 lb/in^2), full-chord laminar flow was maintained upto Re = 19.8 X 10^6, with $C_{D(total)}$ = 0.0017	The C_Q required to maintain full-chord laminar flow decreased with increasing Re. The C_D was 1/2 of that of the 'no suction' case
1952-1954	Carmichael and Raspet	TG-3A Sailplane	Wing with NACA 4416 airfoil. Suction applied through perforated surface	Stabilization of flow in the adverse presure gradient region upto V_∞ = 123 ft./sec (2 X 10^6 < Re < 4 X 10^6)	Location of applied suction and quantity were varied
1952	Burrows and Schwartzberg		Wing with NACA 64 A010 and of chord length 3 ft. Suction applied through 41 suction slots on each surface	Nearly full-chord laminar flow (90% c) was achieved upto Re = 10 X 10^6. 50% drag reduction when compared with case without suction	Extreme surface roughness sensitivity
1952-1953	Loftin and Horton	Langley low turbulence presure tunnel	Wing with NACA 66-(1.8)15 airfoil of 15% thickness and chord length of 5 ft. Suction applied through multiple slots	Full-chord laminar flow was achieved upto Re = 16 -17 X 10^6. Large $C_{D(total)}$ savings. $C_{D(min)}$ = 0.0011 at Re = 16.3 X 10^6	Extreme surface roughness sensitivity
1953	Unpublished work at R.A. E. (refer to ref. 68)	R.A.E.	Untapered, 6.5% thick wing of 60° sweepback and aspect ratio 3. Nose suction through slot	An increase in $C_{L(max)}$ was not attainable, but the usable C_L was considerably raised	
1953-1957	Phenninger and Meyer	Northrop Norair wind-tunnel	1 in. and 2 in. tubes of length 50 ft.	Whole tube laminar flow was maintained upto Re = 14.7 X 10^6	
1953-1957	Goldsmith and Meyer	Northrop Norair wind-tunnel	2 in. diameter tube with hole suction		3-D disturbances due to the hole were experienced which were destabilzing

Time Period	Investigator(s)	Facility/ Airplane	Configuration	Results	Comments
1953	Smith		6.6% thick wing with DESA-2 airfoil of chord length 6 ft. Suction applied through 16 slots (9 upper and 7 lower)	Full-chord laminar flow could not be achieved at $Re = 5.8 \times 10^6$. However, very high stability with respect to T-S waves were established	Hypersensitive to surface roughness
1953	Kay	Closed-circuit Cambridge U. wind tunnel	Flat plate with suction through uniform porous surface	A suction to free-stream velocity ratio, $v_s/V_\infty = 0.001$ was required to stabilize the flow	Minimum C_Q required to maintain laminar flow was the optimum C_Q for drag reduction
1954	Unpublished work at N.P.L. (refer to reference 68)	N.P.L.	Wing with a 8% thick airfoil. Area suction was applied in the vicinity of the knee of the l.e. flap	At a flap deflection angle of 60°, a suction-to-freestream velocity ratio, $v_s/V_\infty = 0.03$ was required to maintain full laminar flow	Separation over flap is best avoided by starting area suction around midway of flap knee (min. pressure point)
1954	Head and Johnson	Vampire Aircraft	Tapered, unswept wing with l.e. at 11.5°. Suction was applied through porous surface	Full-chord laminar flow was achieved upto $Re = 29 \times 10^6$ (M=0.7). Drag reduction of about 70-80% was realized when compared with the 'no-suction' case	
1955	Poppleton		40° sweep wing. Suction was applied in the nose region of the airfoil through both continuous and slot suction	At $Re = 1.3 \times 10^6$, for w/c = 0.004, a $C_{L(max)} = 0.6$ was achieved with $C_Q = 3.7 \times 10^{-3}$ for continuous suction, and $C_Q = 9 \times 10^3$ for slot suction	Continuous suction produced the same C_L's with less C_Q's than slot suction
1955	Gregory and Walker		Wing with NACA 63 A009 airfoil with distributed suction applied over the nose	Separation was avoided at an AOA = 14° at a suction location-to-chord length ratio 0.0275 with $C_Q = 23 \times 10^4$, Re 3.5×10^6	Minimum C_Q required to avoid separation decreased with increasing Re
1955	Head	Avron Anson Aircraft	15% thick low-drag airfoil mounted as fin under fuselage with porous suction	Full-chord laminar flow was achieved upto $Re = 3.3 \times 10^6$	

Time Period	Investigator(s)	Facility/ Airplane	Configuration	Results	Comments
1955-1957	Phenninger, Groth, Carmichael and Whites	F-94 Aircraft	Tapered wing with 13% thick airfoil similar to NACA 65-213. Upper surface wing glove with 12 slots (between 41.5% and 94% c), 69 slots, and 81 slots	For the 12 slot case, full-chord laminarization was achieved upto $Re = 25.64 \times 10^6$, with $C_Q = 0.00034$, $C_D = 0.00051$; for the 69 slot case, upto $Re = 36 \times 10^6$, with $C_Q = 2.91 \times 10^{-4}$, $C_D = 4.82 \times 10^{-4}$	
1955-1958	Groth and Phenninger	Northrop wind tunnel / NASA Ames tunnel	Axisymmetric body of revolution with fineness ratio of 8. Suction applied through slot	Full-length laminarization realized upto $Re = 14 \times 10^6$, at an $AOA = 3°$. For $Re < 11 \times 10^6$, the $C_{D(total)}$ was 1.24 times the C_f for a flat plate	
1956-1966	Burrows (later Landeryou and Porter)	Following Aircraft: Anson, Lancaster, Lincoln.	Dorsal fin mounted on upper fuselage at sweep angles of 42.6° and 45°. Slot suction. Anson, c= 48 in., Lancaster, c = 88 in., Lincoln, c = 100 in.	99% chord laminar flow upto $Re = 1.58 \times 10^6$/ft. 90% chord laminar flow upto $Re = 1.87 \times 10^6$/ft.	
1957	Meyer	Northrop Norair wind tunnel	8 in. diameter tube with suction applied through holes of 1/8 in. diameter drilled 1/2 in. apart	Identified trailing vortices from the holes	
1953-1957	Phenninger, Meyer, Sipe, and Monesss	Northrop Norair wind tunnel	2 in. diameter tube with 80 slots	Full-length laminar flow was achieved upto $Re = 21.2 \times 10^6$. 40% laminar pressure rise. Min CQ's for full laminar flow were 20% smaller than the case with 8 suction slots (mentioned earlier)	27% less suction required with 80 slots than with 8 slots
1957-1959	Phenninger, Gross, Lloyd, Bacon, and Tucker	5 X 7 ft. Michigan wind tunnel	30° sweep wing with 12% thick airfoil. Suction applied through slots (86 slots located from 25%-95% chord), AOA = 0°; 1°, -1°	At AOA = 0°, full-chord laminar flow was achieved upto $Re = 11.8 \times 10^6$, with $C_{D(total)} = 0.00125$	CQ required for full laminar flow was larger than those for a straight wing.
1957	Smith	Douglas wind tunnel	Flat plate with suction through porous surface	Obtained laminarization quite easily upto $Re = 8 \times 10^6$, with rel. low suction rates	Transition occurred $Re = 2.0 - 7.2 \times 10^6$

116

Time Period	Investigator(s)	Facility/ Airplane	Configuration	Results	Comments
1961-1962	Phenninger and Gault	NASA Ames 12 ft. presure tunnel	12% thick wing with NACA 66-012 airfoil and 30° sweep. Suction applied through 93 spanwise slots	Full-chord laminar flow was achieved upto $Re = 29 \times 10^6$, at low speeds	
1962	Gross	Northrop Norair 7 X 10 ft. wind tunnel	4% thick wing with a chord length of 17 ft. Suction applied through 100 suction slots	Full-chord laminar flow was achieved upto $Re = 26 \times 10^6$. At $Re = 25 \times 10^6$, $C_{D(total)} = 0.000375$, with $C_Q = 0.00013$	
1963-1966	Stark	X-21 Aircraft	30° sweep wing with spanwise suction slots	Partial laminarization achieved at $Re = 47 \times 10^6$ (transonic region)	
1964	McCormick	Water tunnel and sea tests	TRI - B bouyantly propelled axisymmetric body, with circumferential slot suction	Nearly full-chord laminar flow at $Re = 4 \times 10^6$	Non uniform circumferential suction caused problems
1964-1965	Gross	Nortrop Norair 7 X 10 ft. wind tunnel	Body of revolution with finess ratio 9:1 and length of 12 ft. Suction through 102 holes	Full-length laminar flow was achieved upto $Re = 20.63 \times 10^6$. At $Re = 20.27 \times 10^6$, $C_{D(total)} = 4.18 \times 10^{-4}$, $C_Q = 2.25 \times 10^{-4}$	At an AOA = 0°, $C_{D(total)}$ was 1.4 times that of a laminar flat plate C_f
1964-1966	Carlson, Phenninger, and Bacon	NASA Ames 12 ft. presure tunnel	33° sweep wing with a NACA 64016 airfoil and of chord length 10 ft. Suction was applied through spanwise slots	90% laminar flow was achieved at $Re = 44.8 \times 10^6$ (low speed enviorenment). At $Re = 29.4 \times 10^6$, $C_D = 0.00088$. At $Re = 43 \times 10$, $C_D = 0.001$	Surface presure had spatial oscillations around x/c = 0.08
1964	Gross	Northrop Norair 7X10 ft. wind tunnel	Sears-Haack body of revolution of length 142 in. and fineness ratio 9:1. Suction applied through 120 slots	Full-length laminar flow was achieved upto $Re = 20.1 \times 10^6$, AOA = 0°. At AOA = 2°, upto $Re = 18.55 \times 10^6$	At $Re = 19.6 \times 10$, $C_{D(total)}$ was 1.8 times that of a laminar flat plate that of a laminar flat plate C_f, $C_Q = 1.75 \times 10^4$
1964	Kosin	X-21 Aircraft (WB-66)	30° sweep wing with approximately 120 slots on the upper surface and 120 slots on the lower surface. Slot widths ranged from 0.0035 in. - 0.01 in.	Full-chord laminar flow was achieved in the outer third of the wing	

Time Period	Investigator(s)	Facility/ Airplane	Configuration	Results	Comments
1965	Van Ingen		Wing with 15% thick airfoil of chord length 1.35 m. Porous suction applied between 30%c and 90%c on both upper and lower surfaces	Transition occured at $Re = 9 \times 10^6$. Location of transition was in approximate agreement with e^9 method	
1973	Zozulya and Cheranovskiy	Remotely Piloted Vehicle	Suction applied through spanwise slots on wing	At low Reynolds numbers, at a $V_\infty = 131$ ft./sec, laminar flow upto 80%c achieved	
1976	Kozlov and Tsyganyuk	Water tunnel experiments	Body of revolution (cylinder) with porous suction surface	At $Re = 3.5 \times 10^6$, and at $C_Q = 6 \times 10^{-4}$ $C_{D(total)}$ was reduced to half the value of that without suction	
1976-1978	George-Flavy		30° sweep wing with suction through slots	Laminarization upto $Re = 6 \times 10^6$, with suction over the first 30% of chord	
1976-1982	Pearce	Douglas wind-tunnel	30° sweep wing with chord length of 7 ft. Suction was applied through: (a) slotted surface (b) porous 'Dynapore' (c) electron beam perforated titanium	At $Re = 1.35 \times 10^6$/ft (comparable to an aircraft flying at $M = 0.74$, at 38,000 ft., at $Re = 1.6 \times 10^6$). 80% laminar flow was achieved with suction upto 70% chord. Total drags were in the order of $C_{D(total)} = 0.00175 - 0.0025$	EB perforated titanium provided the best results compared to the other surfaces. Suction upto 80% chord only on upper surface yielded better results than suction on both surfaces upto 70% c

VITA

Ram Sivakumaran was born on July 30, 1967 in Colombo, Sri Lanka. He completed his elementary, grade, and high school education at Royal College, Colombo.

In 1986, he moved to Saint Louis, Missouri and entered Parks College of Saint Louis University. In December 1988 he graduated with a Bachelor of Science degree in Aerospace Engineering. He then joined the University of Tennessee Space Institute in the fall of 1989, where he served as a Graduate Research Assistant while pursuing his graduate studies. He was awarded the Master of Science degree in Aerospace Engineering from the University of Tennessee in December 1991.

Ram is a member of the American Institute of Aeronautics and Astronautics (AIAA) and the American Helicopter Society (AHS). He is also an alumnus member of the Kappa Delta Rho national fraternity.